UNIVERSITÀ
DEGLI STUDI
FIRENZE

DOTTORATO DI RICERCA IN
Area del Farmaco e Trattamenti Innovativi
(Curriculum Scienze Farmaceutiche)

CICLO **XXIX**

COORDINATORE

Prof.ssa Elisabetta Teodori

"Inhibition studies of Carbonic Anhydrases from pathogenic organisms"

Settore Scientifico Disciplinare CHIM/08

Dottorando
Dott.ssa Sonia Del Prete

Tutore
Prof. Claudiu Supuran

Co-Tutore
Dr. Clemente Capasso

Coordinatore
Prof.ssa Elisabetta Teodori

Anni 2013/2016

Riassunto

La conversione dell'anidride carbonica (CO_2) in bicarbonato (HCO_3^-) e protoni (H^+) è una reazione fisiologicamente rilevante in tutti gli organismi viventi. La reazione $CO_2 + H_2O \leftrightharpoons HCO_3^- + H^+$ non catalizzata è lenta a pH fisiologico e quindi, nei sistemi biologici, è accelerata da catalizzatori enzimatici, noti con il nome di anidrasi carboniche (CA, EC 4.2.1.1). Le CA sono state trovate in quasi tutti i tessuti di mammiferi e tipi cellulari, e sono coinvolte nel trasporto della CO_2 e in altri importanti processi fisiologici.

Nella presente tesi è riportato lo studio sui profili d'inibizione delle CA identificate nel genoma di organismi patogeni per l'uomo, quali *Vibrio cholerae*, *Plasmodium falciparum*, *Porphyromonas gingivalis e Malassezia globosa.*

Le CA codificate dagli organismi suddetti sono state caratterizzate biochimicamente e i loro profili d'inibizione, ottenuti utilizzando gli inibitori classici delle CA, come le sulfonamidi e gli anioni, sono stati ampiamente esaminati. Tale studio ha dato un grande contributo alla ricerca di potenziali antibiotici con un nuovo meccanismo d'azione. Inoltre, la presente tesi ha contribuito alla scoperta di *a*) una nuova famiglia genica di CA, indicata con la lettera greca η; *b*) alla messa a punto di una nuova tecnica, denominata protonografia, utile per l'identificazione dell'attività delle CA su gel di poliacrilamide; e *c*) all'analisi filogenetica delle CA di classe α, β e γ identificate nel genoma dei batteri Gram-positivi e Gram-negativi.

Abstract

The conversion of carbon dioxide (CO_2) to bicarbonate (HCO_3^-) and protons (H^+) is a physiologically relevant reaction in all life kingdoms. The uncatalyzed hydration-dehydration reaction $CO_2 + H_2O \leftrightharpoons HCO_3^- + H^+$ is slow at physiological pH and thus, in biological systems, the reaction is accelerated by enzymatic catalysts, called carbonic anhydrases (CAs, EC 4.2.1.1). CA isozymes have been found in virtually all mammalian tissues and cell types, where they function in CO_2 transport and other physiological processes.

In the present thesis, it has been carried out a wide study concerning the inhibition profiles of CAs identified in the genome of pathogens causing disease in humans, such as *Vibrio cholerae*, *Plasmodium falciparum*, *Porphyromonas gingivalis* and *Malassezia globosa*

CAs from the pathogens aforementioned were biochemically characterized and an extensive inhibition profile was carried out using the classical CAs inhibitors such as sulfonamides and anions. These studies have contributed to the search of antibiotics with a novel mechanism of action. Additionally, the present thesis has contributed to the discovery of the η-CA, a new genetic families of CAs; to the introduction of a new technique, named protonography, useful for the identification of CA activity on a polyacrylamide gel; and to the phylogenetic analysis of the α-, β- and γ-CAs identified in the genome of the Gram-positive and Gram-negative bacteria.

Chapter 1. Introduction

1.1 Carbonic anhydrases

Carbonic anhydrases (CAs, EC 4.2.1.1) are ubiquitous metalloenzymes present in all life kingdoms: Archaea, Bacteria and Eucarya. Formed by the convergent evolution of at least seven families of genes (α, β, γ, δ, ζ, η and θ) (Supuran., 2008 ; Sae Kikutania., *et al*., 2016). CAs have been identified for the first time in red blood cells of bovine (Meldrum N.U. & Roughton F.J. 1933). Later, they have been found in all mammalian tissues, but also in plants, algae and bacteria. CAs owe their ubiquity to the ability to catalyze a simple but physiologically relevant reaction for living being (Capasso C. & Supuran C.T. 2015), i.e. the reversible hydration of carbon dioxide with the formation of bicarbonate and protons according to the following formula:

$$\mathbf{CO_2 + H_2O \leftrightharpoons HCO_3^- + H^+}$$

The reaction of hydration of CO_2 consists of four reactions:

1) $CO_{2(g)} \leftrightharpoons CO_{2(aq)}$ reaction of dissolution in aqueous phase
2) $CO_{2(aq)} + H_2O \leftrightharpoons H_2CO_3$ hydration reaction (carbonic acid production)
3) $H_2CO_3 \leftrightharpoons HCO_3^- + H^+$ ionization reaction (bicarbonate production)
4) $HCO_3^- \leftrightharpoons CO_3^{2-} + H^+$ dissociation reaction (carbonate formation)

In physiological conditions and in the absence of the catalyst, the reaction 2 is the limiting step of the entire process and, the k_{cat} assumes a value of 1.5×10^{-1} s^{-1} (Edsall J.T. 1968). The carbonic anhydrase, able to convert a million molecules of CO_2 per second, increases the value of the k_{cat} from 10^{-1} s^{-1} to 10^5 s^{-1}. CAs are among the fastest enzymes known.

1.2 Physiological role of CAs

CAs in mammals are involved in breathing and transport of carbon dioxide and bicarbonate in tissues and lungs, in the homeostasis of pH and CO_2 in biosynthetic reactions such as gluconeogenesis, lipogenesis, ureagenesis, where the bicarbonate acts as a substrate for the reaction of carboxylation, bone resorption, calcification and tumorigenicity (Supuran C.T., *et al.* 2015). However, in microorganisms, in addition

to the transport of carbon dioxide bicarbonate and its supply of for biosynthetic reactions, carbonic anhydrases are involved in: a) carbon fixation for the photosynthetic process; b) metabolism of xenobiotics (degradation of the cyanate in *E. coli*); c) pH regulation; d) survival of the pathogen within the host organism; d) synthesis of purine and pyrimidine as in the protozoan *Plasmodium falciparum* (Supuran C.T. & Capasso C. 2014).

In mammals, at the level of the peripheral tissue, due to the pressure gradient, the carbon dioxide, produced by the aerobic metabolism, leave the cells and enter the blood, dissolving in the plasma (reaction 1). From here, about 90% of the carbon dioxide enters the red blood cells and, thanks to the action of carbonic anhydrase reacts with water, forming carbonic acid (reaction 2) which in turn dissociates into bicarbonate ion and hydrogen ion (reaction 3). Bicarbonate leaves the red blood cell by a protein antiporter. This transport process, defined exchange of chlorides, exchanges one HCO_3^- ion with a Cl^- ion. The exchange takes place in the ratio of 1: 1 by maintaining electrical neutrality and, consequently, the membrane potential of the cell is not changed. The ion HCO_3^- is converted to carbonate and protons H^+ (reaction 4), which are linked by hemoglobin, which acts as a buffer (Boron W.F. 2010). At the alveolar level, however, the CO_2 concentration is lower than that in the peripheral tissues, while there is a higher concentration of bicarbonate that is pumped inside the red cell. Here, by the action of the reverse reaction catalyzed by the CAs, the bicarbonate is converted into carbonic acid, which will give water and carbon dioxide. The CO_2 thus produced, is released into the blood and, passing by diffusion through the walls of the alveolus, is exhaled. The direction of the reaction, therefore, depends on the concentration of CO_2: if this is low (as in the lungs), the acid is dissociated, with release of carbon dioxide; If this is high, dioxide binds water to form carbonates that are transported by the blood to the lungs (Boron W.F. 2010).

1.3 CA classes

Until now were identified 7 distinct gene families of CAs (Supuran C.T. & Capasso C. 2014):

- α-CA: invertebrates, fungi, protozoa, corals, algae, cytoplasm of green plants and some bacteria

- β-CA: mainly in bacteria, algae and plant chloroplasts mono and dicots, many fungi and Archaea
- γ-CA: mainly in Archaea, some bacteria and plants
- δ-CA: marine phytoplankton (diatoms)
- η-CA: protozoa *Plasmodium falciparum*
- θ-CA: marine diatoms *Phaeodactylum tricornutum*

The α-, β-, δ-, η- and, perhaps θ-CAs use Zn(II) ions at the active site, the γ-CAs are probably Fe(II) enzymes (but they are active also with bound Zn(II) or Co(II) ions), whereas the ζ-class CAs are cambialistic enzymes, active both with Cd(II) or Zn(II) bounded within the active site in order to perform the physiologic reaction catalysis. (Vullo D., *et al*. 2014; Del Prete S., *et al.* 2014; Capasso C. & Supuran C.T. Expert Opin. Ther. Pat., 23 2013).

In mammals, there are only α-CAs, of which 16 isoforms were identified, marked with Roman numbers (Supuran C.T. *et al.*, 2008; Supuran C.T., *et al.* 2004; Scozzafava A., *et al.* 2000; Winum J.Y. *et al.* 2006; Saczewski F., *et al*. 2006; De Simone G., *et al.* 2006). These isoenzymes can be distinguished according to the different tissue distribution, subcellular localization and catalytic activity (Supuran C.T. 2008). In particular, we divide the mammalian α-CAs in:

- Cytosolic (isoenzymes I, II, III, IV, VIII)
- Mitochondrial (isoenzymes VA, VB)
- Membrane-bound (isoenzymes IV, IX, XII, XIV, XV)
- Secreted in saliva (isoenzyme VI)
- Catalytically inactive isoforms (CARP VIII, X and XI)

1.4 Catalytic mechanism

In Figure 1 is reported the alignment of the α-CA amino acid sequences: four human isoforms (hCA I, hCA II, hCAVA and hCAVI) and two bacterial CAs represented by SspCA, identified in the genome of the thermophilic bacterium *Sulfurihydrogenibium yellowstonense* and, VchCA present in the genome of the mesophilic bacterium *Vibrio cholerae*.

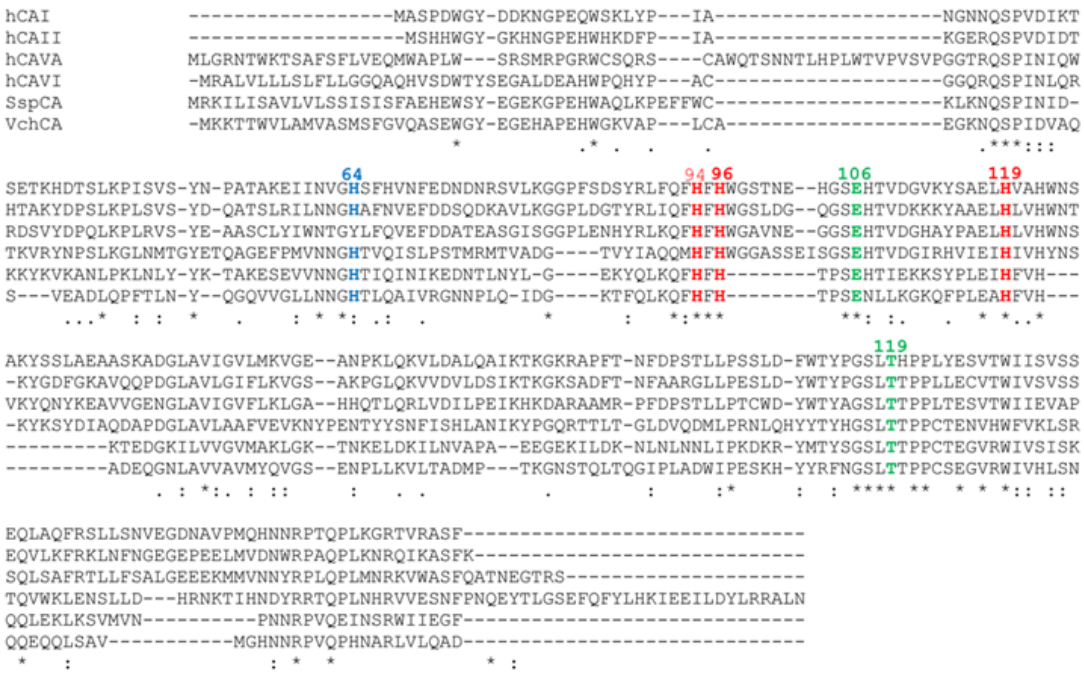

Figure 1. Multialignment of the amino acid sequences of four human and bacterial CAs was realized with the ClustalW program, version 2.1. In red shows the amino acid residues of the catalytic triad, green residues "gate-keeper" and the blue "proton shuttle residual". It was used the numbering system hCA.

The amino acid residues involved in the catalytic mechanism of the α-CAs, which consists of four steps, are colored in the alignment. In the first step zinc ion, present in the catalytic site of the enzyme, is bound to the hydroxyl ion (Figure 2, Panel A). This configuration corresponds to the active form of the enzyme. The substrate CO_2 is bound in a hydrophobic pocket near the Zn(II) ion, defined among others by residues Val121, Val143 and Leu198 (in the human isoform hCA II). Orientated in a favorable position for the nucleophilic attack of the enzyme, CO_2 is transformed into bicarbonate. (Figure 2, Panel B). The bicarbonate ion is then displaced by a water molecule and released in solution (Figure 2, Panel C). In this way, the water molecule coordinated to the zinc, generates the acidic form of the enzyme, which is catalytically inactive (Figure 2, Panel D). The catalytically active form of the enzyme is regenerated through the reaction of transfer of a proton from the active site of the enzyme to the environment (Figure 2, Panel A). The speed of this transfer is highly dependent on the residue His64 known as "proton shuttle residue" (Supuran C.T. 2008)(see Figure 2).

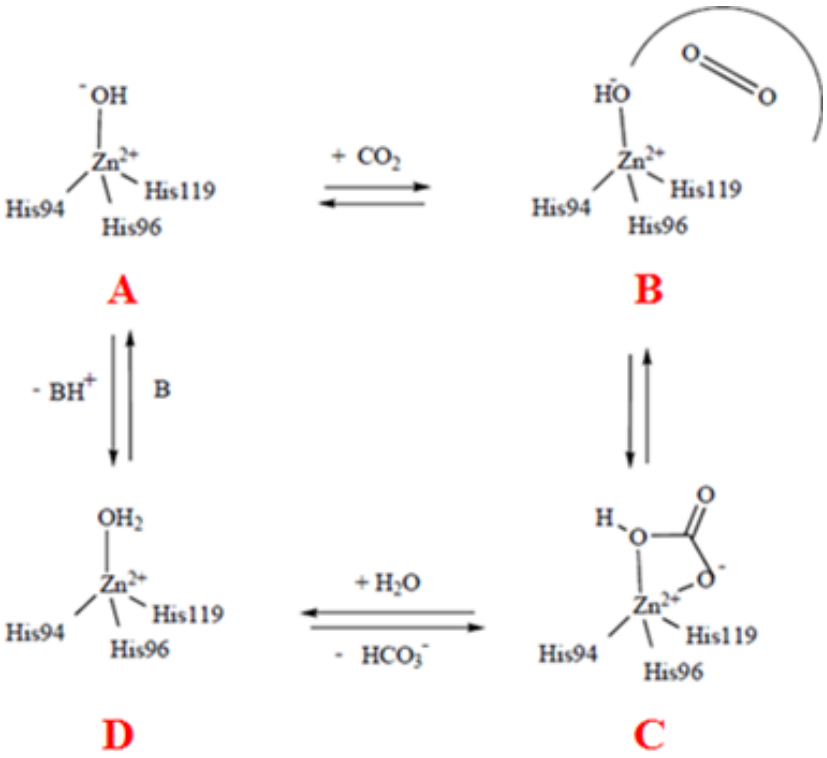

Figure 2. Schematic representation of the catalytic mechanism of a α-CAs.

In the catalytically very active isoenzymes, such as hCAII hCAIV, hCAVII and hCAIX, the transfer process of the proton from the enzyme to the environment is assisted by His64 positioned at the entrance of the active site and, by a cluster of histidine (His4, His3, His17, His15 and His10), which protrude from the edge of the active site of the enzyme on the surface, ensuring efficient removal of the proton by the enzyme (Figure 3). This explains why they are the most active known CAs (k_{cat}/K_M about 1.5 x 10^8 M^{-1} s^{-1}) (Supuran C.T. 2008). In other CA, such as the hCA III, the catalytic efficiency is lower because the residue His64 was absent and in position 198, a phenylalanine replaces the residue of leucine causing a steric hindrance near the catalytic site (Chegwidden W.R., Carter N.D., Edwards Y.H. 2000). α-CAs are also able to catalyze the hydrolysis of esters/thioesters, (for example 4-nitrophenyl acetate (4-NpA) hydrolysis, as well as other hydrolytic reactions); while no esterase activity was detected so far for enzymes belonging to the other five CA genetic families. (Del Prete S, *et al.* 2014; Guzel O., *et al.* 2010).

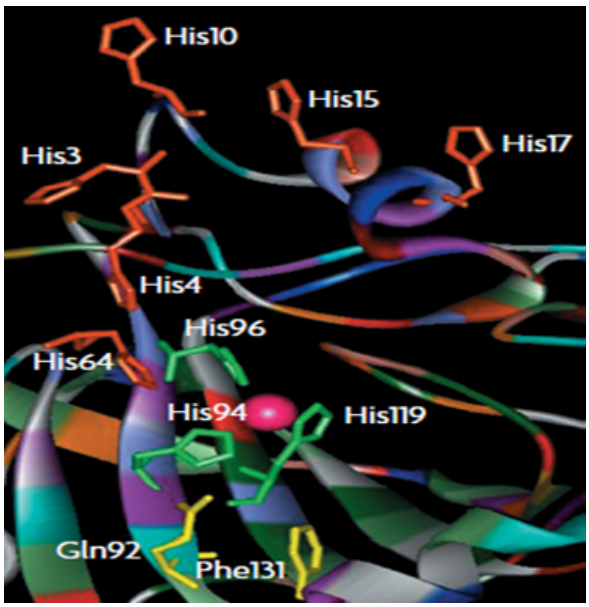

Figure 3. Structure of the active site of hCAII.

Are also known catalytically inactive isoforms of α-CAs, indicated as CARPs (Carbonic Anhydrase Related Proteins). The CARPs occur independently or as domains of other proteins in animals (both vertebrates and invertebrates) and viruses. Although these proteins show a high degree of homology with the other known CA isoforms (hCA I–VII, IX, and XII–XIV), they distinguish themselves from the catalytically active CAs by a salient feature: they lack one, two or all three zinc ligands from the enzyme active site, that is, His94, 96 and 119 (the hCA I numbering system). The phylogenetic analysis shows that these proteins are highly conserved across the species. The three CARPs in vertebrates are known as CARP VIII, X and XI. Most of these CARPs are predominantly expressed in central nervous system. Among the three vertebrate CA isoforms, CARP VIII is functionally associated with motor coordination in human, mouse and zebrafish and certain types of cancers in humans. Vertebrate expression studies show that CARP X is exclusively expressed in the brain. CARP XI is only found in tetrapods and is highly expressed in the central nervous system (CNS) of humans and mice and is also associated with several cancers. CARP VIII has been shown to coordinate the function of other proteins by protein-protein interaction, and viral CARPs participate in attachment to host cells, but the precise biological function of CARP X and XI is still unknown. (Aspatwar A., *et al*. 2014).

1.5 Characteristics of the CA classes

1.5.1 α-CAs

The most studied class of carbonic anhydrase, as well as that of which there are the largest number of three-dimensional structures, is the α-class. They contain the zinc ion (Zn^{2+}) in their active site coordinated by three histidine residues (His94, His96 and His119) and a water molecule/hydroxide ion (see Figure 4). Available α-CA structures, including most isoforms of human CA (hCA), reveal that the zinc ion is located in the pocket of the active site deep 15 Å (Figure 4).

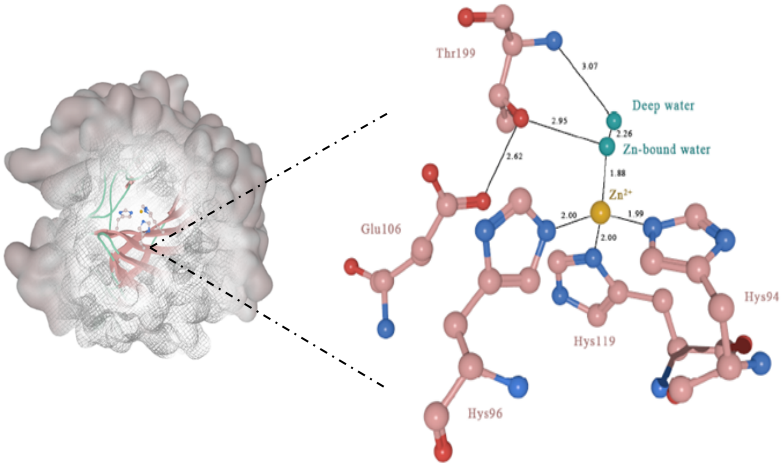

Figure 4. 3D structure and a particular of the active site of the human isoform II (hCAII). Legend: Orange sphere is the zinc ion; His 94, His 96, His119 are the amino acid residues of the catalytic triad; Thr199 and Glu106 are gate-keeping residues.

The water molecule bound to the zinc forms a hydrogen bond with the hydroxyl of Thr199, in turn linked to the carboxyl group of Glu106 (Supuran C.T., 2008). These interactions increase the nucleophilicity of the water molecule bound to the Zn(II) and orient the substrate (CO_2) in a favorable position for nucleophilic attack. It is interesting to note that the above-mentioned residues, are conserved in all human CAs with catalytic activity (Figure 1), with the exception of the human isoform hCAVA where the proton shuttle residues is missing. Up to date are available the crystallographic structures of α class CAs, such as hCA I, hCA II, hCA III, hCA IV, hCA V, hCA IX, hCA XII and hCA XIV (Alterio V., *et al.* 2012). Interesting, two human isoforms hCA IX and XII are associated with cancer and are involved in the

pH regulation and progression of the tumor. The α-CA are normally found in monomeric form with a molecular weight of approximately 29 kDa, with the exception of hCA VI, hCA IX and XII which occur as dimers (Boztas B., *et al.* 2015; Dudutiene V., *et al.* 2014). The bacterial α-CAs, such as those identified in the genome of *Sulfurihydrogenibium yellowstonense*, *S. azorense* and *Neisseria gonorrhoeae*, are dimers formed by two identical active monomers. Among the various classes of CAs, the α-class are the most active. The reactions catalyzed by α-CA, as well as the physiological reaction of hydration of CO_2 (Supuran C.T. 2008) are: hydration of cyanide to carbonic acid (1.1), or of cyanamide to urea (1.2 – 1.3), hydration of aldehydes to geminal diol (1.4), hydrolysis of carboxylic or sulphonic esters (1.5 – 1.6) in addition to other minor hydrolytic processes (1.7 – 1.9). Recently, it has been demonstrated that α-CA possess also the thioesterasic activity (1.10) (Tanc M., *et al*. 2015) (see list below).

List of reactions catalyzed by α-CAs:

(1.1) $O=C=O+ H_2O \leftrightharpoons HCO_3^- + H^+$

(1.2) $O=C=NH + H_2O \leftrightharpoons H2NCOOH$

(1.3) $HN=C=NH + H_2O \leftrightharpoons H_2NCONH_2$

(1.4) $RCHO + H_2O \leftrightharpoons RCH(OH)_2$

(1.5) $RCOOAr + H_2O \leftrightharpoons RCOOH + ArOH$

(1.6) $RSO_3Ar + H2O \leftrightharpoons RSO_3H + ArOH$

(1.7) $ArF + H_2O \leftrightharpoons HF + ArOH$

(1.8) $PhCH_2OCOCl + H2O \leftrightharpoons PhCH_2OH + CO_2 + HCl$

(1.9) $RSO_2Cl + H_2O \leftrightharpoons RSO_3H + HCl$

(1.10) $PhSO_2NHCSSMe \leftrightharpoons C_6H_5SO_2NH_2 + CH_4S + COS$

(Ar = 2,4-dinitrophenyl)
(R = Me; Ph)

1.5.2 β-CAs

Most of bacteria, Archaea as *Methanobacterium thermoautotrophicum*, chloroplasts of algae and higher plants, contain CA belonging to the β-class (Smith K.S. & Ferry J.G. 2000; Smith K.S. & Ferry J.G. 1999; Badger M.R. & Price G.D. 1994; Nishimori I., *et al.* 2007). In β-CAs Zn(II) ion is coordinated by two Cys residues, a residue of His and the carboxyl group of a residue of Asp (Figure 5 and 6A). β-CAs identified in chloroplasts, have as fourth ligand a water molecule (Mitsuhashi *et al*. 2000; Smith K.S., *et al*. 1999; Cronk J.D., *et al.* 2001; Kimber M.S., *et al.* 2000) (Figure 6B). The residues of the catalytic triade are highly conserved (Figure 5).

Figure 5. Multi alignment of amino acid sequences of β-CAs belonging to plants, yeast, fungi and bacteria, made with the ClustalW program, version 2.1. It was used the numbering system of *Pisum sativum*. The ligands of Zn (II) are shown in red. Legend: FbiCA_plant, *Flaveria bidentis*, isoform I; VraCA_plant, *Vigna radiata*; PsaCA_plant, *Pisum sativum*; Can2_fungus; Cryptococcus neoformans; SceCA_yeast, *Saccharomyces cerevisiae*; CalCA_fungus, *Candida albicans*; HpyCA_bacterium, *Helicobacter pylori*.

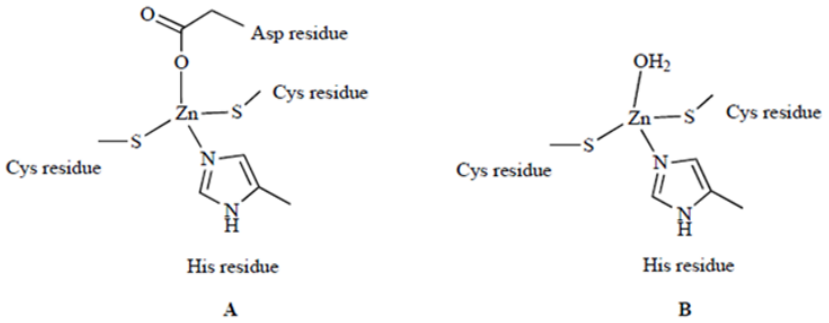

Figure 6. Coordination of Zn (II) in the β-CAs. **A**: *Porphyridium purpureum* and *Escherichia coli*; **B**: *Pisum sativum* and *Methanobacterium thermoautotrophicum*.

It has been demonstrated that at a pH of 7.5 or lower, the active site of carbonic anhydrase β is "locked", since the carboxyl group of an aspartic acid coordinates the zinc ion as a fourth ligand. At pH values higher than 8.3 the enzyme active site is converted in an open one, since the aspartate forms a salt bridge with residue Arg46 (numbering hpβCA) stored in all the carbonic anhydrase from β class (Nishimori I., *et al*., 2007). In this way, the molecule of water/hydroxide ion has the possibility to coordinate the metal ion to the completion of its tetrahedral geometry. As a result, the catalytic mechanism of β-CAs with the active site "open" is rather similar to the enzymes of α class. Respect to the α-class, β-CAs are oligomers formed by two or more identical subunits. Generally, β-CAs are dimers, tetramers and octamers. The monomeric subunit has a molecular weight of 25-30 kDa and the active form of the enzyme requires two subunits to reconstitute the catalytic site. Among the β-classes are available the crystal structures of the CA isolated from red alga *Porphyridium purpureum*, from chloroplasts of *Pisum sativum*, and prokaryotic CAs isolated from *Escherichia coli* and the archaebacterium *Methanobacterium thermoautotrophicum* (Cronk J.D., *et al.* 2001; Strop P., *et al.* 2001).

1.5.3 γ-CAs

The first γ-class carbonic anhydrase identified was isolated from the methanogenic archaebacterium *Methanosarcina thermophila* and is indicated by the acronym "Cam" (Smith K.S. & Ferry J.G. 2000; Kisker C., *et al*. 1996; Iverson T.M.,

et al., 2000; Innocenti A., *et al*. 2004; Alber B.E. & Ferry J.G. 1994). Compared with the α-CA and β-CA, Cam has a number of characteristics that differentiate it from these. In particular, the monomer Cam self-assembles forming an active homo-trimer with an approximate molecular weight of 70 kDa (Figure 7).

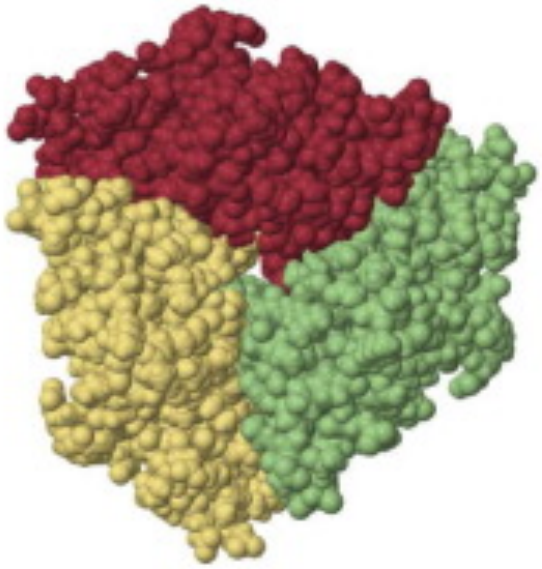

Figure 7. Tridimensional structure of γ-CA. The monomers are indicated in red, yellow and green colors.

The single monomers of the γ-CAs, with molecular weight of about 20 kDa, did not show catalytic activity. The active sites are localized at the interface between the monomers and the ion Zn(II) is coordinated by three histidine residues each coming from a monomer. γ-CA active site assumed a trigonal bi-pyramidal geometry in the Cam containing zinc ion, and an octahedral geometry in enzyme binding cobalt. The catalytic mechanism is similar to that proposed for the α-CA. At present, the mechanism zinc hydroxide, suggested for γ-CA is valid, but it is likely that in the active site of the enzyme may also be a balance between trigonal bi-pyramidal and tetrahedral metal ion species. The ligands in the active site of the enzyme are in contact with the side chain of the residue Glu62, which suggests that this side chain can be protonated. In Cam, which has zinc uncomplexed, the side chains of residues Glu62 and Glu84 seem to share a proton and the residue Glu84 can be in multiple conformations. This suggests that the residue Glu84 performs a function similar to that of residue His64 in α-CA (Supuran C.T. 2008).

1.5.4 δ- e ζ-CAs

Unlike δ-CAs, which are widely distributed throughout the marine phytoplankton, the ζ-CAs are present only in diatoms. Recently in the marine diatom *Thalassiosira weissflogii* have been identified two CA, TweCA (or TWCA1) and CDCA1, belonging respectively to classes δ and ζ (Alterio V., *et al*. 2012). TweCA is a 27 kDa protein, probably a monomer, which does not show significant sequence similarity with other carbonic anhydrases. It is an example of convergent evolution, even if the crystallographic studies show that the active site is similar to that of α-CA, with zinc ion coordinated by three histidine residues and one water molecule (Supuran C.T. 2008). The location of this enzyme in *T. weissflogii* and other diatoms it is not known, although recent studies suggest that TweCA has a cytoplasmic localization and catalyzes the reaction of dehydration of HCO_3^- to CO_2, increasing the concentration in the cytoplasm (Lee R.B.Y., *et al*. 2013).

CDCA1 is a protein belonging to the family of the ζ-CA, is composed of three identical subunits named R1, R2, and R3 that form an active enzyme of 69 kDa. CDCA1 contains in the catalytic site ion Cd(II), although it is able to operate even with the ion Zn(II) (Figure 8). The rapidity of the exchange between the metal ion Zn(II) ion and Cd(II) depends on the availability of the metal ions in the marine environment. In literature is reported the crystallographic structure of the three subunits that comprise it. (Xu Y., *et al*. 2008).

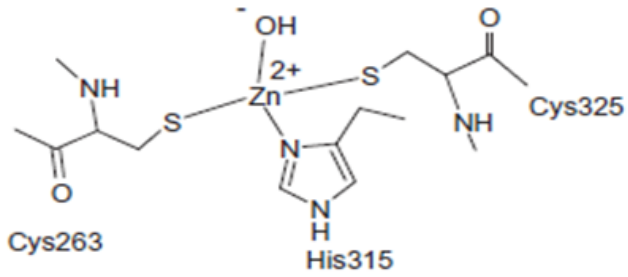

Figure 8. ζ-CA catalytic site. Ion Cd (II) can be replaced by Zn (II) without losing the catalytic activity (numbering of the R1 subunit of the enzyme of *T. weissflogii*).

In the subunit R2, the Cd(II) of the active site it is located in a pocket in the shape of funnel, coordinated by residues Cys263, His315, Cys325 and by a molecule of water. In the R1 subunit of CDCA1, the Cd(II) has coordination identical to the R2 subunit (Figure 8). Since all three subunits have sequence homology rather high, it is

possible that the coordination geometry of the metal ion is similar also for the subunit R3. Since *T. weissflogii* grows in a marine habitat characterized by zinc salts and cadmium, it was hypothesized that the carbonic anhydrase CDCA1 containing cadmium, replace the enzyme TweCA in the mechanism of carbon concentration, when the concentration of marine zinc is very low. The mechanism of carbon concentration has developed in many species of phytoplankton to compensate for the low availability of CO_2 present in the water. In fact, carbonic anhydrases have the function of increasing the CO_2 concentration in proximity of ribulose 1,5-bisphosphate carboxylase/oxygenase (RuBisCo), the primary enzyme involved in carbon fixation, by allowing the enzyme to work efficiently (Xu Y., *et al*. 2008). Therefore, the carbonic anhydrases are key enzymes regarding the acquisition of inorganic carbon for photosynthesis in the phytoplankton.

1.5.5 η-CAs.

The causative agent of human malaria, *Plasmodium falciparum*, was one of the first protozoa to be investigated for the presence of CAs. The open reading frame of the malarial CA enzyme encodes a 600 amino acid polypeptide chain. In 2004, Krungkrai and coworkers cloned a truncated form of *Plasmodium falciparum* CA gene (GenBank: AAN35994.2) encoding for an active CA (named PfCA1) with a primary structure of 235 amino acid residues (Krungkrai SR., *et al*, 2004). The metalloenzyme showed a good esterase activity with 4-nitrophenylacetate as a substrate. The authors observed that the highly conserved α-CA active site residues, responsible for binding of the substrate and for catalysis, were present also in PfCA1 and considered thus the Plasmodium enzyme belonging to the α-CA class (Figure 9).

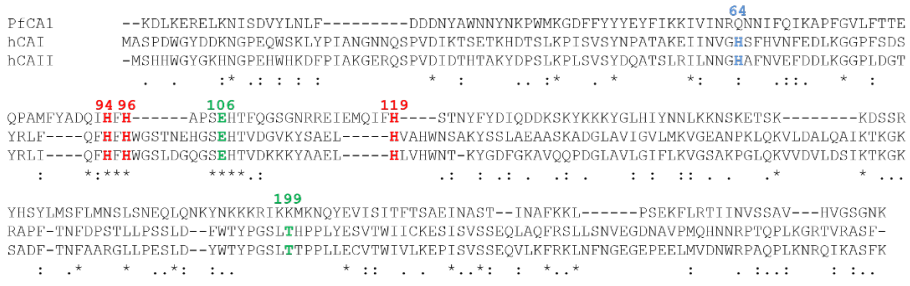

Figure 9. Multialignment of the amino acid sequence of the truncated form of the gene encoding for the PfCA1 with the amino acid sequences of the human isoforms (hCA I and II).

In the present thesis has been showed that *PfCA1* is a new CA-class, denominated with the Greek letter η-CA (Capasso C. & Supuran C.T., 2015). In fact, the alignment of the three-dimensional structures related to PfCA1 and several members of the α-CAs, allowed us to reveal the unique characteristics of the η-CA (De Simone G.*, et al.* 2015): the metal ion is coordinated by two histidine residues (His94, His96) and one residue of glutamine (Glu 119) as described in chapter 7.

1.5.6 θ-CAs, the last discovered class.

The θ-CA is a domain of the Cys-Gly-His–rich (CGHR) protein family (Sae Kikutania., *et al*., 2016)It has been recently targeted into the lumen of the pyrenoid-penetrating thylakoid of the marine diatom *Phaeodactylum tricornutum,* where it seems to play an essential function in photosynthesis, although its reported that CO_2 hydration activity seems to be very low. Probably, its main physiological function is to control the pH gradient across the thylakoid membrane and to supply CO_2 to the Calvin cycle (Sae Kikutania., *et al*., 2016). The detection of Zn in purified θ-CA strongly suggests that at least three residues of the highly conserved CGHR domain amino acid sequence are involved in Zn binding, such as Cys307, Asp309, His349, His363, and Cys387. On the basis of putative active-site amino acids, θ-CA is dissimilar to α- and δ-CAs and most similar to β- and ζ-CAs, which use cysteine, histidine, and sometimes aspartate to coordinate the metal ion. By contrast, the recombinant θ-CA exhibited esterase activity in addition to CA activity. Esterase activity is well known for α- and δ-CAs, thus, the biochemical properties of this θ-CA appear to be distinct from other known CAs.

1.6 Inhibitors

There are two main classes of CA inhibitors (CAIs). The first class comprises the inorganic anions complexing metals, the second class includes organic ligands represented by the sulfonamides and related bioisosteres (sulfamates, sulfamides, hydroxamate and xanthates). Both classes of inhibitors work by coordinating the metal ion in the active site of the enzyme or through a replacement mechanism, forming tetrahedral adducts, or by an addition mechanism, generating trigonal-bi-pyramidal adducts (Figure 10) (Supuran C.T. 2008) according the following single reactions:

A. $E\text{-}Zn^{2+} - OH_2 + I \Leftrightarrow E\text{-}Zn^{2+} - OH_2(I)$ (addition)
Trigonal-bi-pyramidal adduct

B. $E\text{-}Zn^{2+} - OH + I \Leftrightarrow E\text{-}Zn^{2+} - I + H_2O$ (substitution)
Tetrahedral adduct

Since the thirties of the last century, it was known that inorganic ions more effective in inhibiting the activity of CA were cyanate and thiocyanate ions (Meldrum N.U. & Roughton F.J. 1933). Generally, anion inhibitors bind to zinc for addition thereby generating the trigonal-bipyramidal adduct (Figure 10A). The inorganic inhibitors complexing metals find no application in therapy because of their poor selectivity as well as the resulting numerous side effects. Moreover, having a reduced size, it is very complicated, if not impossible, to perform an optimization of their structure (Supuran C.T. 2008).

The sulfonamides derivatives even in this case their activity has long been known. In 1948, Krebs was the first to recognize its inhibitory action on CAs (Krebs HA, 1948) and, as of that date, the CAI entering treatment were dozens, even if, for some of these, the activities anti-CAs was not known. (Dogne J.M., *et al*. 2006; Knudsen J.F., *et al.* 2004; Supuran C.T. 2008). The primary sulfonamides (R-SO2-NH2) are the classic inhibitors of CA and are used for the past half-century as diuretic and anti-glaucoma medications. Recently, they have also been found anticonvulsant, anti-obesity, anti-cancer, anti-infection and anti-panic properties, (Supuran C.T. *et al*. 2009; Winum J. *et al*. 2008; Domsic J.F., *et al*. 2008; Supuran C.T., *et al.* 2008; De Simone G. *et al.* 2008; Mincione F., *et al.* 2009; Krungkrai J. *et al.* 2008).

Figure 10. CAs inhibition mechanisms.

As discussed for the anions inhibitors, the mechanism of action of sulfonamides is based on the interaction of the inhibitor with the metal ion (Figure 10). In fact, the sulfonamide group, in contact with the acid environment of the catalytic site, loses a

proton and forms a dative bond with the Zn (II) by substitution of the hydroxide ion (Figure 10 B). The inhibitor-metal complex is stabilized by two hydrogen bonds between the sulfonamide group and the residue of Thr199 (Figure 11).

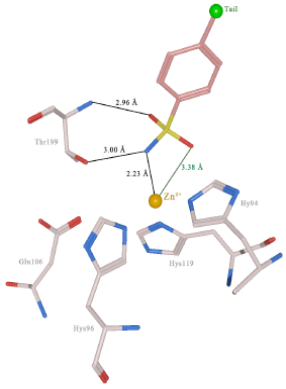

Figure 11. Binding of sulphonamidic CAI.

Some of CAI having significant inhibitory activity, such as sulfonamide derivatives used in clinical (acetazolamide, methazolamide, ethoxzolamide, dichlorophenamide, dorzolamide and brinzolamide) are able to form a second bond with the metal cofactor through one of the sulfonamide oxygen (Supuran C.T. 2008).

The difficulties and problems founded in designing new CAs inhibitors as therapeutical agents are mainly due to the large number of human isoforms (16 human CAs, 13 of which have catalytic activity), the widespread location of the CA in many tissues/organs as well the lack of selectivity of the currently available inhibitors.

For a long time, only primary sulfonamides and inorganic metal complexing anions were known to inhibit CAs, by coordinating to the metal ion from the enzyme active site. These inhibitors are those described above. But, today are known inhibitor classes with a different mechanism of action such as *a*) inhibitors anchoring to the nonprotein metal ion ligand, for example phenols, polyamines, hydrolyzed sulfocoumarins (i.e. sulfonic acids), some carboxylates, 2-thioxocoumarins; *b*) inhibitors occluding the active site entrance, an inhibition mechanism originally discovered for coumarins, which was then demonstrated to be similar to the CA activators (CAAs) binding mode; *c*) inhibitors which are out of the active site binding. This is the case of only one compound, an aromatic carboxylic acid derivative, found bound in an adjacent pocket to the active site entrance; d) inhibitors with an unknown binding mode, such as secondary/tertiary sulfonamide, protein tyrosine kinase inhibitors (e.g. imatinib/nilotinib).

1.7 Activators

Activators of the CAs (CAAs) unlike CAIs, who have been extensively studied and are used in the clinic for prevention and treatment of various diseases, still represent an almost entirely unexplored field. There is a multitude of compounds such as biogenic amines (histamine, serotonin, catecholamines), amino acids, oligopeptides and small proteins, that are capable of effectively activate many CA isoenzymes. Several CAA design studies considered as lead molecules histamine or carnosine (Temperini C., *et al.* 2006; Nishimori I., *et al.* 2007). Through the use of techniques, such us electron spectroscopy, X-ray crystallography and kinetics measurements that activators bind at the cavity of the active site, while CA inhibitors bind to metal core. CAAs participate in the displacement of the protons between the metal ion, bound to a water molecule, and the environment. This determines an increase of the hydroxylated forms of the metal, which corresponds to the catalytically active form of the enzyme (Clare B.W. & Supuran C.T. 1994). In the last few years, have been reported the crystal structures of adducts formed by human isoforms hCA, hCAII and their activators (Temperini C., *et al*. 2007) in addition to those of histamine, dating to 1997 (Briganti F., *et al*. 1997). CAAs participate in a network of hydrogen bonds and hydrophobic interactions with specific amino acid residues or water molecules present in the active site. This explains their different power and ways of interaction with the various isoenzymes.

Chapter 2. Carbonic anhydrases from pathogens as druggable enzymes

2.1 Pathogens

The microorganisms that normally do not cause disease in humans are in a state of commensalism or mutualism with the host (Roux O., *et al.* 2011; Joyce S.A., Watson R.J., Clarke D.J. 2006; Soto W., Punke E.B., Nishiguchi M.K. 2012). This non-harmful condition occurs when the immune system works well, but the same organisms can cause infection when the latter fails. All microorganisms that cause diseases or illnesses to their host are defined as pathogens (Cardoso T., *et al.* 2012).

Pathogens can be distinct into viruses, bacteria, fungi and protozoa. The pathogenicity of microorganisms is defined by the virulence, which is the ability of a pathogen to cause damage more or less severe in the host (Webb S.A. & Kahler C.M. 2008; Grosso-Becera M.V., *et al.* 2015). Genetic characteristics, biochemical and structural properties of the pathogen influence the pathogen virulence, which allows the microorganism to cause disease through a set of actions on the host (Cardoso T., *et al.* 2012). These actions may be its ability to evade and/or fight the immune system, to assimilate nutrients from the host or to perceive environmental changes. All these abilities implicate the action of numerous enzymes. Enzymes considered as virulence factors are generally active against host components and contribute to virulence by damaging host tissues (Schaller M., et al. 2005; Alp S. 2006; Bostanci N. and Belibasakis G.N. 2012; Cox G.M., Mukherjee J., Cole G.T., *et al*. 2000; Cox G.M., McDade H.C., Chen S.C., *et al.* 2001).

2.2 Bacterial CAs

Prokaryotes include several kinds of microorganisms, such as Archaea, bacteria and cyanobacteria (Tibayrenc M. & Ayala F.J. 2012). It has been demonstrated that CAs are enzymes encoded by the genome of many pathogenic organisms. Recently, CAs started to be investigated in detail in several pathogenic bacteria, in the search for antibiotics with a novel mechanism of action, since it has been demonstrated that in many bacteria, CAs are essential for the life cycle of the organism. As reported in Table I, bacteria encode for enzymes belonging to the α-, β-, and γ-CA classes (Vullo D., *et al*. 2014; Nishimori I., *et al*. 2014; Alafeefy A.M., *et al*. 2014; Vullo D., *et al*. 2013).

Table I. CAs from bacteria cloned and characterized so far, and their inhibition studies.

Bacterium	Family	Name	Inhibition studies	
			In vitro	In vivo
Neisseria gonorrhoeae	α	-	sulfonamides, anions	sulfonamides
Neisseria sicca	α	-	sulfonamides	sulfonamides
Helicobacter pylori	α	hpαCA	sulfonamides, anions	sulfonamides
Helicobacter pylori	β	hpβCA	sulfonamides, anions	sulfonamides
Escherichia coli	β	-	NI	NI
Haemophilus influenzae	β	HICA	bicarbonate	NI
Mycobacterium tuberculosis	β	mtCA 1	sulfonamides	sulfonamides, phenols
	β	mtCA 2	sulfonamides	sulfonamides, phenols
	β	mtCA 3	sulfonamides	sulfonamides, phenols
Brucella suis	β	bsCA 1	sulfonamides	sulfonamides
	β	bsCA 2	sulfonamides	sulfonamides
Streptococcus pneumoniae	β	PCA	sulfonamides, anions	NI
Salmonella enterica	β	stCA 1	sulfonamides, anions	NI
	β	stCA 2	sulfonamides, anions	NI
Vibrio cholerae	α	VchCA	sulfonamides, anions	NI
Sulfurihydrogenibium yellostonense	α	SspCA	sulfonamides, anions	NI
Sulfurihydrogenibium azorense	α	SazCA	sulfonamides, anions	NI

- means not named ; NA = no activity in vivo (presumably due to penetration problems); NI = not investigated ;

Thus, the α-CAs from *Neisseria spp*, *Helicobacter pylori* and *Vibrio cholerae* as well as the β-class enzymes from *Escherichia coli*, *Helicobacter pylori*, *Mycobacterium tuberculosis*, *Brucella spp.*, *Streptococcus pneumoniae*, *Salmonella enterica* and *Haemophilus influenzae* have been cloned and characterized in detail in the last few year. The *N. gonorrhoeae* α-CA has a molecular mass of 28 kDa, being rather homologous to mammalian CAs and showing high CO_2 hydratase activity (similar to the human isoforms hCA II) as well as esterase activity for the hydrolysis of p-NpA. Instead, the *H. pylori* α-CA displayed an activity similar to that of the human isoform hCA I for the CO_2 hydration reaction, being thus less efficient catalytically (see Table VI). (Cardoso T., *et al*. 2012; Cox G.M., *et al*. 2000; Cox G.M., *et al*. 2001; Bostanci N. & Belibasakis G.N. 2012; Alp S. 2006; Schaller M., *et al*. 2005;Tibayrenc M., & Ayala F.J. 2012;Roux O., *et al*. 2011; Joyce S.A., *et al*. 2006; Nishiguchi MK. 2012; Krungkrai S.R., *et al*. 2001; Sein K.K. & Aikawa M. 1998; Joseph P., *et al*. 2011; Supuran C.T. 2008).

2.3 Protozoan CAs

Malaria, a mosquito-borne disease of humans and other animal species, is caused by parasitic protozoa species belonging to the genus Plasmodium. Six different Plasmodium species infect humans: *Plasmodium falciparum*, *Plasmodium vivax*, *Plasmodium ovale*, *Plasmodium malariae* and the zoonotic *Plasmodium knowlesi.* Malaria parasites follow a complex lifecycle that involves an intermediate host such as humans and the definitive host, the mosquito vector. Following injection of sporozoite stage parasites from an infected female Anophelene mosquito into a human host, Plasmodium parasites move to the liver and invade hepatocytes where they replicate to form merozoites that are ultimately released into the blood circulation (Figure 12).

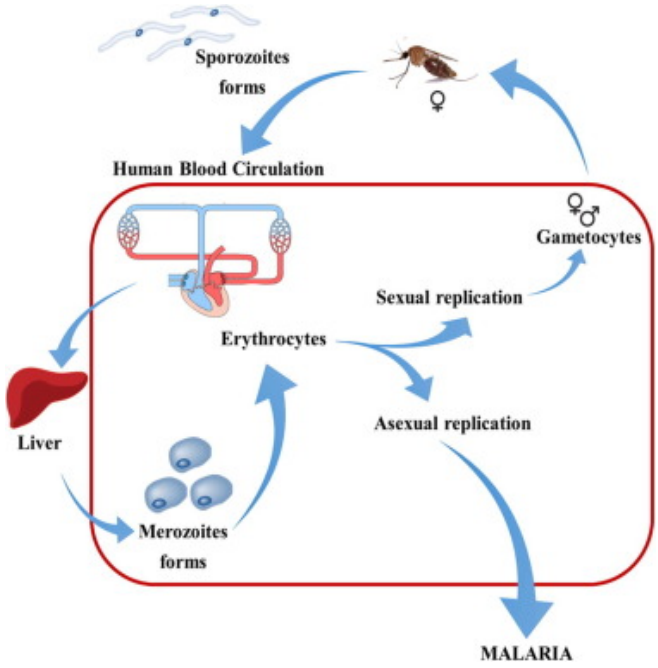

Figure 12. Life cycle of the malaria parasite.

Few protozoan parasites have been investigated for the presence and druggability of CAs. The malaria-provoking organism *Plasmodium falciparum* was undoubtedly the first one. Protozoa utilize purines and pyrimidines for DNA/RNA synthesis during its exponential growth and replication. Plasmodia synthesize pyrimidines de novo from HCO_3^-, adenosine-5'-triphosphate (ATP), glutamine (Gln), aspartate (Asp) and 5-phosphoribosyl-1-triphosphate (PRPP). HCO_3^- is the substrate

of the first enzyme involved in the Plasmodia pyrimidine pathway, which is generated from CO_2 through the action of CA (Figure 13).

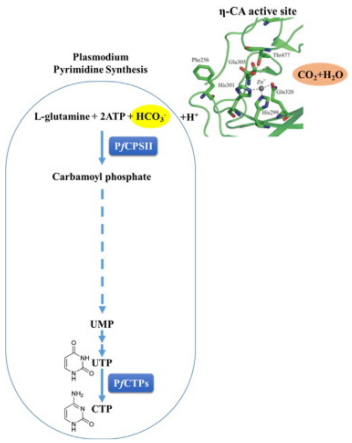

Figure 13. Scheme of the pyrimidine metabolism in *P. falciparum*. Legend: PfCPSII, P. falciparum carbamoyl phosphate synthetase II; PfCTPs, *P. falciparum* cytidine 5′-triphosphate synthase. HCO_3^- is generated from CO2 through the action of the η-CA.

Studies from Krungkrai's and our laboratories showed that *Plasmodium spp*. encode for several α-class CAs, and these enzymes have significant catalytic activity (as esterase with 4-nitrophenyl acetate as substrate) and are inhibited by primary sulfonamides, the main class of CAIs. The best investigated such enzyme has been denominated PfaCA1.

2.4 Fungal CAs

CAs are abundant in fungi and yeasts, but these enzymes have only recently started to be characterized and studied in detail. All known fungal CAs belong either to the α- or β-class (Elleuche & Pouggeler, 2009a). Fungal CA-encoding genes, like the CA multigene families in mammals, algae and plants, have diversified extensively during the evolution of fungi/yeast. The genomes of most filamentous ascomycetes contain three isoforms of β-class CAs and at least one α-class CA, whereas only β-class CAs have been identified in hemiascomycetous yeasts (Elleuche & Po¨ggeler, 2009a). Within the basidiomycetes, only *Cryptococcus neoformans* encodes two β-CAs, while the genome of *Coprinopsis cinerea*, *Laccaria bicolor*, *Malassezia globosa* and *Ustilago maydis* contains single β-CA genes (Elleuche & Po¨ggeler, 2009a). Interestingly, eight genes encoding putative α-CAs can be identified in the genome of *L. bicolor* (S. Po¨ggeler, unpublished). β-CAs have been functionally characterized in only a few fungal species. *Saccharomyces cerevisiae*, *Candida*

albicans and *Candida glabrata* each have only one β-CA, whereas multiple copies of β-CA- and α-CA-encoding genes were reported in other fungi. Recent work demonstrated that these CAs play an important role in the CO_2-sensing of the fungal pathogens and in the regulation of sexual development. In fact physiological concentrations of CO_2/HCO_3^- induce prominent virulence attributes in *C. albicans* (filamentation) and *C. glabrata* or *Cryptococcus neoformans* (capsule biosynthesis) through direct activation of the fungal adenylyl cyclase (Bahn et al., 2007; (Klengel et al., 2005). CO_2/HCO_3^- equilibration by fungal β-CAs equally plays thus a critical part in fungal CO_2 sensing and pathogenesis. For example, the *C. albicans* enzyme CaNce103 or the analogous *C. glabrata* one (CgNce103) are essential for pathogenesis of these fungi in niches where the available CO_2 is limited (e.g., the skin), or essential for the growth of *C. neoformans* in its natural environment (the enzyme from this last pathogen is denominated Can2) (Bahn et al., 2005; Go¨tz *et al*., 1999; Innocenti et al., 2009; Klengel *et al*., 2005). Thus, the link between cAMP signaling and CO_2/HCO_3^- sensing is conserved in fungi and revealed CO_2 sensing to be an important mediator of fungal metabolism and pathogenesis. The gene Nce103 is also present in the model organism *S. cerevisiae* (Cleves., *et al*., 1996). This protein is required to provide sufficient HCO_3^- for essential metabolic carboxylation reactions of the yeast metabolism, such as those catalyzed by pyruvate carboxylase, acetyl-CoA carboxylase, carbamoyl phosphate synthase and phosphoribosylaminoimidazole (AIR) carboxylase (Aguilera *et al.,* 2005b). Thus, this enzyme (called ScCA) has also been cloned and investigated in detail for its inhibition and activation with a range of modulators of activity. Interestingly, an additional putative cab-like β-CA has been identified in the pathogenic yeast *C. albicans* (XP_715817) and in *Pichia stipitis* (XP_001383682.1) (Elleuche & Po¨ggeler, 2009a). Recently, a multigene family of β-CAs was shown to influence the sexual development of the filamentous ascomycete *Sordaria macrospora* (Elleuche & Po¨ggeler, 2009b). CA activity from secreted CA isoforms has also been detected in various Penicillium isolates, and this activity is believed to be involved in limestone dissolution (Li *et al*., 2009). Finally, another yeast, which has been investigated in detail for the presence of CAs is Malassezia globosa, which produces dandruff. As the above-mentioned fungi/yeasts, it contains only one β-CA, denominated MgCA. Only for the Malassezia enzyme (MgCA) some in vivo studies have been performed, but not for the other fungal CAs.

Chapter 3. Scope of the thesis

Cloning the genomes of many pathogenic microorganisms offered the possibility of exploring alternative pathways for inhibiting virulence factors or proteins essential for their life cycle (Sainsbury P.D., *et al.* 2015). Using this approach, carbonic anhydrase has been identified in the genome of bacteria, fungi and protozoa, as a new class of enzymes related to microbial virulence (Capasso C. & Supuran C.T. 2013).

The aims of the present thesis are:

1. **Biochemical studies and inhibition profile of CAs encoded by the genome of two pathogenic bacteria, *Vibrio cholera* and *Porphyromonas gingivalis.***

Vibrio cholerae is the causative agent of cholera. The microorganism colonizes the upper small intestine where sodium bicarbonate is present at a high concentration. Vibrio cholerae genome encodes for three distinct classes: α-CA originated from the cah gene VC0395_0957, a β-CA derived from the gene VC0395_A 0118 and a γ-CA encoded by the gene VC0395_A2463. These CAs were designated as VchCA (α-CA), VchCAβ (β-CA) and VchCAγ (γ-CA). It has been demonstrated that sodium bicarbonate is an inducer of virulence gene expression in *Vibrio* (Cash R.A., *et al.* 1974). Since *V. cholerae* lacks of bicarbonate transporter proteins in its genome, it has been hypothesized that the pathogen utilizes the CAs system to accumulate bicarbonate into the cell to activate its virulence. It was investigated the inhibition profiles of VchCA, VchCAβ and VchCAγ in the presence of inorganic anions complexing metals and organic ligands represented by the sulfonamides and related bioisosteres (sulfamates, sulfamides, hydroxamate and xanthates).

Porphyromonas gingivalis is a pathogen, which colonizes the oral cavity and is involved in the pathogenesis of periodontitis, an inflammatory disease leading to tooth loss. The genome of *P. gingivalis* encodes for β- and a γ-CAs. It has been investigated their inhibition profile with a range of inorganic anions and organic ligands. The role of CAs as possible virulence factors of *P. gingivalis* is poorly understood at the moment but their good catalytic activity and the fact that they might be inhibited by a large number of compounds might pave the way for finding inhibitors with antibacterial activity that may elucidate these phenomena and lead to novel antibiotics

2. Biochemical characterization and inhibition studies of the carbonic anhydrase from *Plasmodium falciparum.*

Plasmodium falciparum is responsible for the most severe and life-threatening form of malaria. The antimalarial drugs represent a keystone of malaria control. Few protozoan parasites have been investigated for the presence and druggability of CAs and *P. falciparum* was one of the first protozoa to be investigated for the presence of CAs. The *P. falciparum* CA gene (accession number AAN35994.2) encodes a 600 amino acid polypeptide chain. In 2004, it was cloned a truncated form of this gene encoding for a polypeptide chain formed by the amino acid residues from position 211–445, named PfaCA1 and designed as a α-CA. Here, it has demonstrated that PfCA1 is not a α-CA but it belongs to the η-class, being however sensitive to sulfonamide inhibitors.

3. Cloning, expression and purification of the β-carbonic anhydrase from the pathogenic yeast *Malassezia globosa*.

The genome of the fungal parasite ***Malassezia globosa***, the causative agent of dandruff, contains a single gene encoding a CA belonging to the β-class (MgCA). Inhibition studies of these enzymes with anions and sulfonamides have been performed, which led to the detection of several inhibitors with high affinity. This study may help a better understanding of the inhibition profile of this enzyme and may offer the possibility to design new such modulators of activity belonging to different chemical classes

4. Protonography

It was set up a simple and inexpensive technique to assay CA activity on SDS-PAGE gels, named "protonography". By using protonography, the conversion of CO_2 into protons can be visualized as a yellow band on a polyacrylamide gel.

5. Phylogenetic analysis of the bacterial CAs

The complex distribution of the various CA classes in Gram-positive and negative bacteria allowed me to find a correlation between the evolutionary history of the bacteria and the three CA classes (α, β and γ) identified in their genome. In the present thesis was demonstrated that the ancestral CA is represented by the γ-CA, while the most evolute form of CA, among all the CA-classes, is the α-CA

Chapter 4. Materials and Methods

4.1 Identification and synthesis of the CA genes.

To determine the presence of carbonic anhydrases have been used similarity searching programs, such as BLAST and FASTA. As query sequences were used the amino acid sequences of CAs belonging to α-, β- or γ-class. The analysis performed on *Vibrio cholerae* genome identified three classes of carbonic anhydrase: the α-CA, indicated with the acronym VchCA; the β-CA, named VchCAβ; and the γ-CA, called VchCAγ. The computational search showed that the genome of *Porphyromonas gingivalis* encoded for β- and γ –CAs, named PgiCAb and PgiCA, respectively. The investigation of the *Malassezia globosa* genome produced as result the identification of a β-CA, named MgCA. In the case of the protozoan *Plasmodium falciparum*, the gene encoding for the η-CA (PfCA1) was kindly provided by Prof. Sally-Ann Poulsen Griffith University, Brisbane, Australia. The GeneArt Company (Invitrogen), specialized in gene synthesis, designed the synthetic genes encoding for VchCA, VchCAβ, VchCAγ, PgiCAb, PgiCA and MgCA. The single genes were inserted in a propagation vector (pMK-T). *Escherichia coli* competent cells (DH5α) were transformed with the aforementioned vector for the gene amplification and storage.

4.2 Bacterial strains used for plasmid propagation and heterologous protein expression.

4.2.1 E. coli DH5α

Competent Cells *Subcloning Efficiency* ™ *DH5α* ™ (Life Technologies) are generally used to propagate plasmids and have good processing efficiency. This strain carries a mutation that inactivates the endonuclease I (endA1) that could degrade the plasmid DNA during the extraction, and a mutation which inactivates the endonuclease EcoK I, but not the methylase activity (hsdR17 (RK, mk +). These cells lack the recombinase recA1 that is responsible for the recombination between the plasmid and the *E. coli* genome, making the plasmid more stable. They can also be used to blue/white screen for bacterial plates containing Blu-gal or X-Gal. More details on the genotype are shown in table II.

4.2.2 E. coli BL21(DE3)

E. coli BL21 host strain is the most used in standard applications of recombinant expression. *BL21-Gold (DE3)* (Agilent) is a robust strain of *E. coli*, able to grow vigorously in minimal media (Chart *et al*., 2000). This strain presents the Hte phenotype, which increases the efficiency of transformation of the cells. In addition, the strain lacks of proteases OmpT and Leon, which can degrade the recombinant protein intact; and of endonuclease (endA), which can degrade the plasmid DNA isolated from mini preparations. The table II shows other details of the cell genotype. The host strain lysogenized from the phage DE3 fragment, presents a copy of the bacteriophage T7 gene 1 integrated in the genome, which encodes the T7 RNA polymerase. Such gene is under the control of the promoter lacUV5 (derivative of the lac promoter) sensitive to the adjustment by the cAMP-CRP complex and inducible by isopropyl-β-D-1-tiogalattopiranoside (IPTG) (Studier & Moffat 1986). The T7 RNA polymerase drives the expression of the gene encoding for the recombinant protein.

4.2.3 E. coli ArcticExpress (DE3)

The strain of competent cells *ArcticExpress (DE3)* (Agilent) has the characteristics described above for the strain *BL21-Gold (DE3)* (Agilent). In addition, these cells are designed to deal with the problem of the insolubility of proteins, which may occur during the expression of the recombinant proteins. *Arctic Express (DE3)* cells, in fact, express proteins chaperone Cpn10 and Cpn60 of the psychrophilic bacterium *Oleispira antarctica*. These chaperonins have an amino acid identity with the chaperonins GroEL and GroES of *E. coli* by 74% and 54%, respectively, and show a good activity of protein folding at temperatures between 4 ° C and 20 ° C. These chaperonins, once expressed in cells ArcticExpress, optimize production of the heterologous protein at low temperatures and, presumably increase the amount of soluble and active recombinant protein produced. See table II for more details on the genotype.

Table II. Host strain genotype

Host strain	Genotype
BL21-(DE3)	*E. coli* B F^- *ompT hsdS*(r_B^- m_B^-) *dcm*$^+$ Tet^r *gal* λ(DE3) *endA* The
ArcticExpress (DE3)	*E. coli* B F^- *ompT hsdS*(r_B^- m_B^-) *dcm*$^+$ Tet^r *gal* λ(DE3) *endA* Hte [*cpn10 cpn60 Gent*^{r}]
Subcloning Efficiency™ DH5α™	F^- Φ80*lac*ZΔM15Δ(*lac*ZYA-*arg*F) U169 *rec*A1 *end*A1 *hsd*R17 (r_k^-, m_k^+) *pho*A *sup*E44 *thi*-1 *gyr*A96 *rel*A1 λ^-

4.3 Culture medium: LB (Luria-Bertani)

The culture medium LB (Luria-Bertani), nutritionally rich and designed for the growth of pure cultures of recombinant strains, is prepared by dissolving 20g of the prepared powder (LB BROTH, LENNOX-Laboratories Conda) per liter of distilled water and sterilized by autoclaving at 121°C for 20 minutes. Heat-labile substances, such as antibiotics and IPTG, are added after sterilization and filtered with Millipore Millex-GP filter (0,22μm) during the preparation.

4.4 Expression vector: pET15b (Novagen)

The expression vector pET-15b (5708 bp) is constituted by an origin of replication and the gene for β-lactamase, which confers resistance to the antibiotic ampicillin, in addition to the viral T7 promoter, a multiple cloning site (MCS) for the enzymes restriction most common and a sequence that encodes a tag of histidines. The recombinant protein is expressed with the tag of histidines at the N-terminal (Figure 14), which allows the rapid purification of the recombinant protein by affinity chromatography using a specific resin loaded with metal ions. Furthermore, in the vector a cutting sequence recognized by the enzyme thrombin allows removal of the fusion tag. The expression of the gene cloned into the vector is controlled by the T7 promote and recognized specifically by the T7 RNA polymerase of E. coli. Its expression is induced by 'isopropyl-β-D-1-tiogalattopiranoside (IPTG). Once the polymerase has reached a sufficient expression level, it binds to the promoter and initiates transcription.

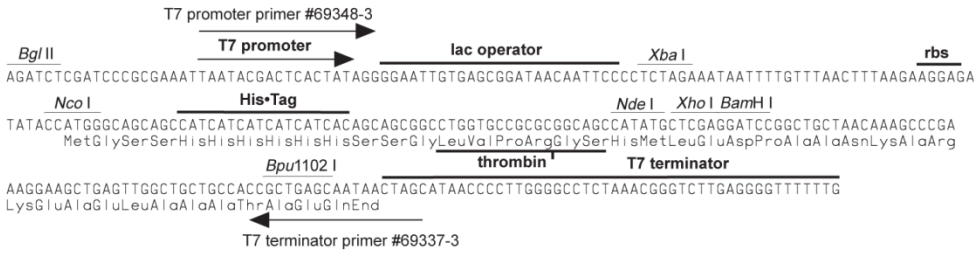

Figure 14. pET-15b Novagen cloning/expression region

4.5 Cloning procedure

4.5.1 Construct preparation

The CA gene encoding for the recombinant protein have been designed using the Life Technologies software. All the genes encoding for a α-CAs were devoid of the signal peptide (first twenty amino acid residues of the peptide sequence) and fused at the *N*-terminal with a tag of histidines essential for the subsequent purification of the protein. These genes were synthetized and inserted by Life Technologies in the plasmid pMK-T, containing cleavage sites for the restriction enzymes NdeI and XhoI at the 5 'end and 3' of the genes, respectively. Subsequently, it was shipped to the laboratory. The 5 µg of plasmid aforementioned in lyophilized form were resuspended in 15µl RNase free water. The concentration was determined using the NanoDrop ™ 1000 Spectrophotometer (Thermo Scientific). The DNA was stored at -20°C.

4.5.2 Plasmid DNA amplification into E. coli DH5α cells

The pMK-T cloning vector prepared as above was amplified using competent cells of *E. coli* DH5α. An aliquot of 50 µl of cells, stored at -80°C, was thawed on ice for 2-5 minutes and transformed with 100 ng of plasmid DNA. The cell suspension was mixed gently and placed on ice for 30 min. and then subjected to heat shock (42° C for 20 sec). After the addition of 950 µL of LB medium preheated, the mixture of transformation was incubated for 1 h at 37 ° C on a horizontal shaker

(CERTOMAT® BS-1), at a speed of 200 rpm. Then, a quantity ≥ 200 L of the mixture of transformation, were plated on solid medium (LB-Agar + kanamycin 50μg / ml) and the plates were incubated over-night at 37 ° C. To obtain higher quantities and a better purity of the plasmid DNA, it was set up a maxi preparation, for which a single bacterial colony was inoculated into 200 ml of LB containing ampicillin 100 mg/ml and made to grow at 37 ° C for 16 hours. The culture was then centrifuged at 5000x*g* for 5 minutes and the pellet treated using The PerfectPrep EndoFree ™ Plasmid Maxi Kit (5 PRIME), following the procedures described in the manual. Briefly, the plasmid DNA was then adsorbed on a column of silica gel and separated from RNA, proteins and other cellular components. The final elution was achieved with ribonuclease free water. The DNA was stored at -20°C.

4.5.3 Vector digestion

The expression vector pET-15b was digested with the restriction enzymes NdeI and XhoI (Biolabs, New England). The digestion of the plasmid DNA was carried out for 60 minutes at 37°C using 50 U of enzyme NdeI, and 50 U of XhoI enzyme in a reaction mixture containing 3 micrograms of BSA in Tris-HCl 6mM pH 7.5 containing 6 mM $MgCl_2$, 50 mM NaCl and 1 mM DTT. The reaction was conducted in a final volume of 30 μl. After digestion, the linearized plasmid was treated with 0.1 U of bovine alkaline phosphatase and incubated at 37°C for 30 minutes. The alkaline phosphatase determines the dephosphorylation of the linearized plasmid to prevent it can reclose on itself. The sample was then loaded on 1% agarose gels in TAE buffer (Tris-acetate-EDTA). The run was conducted using a horizontal electrophoresis apparatus for 40 minutes at 90V. As molecular weight marker was used a mixture of DNA fragments of known size (1 Kb Plus DNA Ladder ™ Thermo Fisher Scientific). Agarose gel was prepared adding ethidium bromide to a final concentration of 1μg/ml, to visualize the fragments of DNA by irradiation of the gel with ultraviolet light. The band corresponding to the linearized plasmid with NdeI and XhoI was excised from the gel and purified using Agarose GelExtract Mini Kit (5 Prime). The concentration of the purified plasmid was determined using the NanoDrop ™ 1000 Spectrophotometer (Thermo Scientific). Similarly, the pMK-T cloning vector, containing the genes coding for the CAs, was digested with the restriction enzymes NdeI and XhoI (Biolabs, New England). The band corresponding to the DNA encoding for CAs (VchCA or VchCAβ or VchCAγ, PgiCAb or PgiCA) was excised from the gel and purified using Agarose GelExtract Mini Kit (5

PRIME). The concentration of the purified fragment was determined by NanoDrop ™ 1000 Spectrophotometer (Thermo Scientific).

4.5.4 Ligation Reaction

50 ng of the fragment corresponding to the DNA encoding for CAs (VchCA or VchCAβ or VchCAγ, PgiCA, PgiCAb) was ligated into the expression vector pET-15b (100 ng). Constructs pET-15b/VchCA, pET-15b/VchCAβ and pET-15b/VchCAγ, pET-15b/PgiCA, pET-15b/PgiCAb were generated. The ligation reaction was carried out at 16 °C for 16 hours in the presence of 400 U of T4 DNA ligase supplied in 10 mM Tris-HCl, pH 7.4, 0.1 mM EDTA, 1 mM DTT, 200 mg / ml BSA and 50% glycerol, and 1X T4 DNA ligase buffer (50 mM Tris-HCl pH 7.5, 10 mM MgCl2, 10 mM DTT, 1 mM ATP, 25 mg / ml BSA) (New England BioLabs).

Three µL of the ligation reaction were used to transform XL10-Gold Ultracompetent cells (Stratagene) with high efficiency of transformation. The transformation was performed by thermal shock, and the cells plated on medium containing as ampicillin 100 µg/ml (pET-15b contain the gene for ampicillin resistance)

4.5.5 Clone identification

Ten colonies grown on LB-agar plate with ampicillin 100 µg/ml were analyzed to verify the presence of the gene encoding the CA of interest in the construct prepared as described above. For this purpose, the plasmid DNA was extracted from the colonies selected using the "The PerfectPrep EndoFree Plasmid Maxi" kit (5 PRIME) based on the method of lysis with alkali as described by Sambrook *et al.* 1992. Each bacterial colony was inoculated in 200 ml of LB containing ampicillin 100 µg/ml and grown at 37°C overnight. The cultures were then centrifuged at 6000xg for 5 min at 4°C and the resulting pellet suspended in Tris-HCl 10 mM pH 8.3. The bacterial suspension was lysed under alkaline conditions and the lysate neutralized in a buffer with a high salt concentration. The plasmid DNA was then adsorbed on a column of silica gel and separated from RNA, proteins and other cellular components. The final elution was achieved by water ribonuclease free. To verify that the gene encoding for VchCA or VchCAβ or VchCAγ or PgiCA or

PgiCAb was correctly inserted, the purified plasmid DNA (100 ng/μL) was sequenced using the PRIMM service.

4.5.6 Construct amplification

The amplification of the expression plasmid pET-15b containing the gene encoding for the CA of interest (VchCA or VchCAβ or VchCAγ or PgiCA or PgiCAb) was performed as described previously.

4.6 Expression of heterologous proteins in *E. coli* cells

4.6.1 Small-scale optimization

To optimize the conditions for the expression of recombinant proteins, growth was performed in a small scale. After the addition of IPTG, the production of proteins of interest was monitored at different times of incubation (2h, 4h, 6h, and overnight). Moreover, it has also been used different concentrations of IPTG (0.1 mm, 0.5 mm, 1 mM). Aliquots of samples were analyzed by SDS-PAGE.

4.6.2 Large-scale expression

For the heterologous expression of VchCA, VchCAβ, PgiCAb and PgiCA it has been used *E. coli* BL21 (DE3) cells; for the expression of VchCAγ and PfCA1 it has used ArcticExpress (DE3) cells and while for the expression of MgCA it has used *E. Coli* BL21 (DE3) Codon Plus. Competent expression cells were transformed using the thermal shock technique, which facilitates the passage of DNA through bacterial wall. Briefly, 50 μl of competent cells stored at -80°C, was thawed on ice for approximately 5 minutes. Then, the cells were incubated with for 10 minutes on ice in presence 1 μl of β-mercaptoethanol (1.42 M) and subsequently transformed with 100 ng of plasmid DNA. The cell suspension was mixed gently and placed on ice for 30 min. After the addition of 950 μL of LB medium preheated, the mixture of transformation was incubated (1 h at 37°C on a horizontal shaker at a speed of 200 rpm). Then, a quantity ≥ 200 L of the mixture of transformation, were plated on solid

medium (LB-Agar + Ampicillin, 100μg/ml) and the plates were incubated overnight at 37°C. Two-three bacterial colonies were inoculated into 100 ml of LB containing ampicillin and grow at 37°C for 16 hours. The culture was diluted 10 times with fresh LB medium containing ampicillin and incubated at 37°C and grown to the value of optical density at 600 nm of 0.6. Differently, ArcticExpress (DE3) and BL21 (DE3) Codon Plus cells were pre-incubated at 30 °C and once reached the 0.6 optical densities at 600 nm shifted to 20 °C. Then the cells transformed with the construct pET-15b/VchCA, pET-15b/VchCAβ, pET-15b/PgiCAb, pET-15b/PgiCA and pET-15b/MgCA were induced with 1 mM IPTG, while those transformed with the construct pET-15b/VchCAγ and pET-43.1a/PfCA1 were induced with IPTG 0.5 mM. After half an hour from the induction with IPTG, $ZnSO_4$ was added to the culture at a concentration of 0.5 mM. The metal ion was added because the zinc ion is essential for the catalytic activity and for the folding of the CA. Depending on the type of construct containing the CA of interest, after 4, 5, 6 or 20 hours cells were harvested by centrifugation at 6000xg for 30 minutes in Sorvall RC 6 Plus ™ (Thermo Scientific).

4.7 Purification and characterization of the recombinant CA

4.7.1 Affinity chromatography

Bacterial cells previously collected were suspended in 10 mM Tris-HCl pH 8.3 (Vf = 50 ml), lysed by sonication using a Branson Digital Sonifier using 15 cycles of 10sec with a 50 % of power. The sonicate was centrifuged at 10000x*g* for 45 minutes in Sorvall RC 6 Plus ™ (Thermo Scientific). All operations were performed at 4 °C. The supernatant was collected and purified by affinity chromatography on column HisTrapTM FF crude 1 ml (GE Healthcare Bio-sciences) connected to an AKTA FPLC system. The column resin (Chelatin SepharoseTM High Performance) is agarose linked to iminodiacetic acid, able to chelate metal ions such as Ni^{2+} ions capable of coordinating the imidazole groups of the His-tag of our proteins (Figure 15).

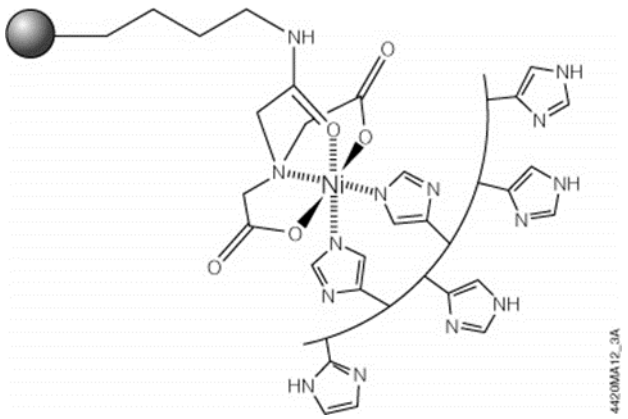

Figure 15. Schematic representation of His-Tag bounded to the beads of HisTrapTM FF column

The column was prepared by passing approximately 20 ml of Milli-Q H_2O (0.5 ml / min) and equilibrated with 10 column volumes of buffer A (20 mM imidazole, 20 mM phosphate buffer, 0.5 M NaCl pH 8 to a flow of 1 ml/min). Sample was loaded on the column at a constant flow of 1ml/min. Subsequently, washing was performed with 40 ml of buffer A. The protein, bound to the resin, was specifically eluted using an elution buffer (250 mM imidazole, 20 mM phosphate buffer, 0.5 M NaCl, pH 8) at a flow rate of 1 ml/min. Fraction were collected by recording the absorbance at 280 nm and dialyzed against 10 mM Tris-HCl, pH 8.3. Dialysis was performed at 4°C and using tubes with a cut-off of 12000 Daltons, in order to remove the high concentration of imidazole used for the elution. The dialyzed protein was collected and analyzed by SDS-PAGE.

4.7.2 SDS-PAGE analysis of protein fractions

The SDS-PAGE analysis of protein fractions obtained as described in the previous section was conducted according to the method described by Laemmli (1970). Each sample was dissolved in SDS Sample Buffer (62.5 mM Tris-HCl pH 6.8; 10% glycerol; 2% SDS; 10% β-mercaptoethanol; Bromophenol Blue 0.05%) and heated for 7 minutes at 100 °C to denature proteins. After this treatment, samples were subjected to vertical electrophoresis by loading 20 µl of each sample on a polyacrylamide gel at 12.5%. The electrophoretic run was performed on Mini-PROTEAN® Tetra Vertical Electrophoresis Cell (BioRad) at a constant voltage of

150 V for about an hour, using the running buffer 1X Tris-Glycine SDS buffer, pH 8.3 (250 mM Tris base, 192 mM glycine and 1% SDS). A molecular weight marker ranging from 10-250 kDa (Precision Plus Protein ™ Dual Color Standards, BioRad) was used as standard. The protein bands were visualized by soaking the gel in the Staining Solution (0.025% Coomassie R-250; 50% methanol; 10% acetic acid; Milli-Q H_2O to a volume of 1 L) and subsequently in destaining Solution (10% methanol; acid 10% acetic; Milli-Q H2O to a volume of 1 L). To calculate the molecular mass of the protein in question has been used the program Compute pI/Mw (Gasteiger et al., 2005), accessible from the server of Molecular Biology ExPASy.

4.7.3 Determination of protein concentration

The protein concentration was determined by the Bradford assay (Bio-Rad Laboratories, Hercules, USA) that is based on the color variation of an acidic solution of Coomassie Brilliant Blue G-250 (Bio-Rad mix, max of absorption at 465 nm) in presence of protein. The color change results in an increase in absorbance from 465 nm to 595 nm, which is proportional to protein concentration. The calibration curve was constructed using known amounts of bovine serum albumin (BSA). For each sample (20 µL) were added 200 µL of the coloring solution Quick Start Bradford Dye Reagent 1x (BioRad) and water to reach the final volume of 1 ml. The blank was prepared with 20 µl of the buffer used for harvesting the cells. The samples thus prepared were incubated 5 minutes at room temperature and read in a spectrophotometer at a wavelength of 595 nm. A three points calibration curve was prepared using known amounts of BSA. The sample unknown concentration was calculated using the first-degree equation determined from the BSA calibration curve.

4.7.4 Determination of the CA hydratase activity in solution

The CAs activity assay is a modification of the procedure described by Chirica (Chirica L.C., *et al.* 1997) and is based on monitoring the change in pH due to the catalytic conversion of CO_2 into bicarbonate. The indicator of the variation of pH is bromothymol blue (BTB) (Sigma-Aldrich). The assay was performed at 0°C in a final volume of 1 ml. The CO_2 saturated water was prepared by bubbling CO_2 into 100 mL of distilled water for about 3 h. To test the activity of the enzyme, 100 µL of 250 mM Tris-HCl pH 8.3 containing BTB (to give a distinct and visible blue color),

were placed in two tubes cooled in ice. Ten to 50 µl of enzyme solution (purified enzyme in 10 mM Tris-HCl pH 8.3) were added to a test tube and, an equivalent amount of buffer was added to the second tube as a control. Immediately have been added 500 µl of water saturated with CO_2 and 400 µl of Milli-Q water and simultaneously a stopwatch was started. The time taken for the color change of the solution from blue (alkaline pH) to yellow (acidic pH) was recorded (the range of color change is between pH 6.0 and pH 7.6). The production of H^+ during the reaction of hydration of CO_2 lowers the pH of the solution up to the transition point of the dye. The time required for the color change is inversely proportional to the quantity of CA present in the sample. Next, we have calculated the Wilbur-Anderson units (WAU). One WAU of activity is defined as: $(T_0 - T) / T$, where T_0 (reaction not catalyzed) and T (reaction catalyzed) represent the time (in seconds) necessary so that the pH falls from 8, 3 up to the transition point of the dye, in the control buffer, and in the sample in which is present enzyme respectively.

4.7.5 α-CA esterase activity assay

Differently from the other CA classes, the α-CAs are able to hydrolyze the ester p-nitrophenyl acetate (p-NpA) in p-nitrophenolate and acetate. The activity of hydrolysis of p-NpA was determined using a modification of the method proposed by Armstrong (Armstrong J.M., *et al.* 1966). The reaction mixture was composed as follows: 300 µl of p-NpA 3mM, 700 µl 15mm Tris Sulfate buffer at pH 7.6 and 10µl of enzyme. The hydrolysis of p-NpA was monitored by the increase of p-nitrophenolate, which was measured at 348nm for 5 minutes using a spectrophotometer Varian's Cary 50 (Agilent Technologies). The catalyzed reactions were corrected for the non-enzymatic reaction. One unit of enzyme was defined as the amount of enzyme capable of producing an $OD_{348nm} = 0.03$ in 5 minutes.

4.7.6 Protonography

It was set up a simple and inexpensive method, similar to zymography, which allowed the detection of CA activity on the polyacrylamide gel following the formation of H^+ ions produced by hydratase of CAs. The technique was called "protonography" (De Luca V., *et al.* 2015). Briefly, samples were run on SDS-PAGE at a concentration of about 4 µg per well. The commercial bovine CA (bCA) was used as a control. SDS-Page was carried out as described in the section "SDS-PAGE analysis of protein fractions", with the exception that the SDS sample buffer didn't

contain the β-mercaptoethanol and samples were not heated. Two SDS-PAGE gels were prepared: one was stained with Coomassie blue; the other was used to develop the protonogram. The last one was, in fact, treated with Triton X-100 at 2.5% and kept under stirring for one hour to remove the SDS. The gel was subjected to a washing step of 20 min with 100 mM Tris-HCl, pH 8.3, containing 10% isopropanol. It was washed two times for 10 minutes. Finally, the gel was incubated for 30 minutes at 4 °C under stirring with 0.1% bromothymol blue (BTB) in 100 mM Tris-HCl pH 8.3. BTB is a pH indicator. To detect the hydratase activity, the gel was immersed in distilled water saturated with CO_2 prepared by bubbling CO_2 into 200 mL of distilled water for about 3 h. The localized decrease of the pH value, due to the presence of the enzymatic activity of CAs, was detected through the formation of yellow band due to the change of color of the BTB from blue (alkaline pH) to yellow (acidic pH).

4.7.7 Thermoactivity

The temperature dependence activity of VchCA was determined using the p-NpA as substrate. The results were compared with that obtained for the bovine CA (bCA). In the assay were used 300 ng of protein. The reaction mixture was set up as described in the previous paragraph and the activity was measured at the temperatures ranging from 25 to 100°C.

4.7.8 Thermostability

The CA thermal stability was evaluated through experiments of thermal inactivation. The recombinant CAs were incubated at 25, 40, 50, 60, 70, 80, 90 and 100°C and aliquots were withdrawn at different times (30, 120 and 180min). Enzyme concentration was 3µg/mL in a buffer composed of Tris-HCl 10 mM, pH 8.3. The enzyme residual activity, expressed in percent of WAU, was measured at 0°C using CO_2 as a substrate. The results were compared with those obtained for a mesophilic enzyme (bCA)

4.7.9 Determination of the kinetic and inhibition constants

The kinetic and inhibition constants were obtained using the “stopped flow” apparatus. The apparatus (Applied Photophysics) is positioned in the laboratory

direct by Prof. Claudiu Supuran, where have been collected all the kinetic results. The apparatus is made up of two main components: the mixing chamber and the observation chamber. As pH indicator it has been used phenol red (0.2mM), which operates at a maximum absorbance of 557 nm with HEPES buffer (acid 4-2-hydroxyethyl-1-piperazinyl-ethanesulfonic acid, an organic substance used to maintain the stable pH) 10 mM at pH 7.5 (for the α-CAs) or 20 mM Tris (pH 8.3 for β- and γ- CA) and 0.1 M $NaClO_4$ (to maintain ionic strength constant) at 20°C. The reaction was followed for a period of 10-100 sec (the reaction is not catalyzed needs about 60-100 sec under the test conditions, while the reactions catalyzed need about 6-10 sec). For the determination of kinetic parameters and inhibition constants, the concentrations of CO_2 are comprised between 1.7 and 17 mM. Stock solutions of inhibitor (10-50 mM) were prepared in deionized-distilled water and then, with the Assay Buffer were made dilutions to 0.01 μM. The inhibitor and the enzyme solutions were pre-incubated for 15 minutes at room temperature before assay, in order to allow the formation of the E-I complex (enzyme-inhibitor) or to the possible hydrolysis of the inhibitor, mediated by the active site. The kinetic parameters were determined using the diagram Lineweaver-Burk plot (or diagram of the double reciprocal), while the inhibition constants were obtained by the method of nonlinear least squares using PRISM 3 and represent the average of at least three different determinations.

Chapter 5. *Vibrio cholerae* CAs

Bacteria can increase cytosolic levels of bicarbonate through the transporters of the bicarbonate or through the action of enzymes, the carbonic anhydrase (CA), which convert the CO_2 to bicarbonate or metabolic than atmospheric entry into the cells by simple diffusion (Smith K.S. & Ferry J.G. 2000). The analysis of the genome of *Vibrio cholerae* through the use of the program FASTA (Pearson W.R., 1994) has evidenced the absence of nucleotide sequences of the bicarbonate transport system similar to those identified in *S. elongates*. It was hypothesized that *V. cholerae* uses the enzymatic system of the carbonic anhydrase to accumulate bicarbonate inside the cell. (Del Prete S., *et al.* 2014). From the inspection of the *V. cholerae* genome, carried out using the BLAST program, it was found that the pathogen encoded for three classes of carbonic anhydrase: the α-class CA, encoded by the gene cah (VC0395_0957), indicated by the acronym VchCA; the β-CA derived from the gene VC0395_A 0118, indicated by the acronym VchCAβ and a γ-CA encoded by the gene VC0395_A2463, indicated with the acronym VchCAγ. In prokaryotes, the existence of genes encoding CAs from at least three classes (α-, β- and γ-class) suggests that these enzymes play an important role in the prokaryotic physiology.

5.1 VchCA

VchCA is a carbonic anhydrase belonging to α class and consists of 239 amino acid residues. The figure 16 shows the alignment of VchCA with human (isoform hCAI and II) and bacterial α-CAs (hpyCA identified in the bacterium *Helicobacter pylori*; NgonCA identified in *Neisseria gonorrhoeae*).

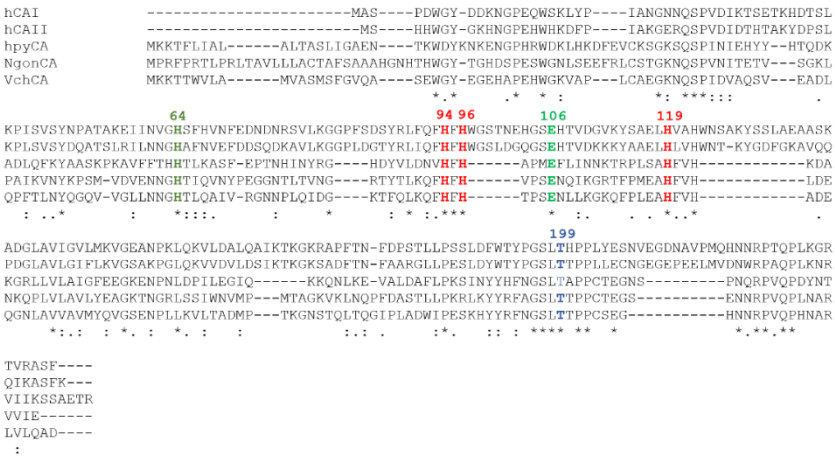

Figure 16. Multialignment of amino acid sequences of the α-CAs encoded by the genome of *Vibrio cholerae* and other sources (see text for details) performed with the ClustalW program, version 2.1. Numbering system of hCAI was used. It has been reported the proton shuttle residue (dark green) and the gate-keeping residues (Asp, light green; Thr, blue).Legend: hCAI, *Homo sapiens*, isoform I; hCA II, *Homo sapiens*, isoform II; hpyCA, *Helicobacter pylori*; NgonCA, *Neisseria gonorrhoeae*; VchCA, *Vibrio cholerae*.

VchCA shows an identity of about 30% with the two human isoforms and 40% with bacterial CAs. Moreover, VchCA conserved all the characteristics common to other α-CAs, for example the amino acid residues of the catalytic triad, the proton shuttle and the gate-keeping residues. (Figure 16).

5.2 VchCAβ

VchCAβ is a β-CA formed by a polypeptide chain of 222 amino acid residues showing an identity of 40%, when compared with the β-CAs from *Flaveria bidentis* (FbiCA) and *Pisum sativum* (PsaCA) and, 30% when compared with the bacterial β-CAs from *Porphyromonas gingivalis* (PgiCA) and *Brucella suis* (BsuCA). The catalytic triad of a β-CAs is perfectly conserved in all these enzymes (Figure 17). Moreover, VchCAβ showed all the characteristics of a classical β-CA: the two cysteines and one histidine amino, which are the amino acid residues responsible for the catalytic mechanism (Figure 17).

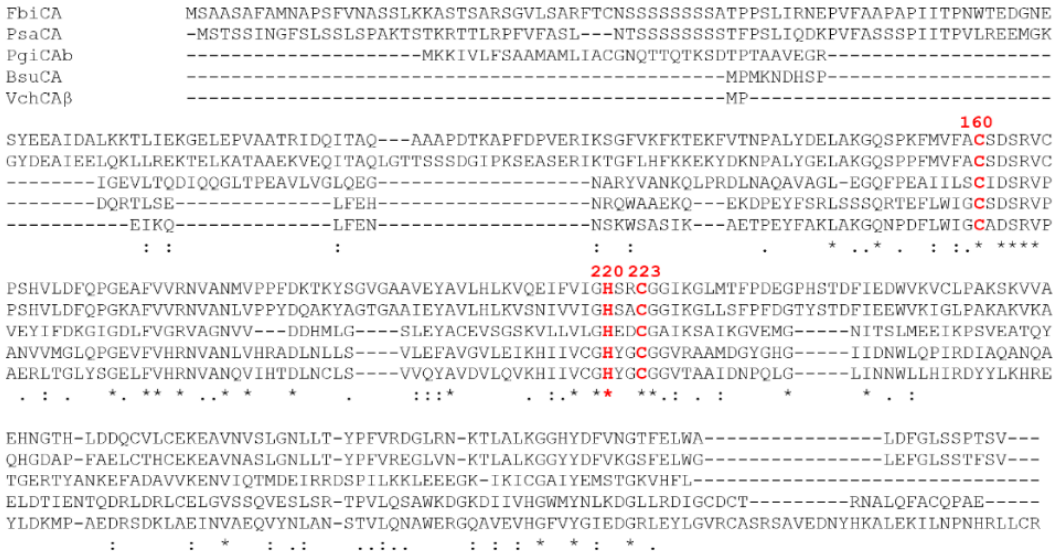

Figure 17. Multialignment of the amino acid sequences of the β-CA belonging to plants and bacteria, obtained with the ClustalW program, version 2.1. It was used the numbering system of *Pisum sativum*. The ligands of Zn(II) are shown in red. Legend: FbiCA, *Flaveria bidentis*, isoform I; PsaCA, *Pisum sativum*; PgiCAb, *Porphyromonas gingivalis*; BsuCA, *Brucella suis*; VchCAβ, *Vibrio cholerae*.

5.3 VchCAγ

VchCAγ is a CA belonging to γ class with a polypeptide chain of 184 amino acid residues. It shows an identity of 25-26% when compared with the two prototypes of the γ-CAs, CAM and CAMH, while presenting an identity of 38% when compared with PgiCA (γ-CA of *Porphyromonas gingivalis*). In figure 18 is shown the multialignment of VchCAγ with other bacterial γ-CAs identified in *Porphyromonas gingivalis* (PgiCA), *Clostridium perfringes* (CpeCA) and *Methanosarcina termophila* (CAMH and CAM). From figure 18 it is possible to see that VchCAγ retains the three histidines (His81, 117 and 122), responsible for the catalytic mechanism in all γ-CAs studied to date.

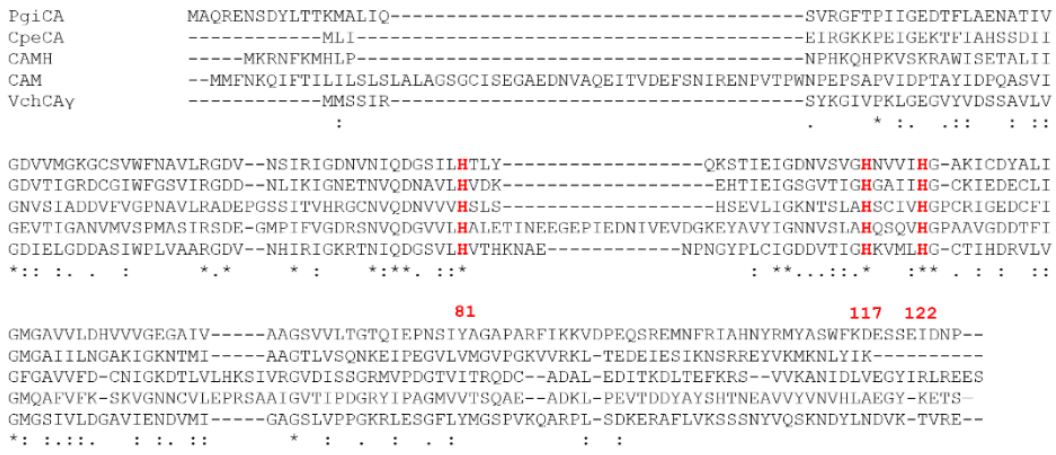

Figure 18. Multialignment of amino acid sequences of the γ-CA belonging to bacteria, achieved with the ClustalW program, version 2.1. It was used the numbering system of CAMH. The ligands of Zn (II) are shown in red. Legend: PgiCA, *Porphyromonas gingivalis*; CpeCA, *Clostridium perfringes*; CAMH, *Methanosarcina temophila*; CAM, *Methanosarcina temophila*; VchCAγ, *Vibrio cholerae*.

5.4 Cloning sequencing and production of expression vector

The three classes of CAs belonging to *V. cholerae* (VchCA, VchCAβ and VchCAγ) have been prepared using the DNA recombinant technology. The synthetic genes encoding for VchCA (657bp) or VchCAβ (669bp) or VchCAγ (552bp) were cloned into the expression vector pET-15b (see "Material and Methods")

5.5 Growing condition and recombinant protein production

Time course experiments were performed to optimize the protein expression. For this propose, bacterial cells were transformed with the appropriate expression vectors, grown in rich medium and, after induction with IPTG and metal addition, samples were collected at various time points as described in the experimental section. Compute pI/MW program calculated a theoretical molecular weight of 25 kDa for VchCA, of 29 kDa and 24 kDa for VchCAβ for VchCAγ. In this calculation was included also the His-Tag fragment. After the induction with IPTG, the SDS-PAGE showed that most of protein present in the soluble fraction was obtained after 5 hours for VchCA, 4 hours for VchCAβ and 6 hours for VchCAγ (data not shown).

Once defined the optimum growth conditions a bacterial culture of 2.0 L has been prepared by using the bacteria transformed with the construct of interest (pET-15b/VchCA, pET-15b/VchCAβ, pET-15b/VchCAγ). Protein expression was performed as described in the experimental section and the bacterial pellet was resuspended in Tris-HCl 10 mM, pH 8.3 and disrupted by sonication.

5.6 Purification

The bacterial extract obtained by sonication was purified by Nichel affinity chromatography as described in "Materials and Methods". The fractions containing the protein of interest were dialyzed against 10 mM Tris-HCl pH 8.3. The yield of the protein at the end of the purification process was 30 mg for VchCA and VchCAβ, while VchCAγ was recovered with a yield of about 0.7 mg. The recombinant proteins were analyzed by SDS-PAGE as shown in Figure 19.

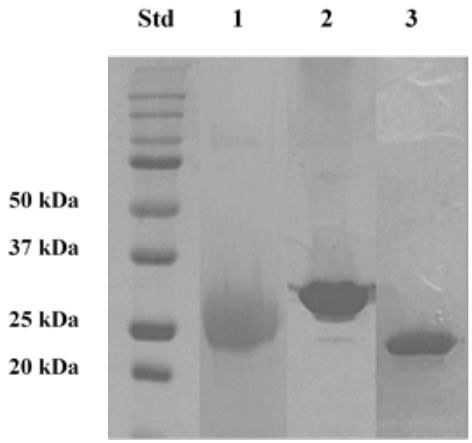

Figure 19. SDS-PAGE after affinity chromatography. Std: standards; 1: VchCA; 2: VchCAβ; 3: VchCAγ.

5.7 Biochemical characterization

5.7.1 Specific Activity

The Vibrio CAs produced as described above were assayed in solution using CO_2 as a substrate and following the procedure described by Chirica *et al.* Enzyme activity was expressed as Wilbur-Anderson units (WAU). Table III shows specific

activities of VchCA, VchCAβ and VchCAγ compared with those obtained for the bovine enzyme bCA (α-CA). The specific activity of VchCA is 5.4 times higher than the commercial bovine enzyme (bCA), 16 times greater than that calculated for VchCAβ and 8 times that of VchCAγ. The results obtained demonstrate that the VchCA (α-CA) was the most active. Interestingly VchCAγ, is more active than VchCAβ (respectively the γ-class and β-class CAs founded in *V. cholerae* genome). Generally, γ-CA are reported to be less active than β-CAs

Table III. Specific activity of the three classes of CAs identified in the genome of *V. cholerae* and of bovine α-CA.

	Class	**Specific activity** (WAU/mg protein)
VchCA	α	26232
VchCAβ	β	1600
VchCAγ	γ	3200
bCA	α	4845

As described in literature α-class CAs, in addition to the hydration reaction of CO_2, catalyze such as secondary reaction the reversible reaction of hydrolysis of esters. The esterase activity of VchCA, identified in the genome of *V. cholerae*, was determined using as substrate the p-NpA. VchCA presents a very low esterase activity (19 U/mg) compared with that of the commercial bCA (Table IV).

Table IV. Esterase activity of VchCA and bCA.

	Class	**Specific activity** (WAU/mg protein)
VchCA	α	19
bCA	α	1100

5.7.2 Kinetic constants

In Table V are shown the rate constants ($k_{cat,}$ K_M and k_{cat}/K_M) of the three classes of CA identified in the genome of *V. cholerae* and the inhibition constant (K_I) using the inhibitor acetazolamide. These constants were compared with the kinetic parameters of other CAs belonging to α-, β- and γ-classes identified in different organisms and microorganisms.

Table V. Determination of the kinetic constants for the hydratase reaction catalyzed by CAs identified in the genome of *V. cholerae.* The results were compared with those obtained for CAs identified in other organisms. The inhibition constant (K_I) was obtained for the classical sulfonamide inhibitor, acetazolamide.

Class	CA acronym	Species	k_{cat} (s^{-1})	K_M (M)	k_{cat}/K_m (M^{-1} s^{-1})	K_I (nM) (acetazolamide)
α	hCA I	*Homo sapiens*	2.00×10^5	4.0×10^{-3}	5.0×10^7	250
	hCA II	*Homo sapiens*	1.40×10^6	9.3×10^{-3}	1.5×10^8	12
	hpαCA	*Helicobacter pylori*	2.5×10^5	16.6×10^{-3}	1.5×10^7	21
	SazCA	*Sulfurihydrogenibium yellostonense*	4.40×10^6	12.5×10^{-3}	3.5×10^8	0.90
	SspCA	*Sulfurihydrogenibium azorense*	9.35×10^5	85×10^{-3}	1.1×10^8	4.5
	VchCA	***Vibrio cholerae***	$\mathbf{8.23 \times 10^5}$	$\mathbf{11.7 \times 10^{-3}}$	$\mathbf{7.0 \times 10^7}$	**6.8**
β	FbiCA1	*Flaveria bidentis*	1.2×10^5	1.6×10^{-3}	7.5×10^6	27
	BsuCA219	*Brucella suis*	6.4×10^5	16.4×10^{-3}	3.9×10^7	63
	BsuCA213	*Brucella suis*	1.1×10^6	1.2×10^{-3}	8.9×10^7	303
	PgiCAb	*Porphyromonas gingivalis*	2.8×10^7	18.6×10^{-3}	1.5×10^7	214
	hpβCA	*Helicobacter pylori*	7.1×10^5	14.7×10^{-3}	4.8×10^7	40
	VchCAβ	***Vibrio cholerae***	$\mathbf{3.34 \times 10^5}$	$\mathbf{8.1 \times 10^{-3}}$	$\mathbf{4.1 \times 10^7}$	**451**
γ	PgiCA	*Porphyromonas gingivalis*	4.1×10^5	7.5×10^{-3}	5.4×10^7	324
	CAM	*Methanosarcina thermophila*	6.1×10^4	7.0×10^{-3}	8.7×10^5	63
	VchCAγ	***Vibrio cholerae***	$\mathbf{7.39 \times 10^5}$	$\mathbf{11.5 \times 10^{-3}}$	$\mathbf{6.4 \times 10^7}$	**473**

VchCA showed a k_{cat} of 8.23×10^5 s^{-1}, a K_M of 11.7 mM and a k_{cat}/K_M of 7.0×10^7 M^{-1} s^{-1}. VchCA was more active of the human isoform hCAI ($k_{cat} = 2.0 \times 10^5$ s^{-1}) and hpαCA ($k_{cat} = 2.5 \times 10^5 s^{-1}$), it has an activity of an order of magnitude lower than hCA II and SazCA, an extremophilic CA from the genome of *Sulfurihydrogenibium azorense*. Furthermore, VchCA was inhibited by acetazolamide ($K_I = 6.8$ nM) better than the hCA II and hpαCA.

VchCAβ had a k_{cat} of $3.34 \times 10^5 s^{-1}$ and a K_M of $8.1 \times 10^{-3} s^{-1}$and a catalytic efficiency of 4.1×10^7 M^{-1} s^{-1}. The enzyme showed a k_{cat} similar to that of the enzyme identified in plant (FbiCA1) and its catalytic efficiency is very similar to that of other bacterial enzymes, but it was two orders of magnitude lower compared to the β-class enzyme identified in the bacterium *Porphyromonas gingivalis* (PgiCAβ*)*. In addition, acetazolamide was found to be a less effective inhibitor for VchCAβ than VchCA, showing an inhibition constant of 451 nM (Table V).

VchCAγ showed a k_{cat} of $7.39 \times 10^5 s^{-1}$, an order of magnitude higher than that of γ-CA (CAM) identified in the thermophilic Archeon *Metanosarcina thermophila* and, slightly higher than the k_{cat} of the bacterial γ-CA PgiCA. Interestingly, VchCAγ resulted more active than VchCAβ, while the acetazolamide shows an inhibition constant of 473 nM.

5.7.3 Thermoactivity and Thermostability

Thermoactivity was only determined for VchCA because this is the unique class of CA (α-CA) that possesses an esterase activity. The results were compared with

those obtained for the bovine enzyme, bCA. In Figure 20 is shown that VchCA activity is shifted of 10 degrees respect to that of the mammalian enzyme. bCA, in fact, showed a maximum peak of enzyme activity at 60 °C, while for VchCA this peak was at 70 °C (Figure 20).

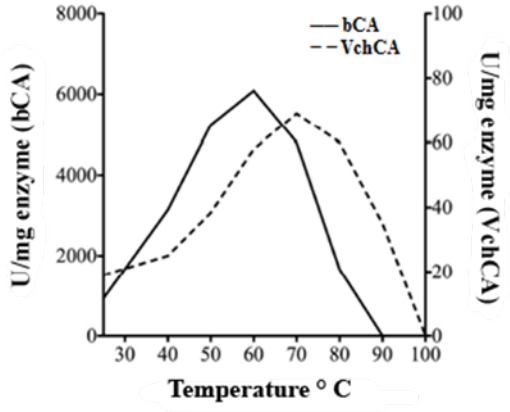

Figure 20. Comparison of the thermoactivity of VchCA and bCA. The enzyme activity was measured at the indicated temperatures on the x-axis using the p-NpA as a substrate. Each point is the mean ± SEM of three independent determinations

This variation may be due to the fact that the enzyme of *Vibrio cholerae* is characterized by an amino acid sequence shorter than bCA, which probably confers stability to the bacterial enzyme.

Thermostability of VchCA, VchCAβ, VchCAγ and bCA were investigated incubating each enzyme at 30, 40, 50, 60, 70, 80 and 90 °C. After 30 and 120 minutes of incubation, an aliquot of each enzyme was taken and assayed using CO_2 as a substrate. Figure 21 showed that after 30 minutes of incubation the activity of the bovine enzyme (bCA) decreases faster than that of VchCA. In fact, at 80 °C the residual activity for VchCA is 40%, while for bCA is 0. VchCAγ and VchCAβ have a behavior very similar to the bovine enzyme (Figure 21). After 120 minutes of incubation, bCA and VchCAβ are inactive at temperatures higher than 60 °C, VchCAγ is inactivated at 70 °C, while VchCA is completely inactive at 80 °C. These results demonstrated that VchCA is more stable respect to the β and γ-CAs identified in the genome of *Vibrio cholerae*.

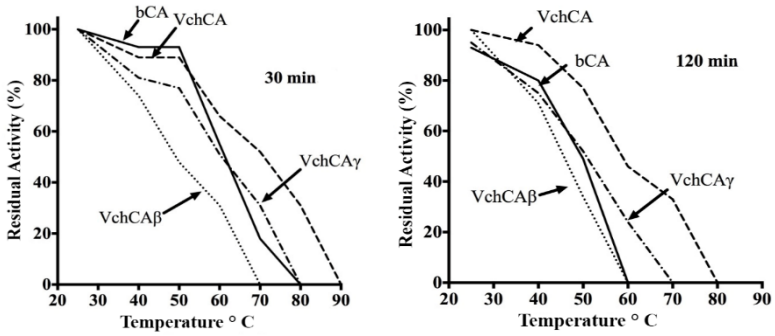

Figure 21. Thermostability of VchCA, VchCAβ, VchCAγ and bCA. The enzymes were incubated for 30 to 120 minutes at the indicated temperatures on the x-axis and assayed using CO_2 as a substrate. Each point is the mean ± SEM of three independent determinations.

5.7.4 Protonography

The activity of proteolytic enzymes, capable of refold and acquire the proteolytic activity after treatment with SDS, can be determined by SDS-PAGE after the removal of the detergent. Such a technique is known with the name of zymography. It has developed a technique to identify the activity of CA hydratase on SDS-PAGE (see Materials and Methods), we named this technique protonography, because during the CO_2 hydratase reaction are produced protons, which are then responsible of the change of color that appears on the gel, in correspondence of the CA (see Material and Methods). In figure 22 are reported the protonograms obtained using the commercial bovine bCA (α-CA class) and the recombinant CAs (α, β and γ) from *V. cholerae*. Protonograms of VchCA, VchCAβ and VchCAγ showed the different behavior that the three bacterial CAs assumed during the SDS-PAGE. It is known that mammal α-CAs are monomeric and the protonogram of bCA showed a single band of activity corresponding to a monomer of 30 kDa (Figure 22 A). The bacterial α-CAs are generally dimeric enzymes and the protonogram showed three bands of activity: a monomer (25 kDa), a dimer (50 kDa) and a tetramer (100 kDa) (Figure 22 A). Therefore, unlike bCA, VchCA is present in three different oligomeric states. The protonogram of VchCAβ (Figure 22 B) showed two bands of activity: a band corresponding to the monomeric form (29 kDa) and one at the dimeric form (58 kDa). The protonogram of VchCAγ showed a band of activity in correspondence of the monomer (24 kDa) and the trimer (69 kDa) (Figure 22 C). The yellow bands found in correspondence of the inactive monomeric form of VchCAβ or VchCAγ, is due to the fact that at the end of the electrophoretic run, the SDS is removed from the gel. This procedure may lead to the rearrangement of β- or γ-CA monomers in the

gel and the final result is the reconstitution of the active dimeric (β -CA) or trimeric forms (γ -CA). Protonography allowed us to distinguish not only the active enzyme, but also oligomeric states of the CA.

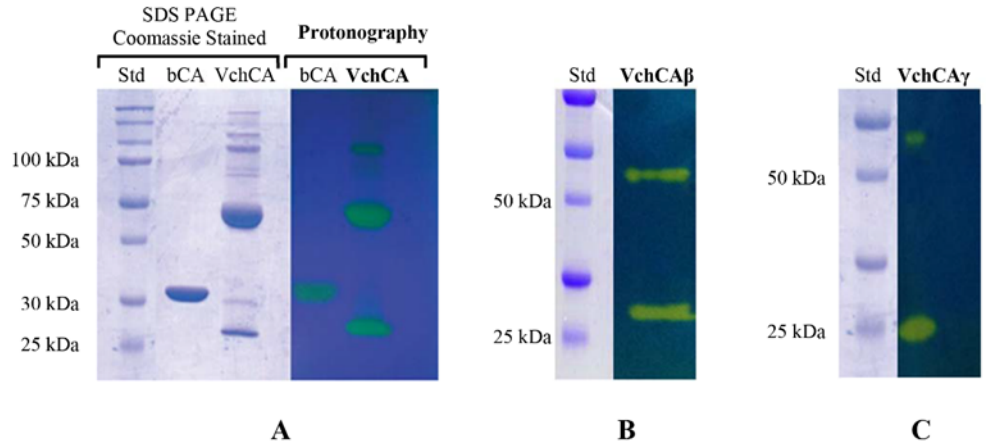

Figure 22. A: protonogram and SDS-PAGE stained with Coomassie compared. Both Gels were run in non-reducing denaturing conditions and loaded with 4 micrograms of bCA and VchCA. The appearance of the band occurred after 5 seconds of incubation in CO_2 saturated water. **B**: protonogram of VchCAβ with a molecular weight marker (Coomassie gel not shown). The band appeared after 40 seconds of incubation in CO_2 saturated water. **C**: protonogram of VchCAγ with a molecular weight marker (Coomassie gel not shown). The band appeared after 25 seconds of incubation in CO_2 saturated water.

5.8 Inibition

5.8.1 Sulfonamides and the bioisosteres

In collaboration with Prof. C. Supuran, University of Florence, a large number of sulfonamides and sulfamates were tested to evaluate their effectiveness on the inhibition of *V. cholerae* CA.

Simple aromatic and heteroaromatic sulfonamides of types **1-24** were among them, as well as derivatives **AAZ-IND**, which are clinically used drugs or agents in clinical development (Figure 34). Acetazolamide **AAZ**, methazolamide **MZA**, ethoxzolamide **EZA** and dichlorophenamide **DCP**, are the classical, systemically acting CAIs. Dorzolamide **DZA** and brinzolamide **BRZ** are topically-acting antiglaucoma agents, benzolamide **BZA** is an orphan drug belonging to this class of pharmacological agents, whereas topiramate **TPM** and zonisamide **ZNS** are widely used antiepileptic drugs. Sulpiride **SLP** and indisulam **IND** were recently shown by this group to belong to this class of pharmacological agents. Sulfonamides **1-24** and

the clinically used agents investigated in this study were either commercially available, or were prepared as reported earlier by our group (Figure 23).

The study of inhibition profiles has the aim to identify the existence of selective inhibitors for the CA identified in the genome of *V. cholerae*. Some of these compounds are excellent inhibitors of bacterial enzymes (Table VI). These results will be of great assistance for the realization of new inhibitors characterized by a high selectivity towards the bacterial CAs.

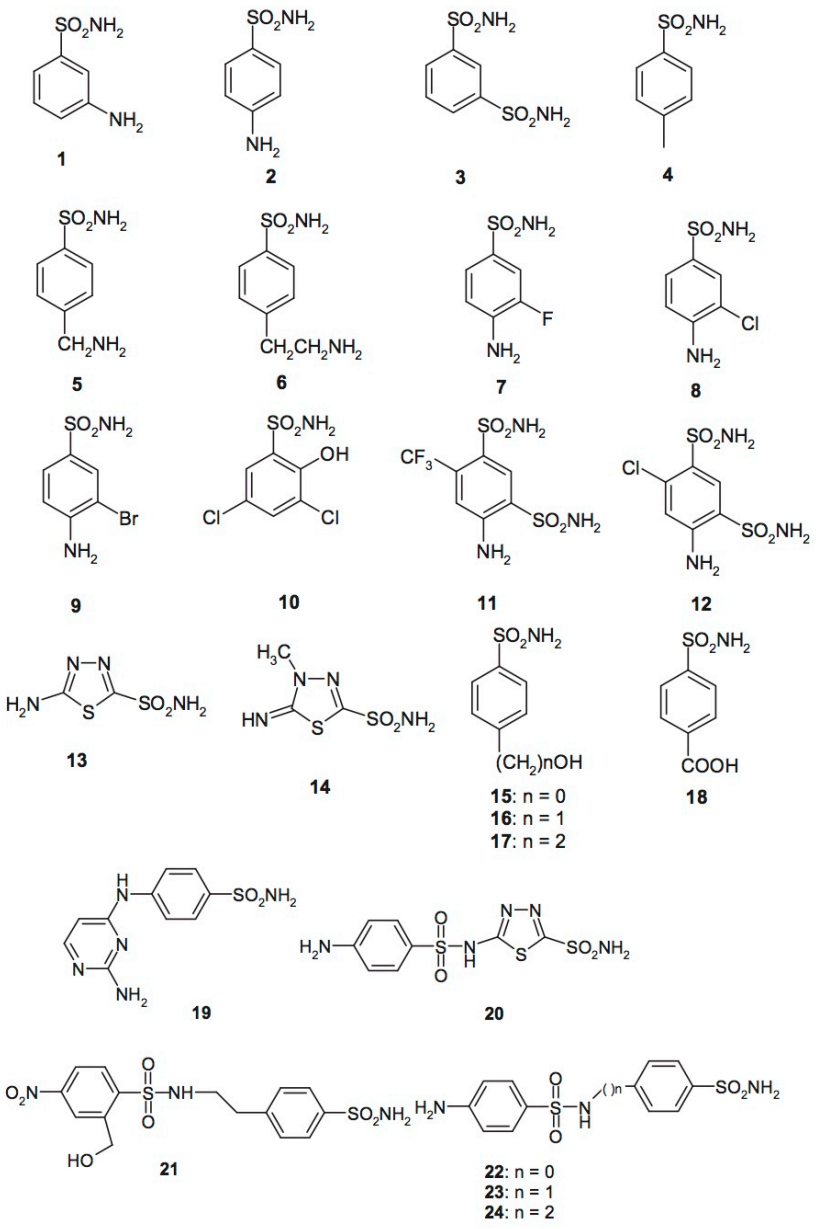

Figure 23. Sulfonamides and bioisosteres inhibitors structures

Table VI. Sulfonamides and bioisosteres inhibition constants for the human α-CA isoform I and II, the α-CA of *H. pylori* (hpαCA) and the three classes of CA identified in the genome of *V. cholerae*, obtained with the technique of "stopped flow" at 20 ° C and pH 7.5.

	K_Is* (nM)				
Inhibitor	hCA I	hCA II	VchCA	VchβCA	VchγCA
1	45,400	295	440	463	672
2	25,000	240	471	447	95.3
3	28,000	300	125	785	93.6
4	78,500	320	219	>10,000	76.3
5	25,000	170	447	>10,000	80.6
6	21,000	160	402	>10,000	69.0
7	8300	60	199	>10,000	73.6
8	9800	110	139	9120	73.6
9	6500	40	133	>10,000	95.3
10	6000	70	99.1	>10,000	544
11	5800	63	62.9	879	87.1
12	8400	75	45.3	4450	563
13	8600	60	23.5	68.1	66.2
14	9300	19	12.1	82.3	69.9
15	6	2	4.2	349	88.5
16	164	46	42.7	304	556
17	185	50	30.3	3530	6223
18	109	33	59.8	515	5100
19	95	30	4.7	2218	4153
20	690	12	0.59	859	5570
21	55	80	54.5	4430	764
22	21,000	125	56.7	757	902
23	23,000	133	71.5	817	273
24	24,000	125	52.1	361	73.3
AAZ	250	12	6.8	4512	473
MZA	50	14	3.6	6260	494
EZA	25	8	0.69	6450	85.1
DCP	1200	38	37.1	2352	1230
DZA	50,000	9	6.3	4728	87.3
BRZ	45,000	3	2.5	845	93.0
BZA	15	9	4.2	846	77.6
TPM	250	10	>1000	874	68.8
ZNS	56	35	982	8570	725
SLP	1200	40	>1000	6245	77.9
IND	31	15	8.1	7700	91.3
VLX	54,000	43	89.7	8200	817
CLX	50,000	21	>1000	4165	834
SLT	374	9	88.4	455	464
SAC	18,540	5959	>1000	275	550
HCT	328	290	79.5	87.0	500

* Mean from 3 different assays. Errors in the range of ±10% of the reported values (data not shown).

Table VI showed inhibition data for this panel of sulfonamides (and one sulfamate, TPM) against the human α-CAs (isoforms hCAI and hCAII) and the recombinant α, β and γ CAs from *Vibrio cholera*. The following should be noted regarding a comparison of *V. cholerae* enzymes inhibition with the compounds investigated in this study: Topiramate **TPM**, a sulfamate, sulpiride **SLP**, a primary sulfonamide, as well as saccharin **SAC**, an acylsulfonamide, were ineffective VchCA inhibitors (K_{Is}>1000 nM). Moreover, **SAC** was a bad inhibitor for VchCAβ and VchCAγ, while **TPM** and **SLP** were effective inhibitors of VchCAγ. These compounds (except saccharin) generally act as good inhibitors of other bacterial or mammalian α-CAs. Zonisamide, **ZNS**, an aliphatic primary sulfonamide was also a very weak inhibitor for the bacterial enzymes but effective towards the human enzymes (K_Is ≥725 nM). A large number of simple aromatic sulfonamides, such as derivatives **1-9**, showed moderate VchCA and VchCAγ inhibitory properties, with inhibition constants in the range of 125 – 672 nM (Table VI). It may be observed that all these derivatives are benzenesulfonamides with one or two simple substituents in *ortho-, para-* or the 3,4-positions of the aromatic ring with respect to the sulfamoyl zinc-binding moiety. Most of these CAIs were ineffective towards VchCAβ with K_Is ≥ 9120 nM. Most of the sulfonamides investigated here showed a potent inhibitory effect against VchCA, VchCAβ and VchCAγ with inhibition constants in the range of 23.5 – 88.5 nM. These derivatives include compounds **13-15**. It is interesting to note that compounds **10-13**, **16-18**, **21-24**, **DCP**, **VLX**, **SLT** and **HCT** showed a potent inhibitory effect against VchCA. Some of them are effective towards VchCAβ or VchCAγ but never effective for all the three classes identified in the genome of *V. cholerae* (Table VI). Several very potent VchCA inhibitors were detected, such as compounds **14**, **15**, **19**, **20**, **AAZ**, **MZA**, **EZA**, **DZA**, **BRZ**, **BZA**, and **IND**, which showed K_{Is} in the range of 0.59 – 12.1 nM (Table VI). Most of the sulfonamides used were effective inhibitors of VchCAγ but the K_{Is} was always ≥ 69 nM. The inhibition profile of VchCA, VchCAβ or VchCAγ was different from that of the other bacterial or mammalian CAs investigated up until now, proving that probably it will be possible to design VchCA-,VchCAβ- or VchCAγ-selective inhibitors using the scaffold of leads detected here.

5.8.2 Anions

In addition to sulfonamides and bioisosteres, another class of CA inhibitors is represented by anions. In the table VII is shown the inhibition profile of VchCA,

VchCAβ and VchCAγ with a series of simple and complex inorganic anions in comparison with those obtained for the human isoforms (hCA I and II) and the bacterial enzyme of *Helicobacter pylori* (hpαCA).

Table VII. Anions inhibition constants for the human α-CAs isoforms I and II, α-CA of *H. pylori* and the three classes of CA identified in the genome of *V. cholerae*, obtained with the technique of "stopped- flow "at 20 ° C and pH 7.5.

	K_I[a] (mM)					
Inhibitor	hCA I	hCA II	hpαCA	VchCA	VchβCA	VchγCA
F^-	>300	>300	4.08	0.80	8.7	21.3
Cl^-	6	200	2.70	0.93	8.1	8.8
Br^-	4	63	2.41	28.0	7.4	8.7
I^-	0.3	26	6.05	9.73	9.0	6.3
CNO^-	0.0007	0.03	0.60	0.075	7.1	2.6
SCN^-	0.2	1.60	4.10	0.82	9.5	13.1
CN^-	0.0005	0.02	0.76	0.033	5.7	8.4
N_3^-	0.0012	1.51	0.83	0.76	20.5	8.7
HCO_3^-	12	85	0.75	5.13	5.9	3.0
CO_3^{2-}	15	73	0.66	4.64	6.7	8.2
NO_3^-	7	35	0.81	0.67	8.4	7.8
NO_2^-	8.4	63	0.93	34.1	9.1	8.7
HS^-	0.0006	0.04	0.69	0.074	21.3	7.9
HSO_3^-	18	89	0.99	0.068	>200	>200
SnO_3^{2-}	0.57	0.83	0.55	5.32	3.1	2.9
SeO_4^{2-}	118	112	0.72	60.8	3.4	9.1
TeO_4^{2-}	0.66	0.92	0.34	14.5	2.3	7.2
$P_2O_7^{4-}$	25.8	48.5	0.66	2.96	15.1	7.3
$V_2O_7^{4-}$	0.54	0.57	0.27	0.84	7.9	8.3
$B_4O_7^{2-}$	0.64	0.95	0.56	16.6	3.4	7.2
ReO^{4-}	0.11	0.75	0.88	5.11	6.3	>200
RuO^{4-}	0.101	0.69	0.36	0.61	8.4	>200
$S_2O_8^{2-}$	0.107	0.084	0.92	84.1	3.4	>200
SeCN	0.0085	0.086	0.73	0.76	5.3	8.7
CS_3^{2-}	0.0087	0.0088	0.38	0.088	7.0	8.8
$Et_2NCS_2^-$	0.79	3.1	0.005	0.043	0.73	0.44
SO_4^{2-}	63	>200	0.82	0.85	>200	9.6
ClO_4^-	>200	>200	10.1	>200	>200	>200
BF_4^-	>200	>200	>200	>200	>200	>200
FSO_3^-	0.79	0.46	0.91	86.1	8.9	7.5
$NH(SO_3)_2^{2-}$	0.31	0.76	0.54	88.2	>200	8.1
$H_2NSO_2NH_2$	0.31	1.13	0.073	0.008	0.054	0.084
H_2NSO_3H	0.021	0.39	0.080	0.031	0.086	0.087
$PhB(OH)_2$	58.6	23.1	0.097	0.007	0.085	0.081
$PhAsO_3H_2$	31.7	49.2	0.44	0.023	0.079	0.091

[a] Error in the range of 3–5% for the reported values.

Interestingly, the carbonate and bicarbonate are not very effective inhibitors for *V. cholerae* CA (K_I = 3.0 to 8.2 mM). This result is in agreement with the fact that *V. cholerae* colonizes the upper part of the small intestine characterized by high concentrations of bicarbonate, in turn considered a potent inducer of the expression of the genes involved in the virulence of the pathogen. This is an example of evolutionary adaptation of the *Vibrio* CAs to the high concentrations of bicarbonate. Interesting, also for two human isoforms (hCAI and hCAII) carbonate and bicarbonate are not effective inhibitors (K_I = 12-85 mM). In fact, these anions are present in the plasma at high concentrations.

5.9 Tridimensional structure of VchCAβ

In collaboration with Dr. Marta Ferraroni, University of Florence, it was determined the crystallographic structure of the VchCAβ. The X-ray structure of VchCA was solved by molecular replacement using the coordinates of the β-CA from *E. coli*. The X-ray crystal structure of this new enzyme was similar to the structures of the other β-CAs. As described in literature, X-ray crystallographic analysis of β-CAs revealed two distinct subtypes of this enzyme class based on active-site organization, denoted type I and type II β-CAs (Figure 24A). In the enzymes from *P. sativum*, *M. thermoautotrophicum* and *M. tuberculosis* Rv1284, the active-site zinc ion is coordinated by one histidine and two cysteine residues, with a fourth coordination site occupied by water or a substrate analogue (the so-called open conformation). In contrast, the other subclass of β-CAs, exemplified by the structures of the enzymes from *H. influenzae*, *E. coli*, *P. purpureum* and *M. tuberculosis* Rv3588c, has a unique zinc-coordination geometry in which the water molecule has been replaced by an aspartate side chain, forming a noncanonical CA active site (the closed conformation). The latter group of CAs (type II β-CAs) are characterized by little or no CO_2 hydration activity at pH values less than 8.0, compared with the former group (type I β-CAs) that shows catalytic activity at pH values from as low as 6.5 to greater than 9.0. Type II β-CAs also show highly cooperative pH-rate profiles and cooperative inhibition by HCO_3^-, whereas type I β-CAs are not inhibited by HCO_3^- (Rowlett. *et al*, 2010).

The X-ray crystal structure of this new enzyme was solved at 1.9Å resolution from a crystal that was perfectly merohedrally twinned, revealing a tetrameric type II β-CA with a closed active site in which the zinc is tetrahedrally coordinated to Cys42, Asp44, His98 and Cys101 (Figure 24B). The substrate bicarbonate was found bound

in a noncatalytic binding pocket close to the zinc ion (Figure 24C), as reported for a few other β-CAs, such as those from *Escherichia coli* and *Haemophilus influenzae*. It has already been observed that the binding of the bicarbonate ion to this noncatalytic site enforces a closed conformation of the active site in type II β-CA structures.

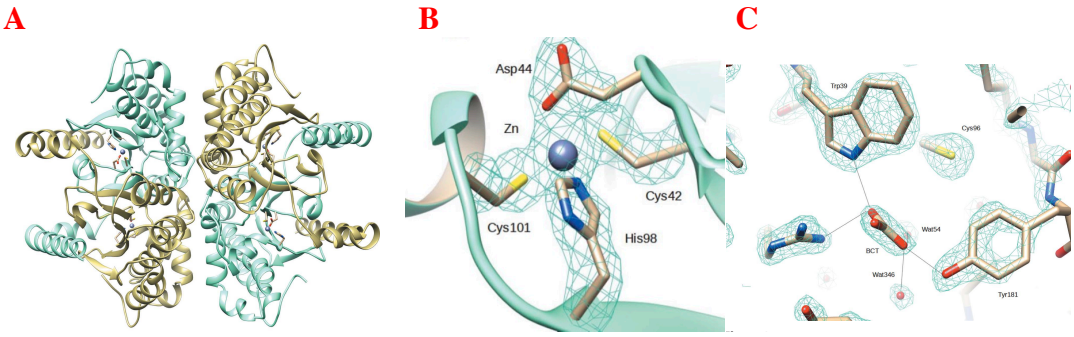

Figure 24 A: Ribbon structure showing the tetrameric arrangement of VchCA; **B:** the active site of VchCA exhibiting a 'closed' configuration; **C:** the noncatalytic bicarbonate-binding site.

However, the alternative open configuration has not been observed in any type II β-CA structure, regardless of the crystallization pH and the concentration of bicarbonate in the crystallization medium, but the kinetic data suggest that these enzymes adopt this conformation in order to function in a highly cooperative manner. The active form can be inferred from the crystal structures of type I β-CAs in which Asp44 is detached from the catalytic zinc ion and is hydrogen-bonded in a bidentate mode to Arg46.

Chapter 6. *Porphyromonas gingivalis* CAs

The microbiota of the human oral mucosa consists of a myriad of bacterial species that normally exist in commensal harmony with the host. Among the bacterial species living in the oral cavity, a bacterial complex named "red complex" and composed of *Porphyromonas gingivalis*, *Treponema denticola*, and *Tannerella forsythia* has been strongly associated with advanced periodontal lesion. *Porphyromonas gingivalis* is one of the few major pathogens responsible for the development of chronic periodontitis and a successful colonizer of the oral epithelium. The perturbation of epithelial cells by bacteria is the first stage in the initiation of inflammatory and immune processes causing eventually destruction of the tissues surrounding and supporting the teeth, which ultimately result in tooth loss. From the inspection of the *P. gingivalis* genome, carried out using the BLAST program, it was found that the pathogen encoded for two classes of carbonic anhydrase: the β-class CA, indicated with the acronym PgiCAb; the γ-CA, named PgiCA.

6.1 PgiCAb (β-CA)

The full nucleotide sequence showed an open reading frame encoding a 242 residues polypeptide chain which contained all the typical features of a β-CA, including the three residues that are involved in the catalytic mechanism of the enzyme (two cysteines and one histidine, more precisely Cys90, His143 and Cys146, see Figure 25). Furthermore, the catalytic dyad (Asp92-Arg94) involved in the activation of the water molecule coordinated to the zinc ion from the enzyme active site, is also conserved in PgiCAb, as for the other investigated β-CAs such as the two enzymes from *Legionella pneumophila* lpCA1 and lpCA2, *H. pylori* enzyme, HpyCA, as well as the two β-CAs from *Salmonella typhimurium*, stCA1 and stCA2.

Figure 25. Amino acid sequences alignment of selected β-CAs from several bacterial species. The LpCA1 numbering system was used. Amino acid residues participating in the coordination of the metal ion are indicated in red and bold (Cys90, His143 and Cys146, respectively), whereas the catalytic dyad involved in the activation of the water molecule coordinated to zinc (Asp92–Arg94) is shown in blue and bold. The asterisk (*) indicates identity at a position; the symbol (:) designates conserved substitutions, whereas (.) indicates semi-conserved substitutions. The multiple sequence alignment was performed with the program MUSCLE and refined using the program Gblocks. Legend: PgiCAb, *Porphyromonas gingivalis* (YP_001929649.1); lpCA1, *Legionella pneumophila*, isoform 1 (WP_014844650.1); lpCA2, *Legionella pneumophila*, isoform 2 (WP_014842179.1); HypaCA, *Helicobacter pylori* (YP_005769368.1); stCA1, *Salmonella typhimurium*, isoform 1 (NP_459176.1); stCA2, *Salmonella typhimurium*, isoform 2

6.2 PgiCA (γ-CA)

The open reading frame of the P. gingivalis gene encodes a 192 amino acid polypeptide chain, which displays 33% and 30% identity when compared with the prototypical γ-CAs CAM and CAMH, respectively (Figure 26). CAM and CAMH both belong to the γ-CA class and were isolated from the Archaeon *Methanosarcina thermophila*; they have been thoroughly characterized by Ferry's group (A. Zimmerman., *et al*., 2009)

Figure 26. Amino acid sequence alignment of the γ-CAs: PgiCA, CAMH and CAM. The metal ion ligands (His81, His117 and His122) are indicated in red; the catalytically relevant residues of CAM, such as Asn73, Gln75 and Asn202 which participate in a network of hydrogen bonds with the catalytic water molecule, are indicated in green; the acidic loop residues containing the proton shuttle residues (Glu84) is also colored in green, but it is missing in CAMH and PgiCA (CMA numbering system). The asterisk (*) indicates identity at all aligned positions; the symbol (:) relates to conserved substitutions, while (.) means that semi-conserved substitutions are observed. The multialignment was performed with the program Clustal W.

Data of Figure 26 show that the three His residues involved in the Zn(II) coordination (His81, 117 and 122, CAM numbering system) are conserved in PgiCA, similar to all other γ-class CAs studied. In the γ-CAs, or at least for CAM, the residue acting as a proton shuttle seems to be a glutamic acid (Glu84). The results of Ferry's group suggest that the majority of the γ class CAs belong to a subclass of proteins distinct from CAM, probably more related to CAMH. Furthermore, the catalytic activity of many of these proteins is uncertain or anyhow, poorly investigated at this moment. The analysis of the amino acid sequence of CAM, CAMH, and PgiCA, suggest that PgiCA is more similar to CAMH than CAM.

6.3 Cloning, expression and purification of PgiCAb and PgiCA

The two classes of CAs belonging to *P. gingivalis* (PgiCAb and PgiCA) have been prepared using the DNA recombinant technology. The synthetic genes encoding for PgiCA (588 bp) or PgiCAb (741 bp) were cloned into the expression vector pET-15b

(see "Material and Methods"). Once defined the optimum growth conditions a bacterial culture of 2.0 L was prepared to produce PgiCAb and PgiCA. At the end of the purification procedure the two recombinant proteins were analyzed by SDS-PAGE. The enzymes were at least 90% pure as shown in Figure 27.

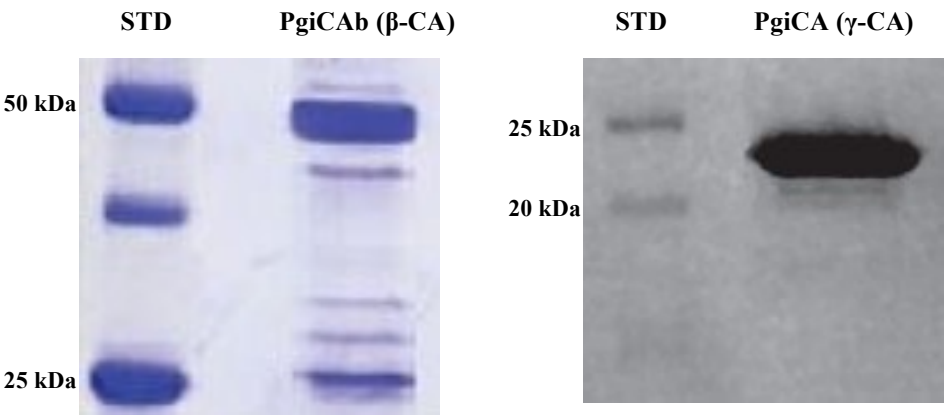

Figure 27. SDS-PAGE after affinity chromatography. Legend: Std, standards; PgiCA, γ-CA; PgiCAb, β-CA

6.4 Biochemical characterization

6.4.1 Determination of oligomeric state

Analysis by SDS-Page of PgiCAb showed two main bands of about 25 kDA (monomeric form) and 50 kda (dimeric form) under reducing condition, while PgiCA showed a single band of about 22kDA. PgiCA was subject to a HPLC gel-permeation chromatography under native conditions to determine the oligomeric state of the protein. PgiCA was eluted from the gel-filtration column as a protein with an estimated molecular mass of 65 kDa (Figure 28). Given a calculated subunit molecular mass of 20.8 kDa, these results suggest that the recombinant enzyme self-associate in a homotrimer. This is in agreement with Ferry's studies on the γ-class CA. The carbonic anhydrase from the thermophilic methanoarchaeon *Methanosarcina thermophila*, CAM, is the prototype of the γ-class and the only γ-CA that has been characterized. CAM showed a homotrimer structure with an approximate molecular mass of 70 kDa (data reported by Ferry's group).

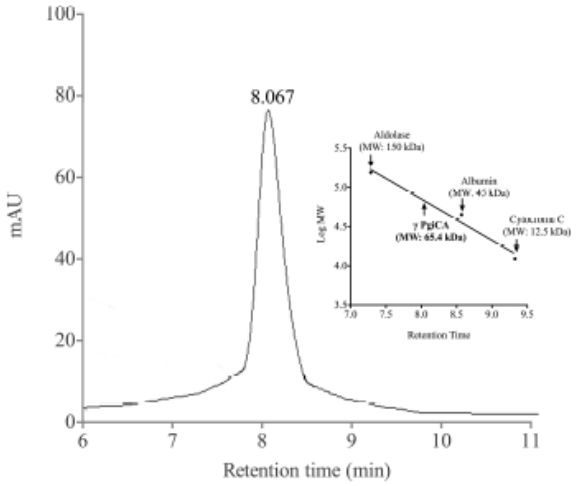

Figure 28. Size exclusion chromatography column of the purified PgiCA enzyme carried out by HPLC. Dialyzed fractions from the His-tag affinity column chromatography step were concentrated and chromatographed on a BioSep-SEC-s2000 column (300 × 4.6 mm). The elution profile has been reordered at 280 nm. The peak at the retention time of 8.067 min corresponds to a MW of 65.4 kDa. The three points calibration curve indicated in the insert has been obtained using as standards the rabbit aldolase, the chicken egg albumin and the bovine cytochrome C (12.5 kDa).

6.4.2 Kinetics constants

Using the stopped-flow techniques and CO_2 as a substrate, the kinetic parameters were determined for the purified recombinant PgiCAb and PgiCA. PgiCAb showed a significant catalytic activity, with a k*cat* of 2.8 x10^5 s-1 and a k_{cat}/K_m of 1.5 x 10^7 M^{-1} x s^{-1}. PgiCA showed a kcat of 4.1 x 10^5 and a k_{cat}/K_m of 5.4 x 10^7 M^{-1} x s^{-1} (Table VIII).

Table VIII . Kinetic parameters for the CO_2 hydration reaction catalyzed by various CAs belonging to the various families. Inhibition data with the clinically used sulfonamide acetazolamide (5-acetamido-1,3,4-thiadiazole-2-sulfonamide) are also provided. All data were obtained in similar conditions.

Isozyme	Class	Organism	k_{cat} (s^{-1})	k_{cat}/K_m ($M^{-1} \times s^{-1}$)	K_I (acetazolamide) (nM)
SspCA	α	Bacterium	9.35×10^5	1.1×10^8	4.5
SazCA	α	Bacterium	4.4×10^6	3.5×10^8	0.9
Can2	β	Fungus	3.9×10^5	4.3×10^7	10.5
FbiCA1	β	Plant	1.2×10^5	7.5×10^6	27
PgiCAb	β	Bacterium	2.8×10^7	$1.5 \times 10_7$	214
PgiCA	Γ	Bacterium	4.1×10^5	5.4×10^7	324
CAM	Γ	Archaeon	6.1×10^4	8.7×10^5	63

In Table VIII is reported the comparison of the kinetic parameters of PgiCAb and PgiCA with other CAs belonging to different family and from different organisms. SazCA (α-CA) from the extremophilic bacterium *Sulfurihydrogenibium azorense* resulted the faster CAs known to date, i.e. showed a k*cat* of 4.4 x10^6 s^{-1}; whereas the β- and γ-CAs showed kinetic constants ranging from 10^4 to 10^5 s^{-1}. Interestingly, in general the catalytic efficiency of the γ-CAs is lower compared to the β-CAs, which in turn are also less efficient catalysts compared to many bacterial α-CAs (Table VIII). However, PgiCAb is about 2.3 times faster than the β-CA isolated from *Flaveria bidentis* but 1.5 times slower when compared with the γ-class enzyme PgiCA. It may also be observed that the CO_2 hydrase activity of PgiCAb is inhibited by the clinically used sulfonamide acetazolamide, with an inhibition constant of 214 nM. Enzyme kinetic analysis showed that PgiCA is 62 times more effective as a catalyst compared to CAM, the only other γ-CA characterized in detail kinetically (Vullo., *et al.* , 2013). It has been noted that the enhanced efficiency of PgiCA compared to CAM is due both to the fact that the kinetic rate constant of the *P. gingivalis* enzyme is 6.7 times higher compared to that of the archaeal enzyme, as well as because the Km of the PgiCA is much lower (around 7.5 mM) compared to the one of CAM (around 70 mM). Thus, the enhanced catalytic efficiency of PgiCA compared to CAM is due to both kinetic (higher kcat) and thermodynamic factors (lower Michaelis-Menten constant for the binding of the substrate within the active site of the enzyme). It was also noted that PgiCA is more active catalytically than other α- or β-CAs, such as hCA I (human isoform), Can2 (fungal enzyme), FbiCA (plant enzyme), being only slightly less efficient compared to hCAII, a highly effective catalyst for the CO_2 hydration reaction together with SspCA and SazCA.

6.4.3 Thermostability of PgiCA

It has been investigated the effect of the temperature on the stability of PgiCA. The enzyme stability was studied in the 25 – 90 °C temperature range incubating the enzyme for 10, 30, 60 and 120 min (Figure 29). After 10, 30, 60 and 120 min of incubation, enzyme activity was determined using CO_2 as substrate. Interesting, the enzyme was stable up to 80 °C when the incubation time did not exceed the 30 minutes. As shown in Figure 28, the residual activity at this incubation time and 80 °C is still 35 %, and starts to decline at 15 and 0 % when the incubation time is 60 and 120 min, respectively. However, when the incubation time is 120 min the enzyme is completely inactivated.

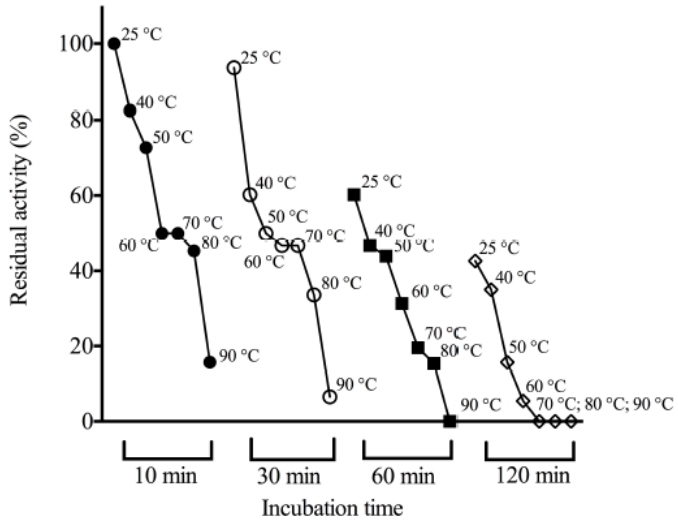

Figure 29. Thermostability of PgiCA. The enzyme was incubated at 25, 40, 50, 60 70, 80 and 90 °C for 10, 30, 60 and 120 and assayed using CO_2 as substrate.

6.5 Inhibition studies

6.5.1 PgiCA (γ-CA)

a) Sulfonamide inhibition

A library of 40 compounds, comprising 39 sulfonamides and one sulfamate were included in our study. Data of Table IX show the inhibition data of PgiCA with the 40 derivatives mentioned above. Inhibition data of the human (h), possibly off target isoforms hCA I and II, of a β-class CA, LdcCA (from the protozoan pathogen *Leishmania donovani chagasii*) and of CAM, the only other γ-CA investigated in detail, are also presented in Table IX. A large number of compounds, among which **1, 3, 5, 6, 12, 20–24, DCP, and TPM** were weak PgiCA inhibitors (KIs in the range of 1.035–4.65 lM) or were totally ineffective against this enzyme (compound 3 and TPM has inhibition constants of >100 lM). It may be observed that apart the sugar sulfamate TPM, most other compounds are simple benzenesulfonamides incorporating small, compact moieties such as amino, aminoalkyl, halogeno, etc., Compounds 20–24 on the other hand are aromatic/ heterocyclic sulfonamides incorporating arylsulfonylamido moieties, possessing thus a rather elongated molecule. The best inhibitory power against PgiCA among the investigated sulfonamides was observed for the following derivatives: **9, 10, 15–17, AAZ, MZA,**

ZNS, IND, CLX, **SAC** and **HCT**, which showed inhibition constants in the range of 131–380 nM (Table IX). 9 and 10 are benzenesulfonamides incorporating amino and

Table IX Inhibition of human isoforms hCA I and hCA II, of the protozoan one from L. donovani chagasi (LdcCA) as well as the bacterial enzyme from *Metanosarcina thermophila* (CAM) and *Porphyromonas gingivalis* (PgiCA) with sulfonamides 1–24 and the clinically used drugs AAZ—HCT, by a CO_2 hydrase, stopped-flow assay

Inhibitor	K_I^* (nM)				
Enzyme class	hCA I α	hCA II α	LdcCA β	CAM γ	PgiCA γ
1	28,000	300	5960	nt	4220
2	25,000	240	9251	250	893
3	79	8	8910	170	>100,000
4	78,500	320	>100,000	nt	945
5	25,000	170	>100,000	350	3600
6	21,000	160	>100,000	270	3840
7	8300	60	15,600	970	680
8	9800	110	9058	140	662
9	6500	40	8420	1720	201
10	7300	54	9135	nt	218
11	5800	63	9083	830	711
12	8400	75	4819	120	1040
13	8600	60	584	nt	510
14	9300	19	433	nt	595
15	5500	80	927	nt	326
16	9500	94	389	nt	223
17	21,000	125	227	nt	178
18	164	46	59.6	nt	560
19	109	33	>100,000	nt	685
20	6	2	95.1	nt	1450
21	69	11	50.2	nt	3540
22	164	46	136	nt	4100
23	109	33	87.1	180	4650
24	95	30	73.4	nt	3400
AAZ	250	12	91.7	63	324
MZA	50	14	87.1	140	343
EZA	25	8	51.5	200	613
DCP	1200	38	189	190	1035
DZA	50,000	9	806	410	685
BRZ	45,000	3	764	nt	722
BZA	15	9	236	nt	741
TPM	250	10	>100,000	1020	>100,000
ZNS	56	35	>100,000	nt	157
SLP	1200	40	>100,000	nt	418
IND	31	15	316	nt	131
VLX	54,000	43	338	130	755
CLX	50,000	21	705	140	169
SLT	374	9	834	nt	424
SAC	18,540	5959	>100,000	nt	273
HCT	328	290	50.2	nt	380

nt = not tested.

* Errors in the range of 5–10% of the shown data, from 3 different assays.

halogen or OH and halogen groups, and these substitution patterns greatly increase the PgiCA inhibitory power compared to the sulfanilamide lead 2, which is a rather

ineffective inhibitor of this enzyme (Table IX). Interestingly, 15–17 are also quite simple benzenesulfonamide derivatives, incorporating 4- OH, 4-hydroxymethyl and 4-hydroxyethyl moieties, and their inhibition constants (in the range of 178–326 nM) are much better compared to the corresponding amino-derivatives 2, 5 and 7 (KIs of 893–3840 nM, Table IX) Dichlorophenamide, topiramate and many simple aromatic/heterocyclic sulfonamides were ineffective as PgiCA inhibitors whereas the best inhibition was observed with halogenosulfanilamides incorporating heavy halogens, 4-hydroxy- and 4-hydroxyalkyl-benzenesulfonamides, acetazolamide, methazolamide, zonisamide, indisulam, celecoxib, saccharin and hydrochlorothiazide (K_Is in the range of 131– 380 nM). The inhibition profile of PgiCA was very different from that of CAM, hCA I and II or the β-CA from a protozoan parasite.

b) Anion inhibition study

We have also investigated the inhibition profile of the new enzyme with a range of inorganic anions as well as other small molecules known to interact with zinc enzymes, such as sulfamide, sulfamic acid, boronic and arsonic acids (Table X). Both simple, inorganic anions such as halides, pseudohalides, bicarbonate, carbonate, sulfate (and anions isoelectronic with them) as well as complex inorganic anions were included in our study. Inhibition data of the human predominant isoform (hCAII, α-class) and CAM (γ-class, when available) are also reported in Table X, for comparison reasons. Perchlorate and tetrafluoroborate did not inhibit appreciably PgiCA. In fact these two anions were generally noninhibitory against most CAs (belonging to all genetic families) investigated so far, probably due to their relatively low affinity for metal ions (compared to most other complexing anions). Weak PgiCA inhibition has been observed with selenate, tellurate, diphosphate, divanadate, tetraborate and fluorosulfonate, which showed inhibition constants in the range of 18.5–89.5 mM. Another group of ineffective PgiCA inhibitors (but better ones compared to those mentioned above) included iodide, nitrate, nitrite, hydrogensulfite, sulfate, stannate, perruthenate, peroxydisulfate and iminodisulfonate, which showed inhibition constants in the range of 3.1–10.8 mM (Table X). The following anions showed submillimolar inhibition of PgiCA: fluoride, chloride, bromide, cyanate, bicarbonate, carbonate, perrhenate, and selenocyanide. These anions possessed K_Is in the range of 0.71–0.96 mM. It should be noted that in the halides series, the first three (light) halides showed a rather similar, submillimolar affinity for PgiCA, whereas iodide was a rather weak inhibitor. This is very different from the situation

observed for hCA II for which the inhibition increased with the atomic weight of the halogen, or for CAM, for which fluoride and chloride were not at all inhibitory whereas bromide and iodide were very weak inhibitors (Table X).

Table X Inhibition constants of anionic inhibitors against the h-CA (human) isoform hCAII, and the **γ-CAs,** Zn-CAM and PgiCA, for the CO_2 hydration reaction

Inhibitor	K_I [mM][b]		
	hCA II	Zn-CAM	PgiCA
F^-	>300	>200	0.95
Cl^-	200	>200	0.94
Br^-	63	60	0.92
I^-	26	160	8.7
CNO^-	0.03	0.09	0.71
SCN^-	1.6	7.0	0.093
CN^-	0.02	0.68	0.041
N_3^-	1.5	5.8	0.073
HCO_3^-	85	42	0.96
CO_3^{2-}	73	6.7	0.89
NO_3^-	35	36.5	8.5
NO_2^-	63	6.8	3.1
HS^-	0.04	0.05	0.092
HSO_3^-	89	11.7	9.3
SO_4^{2-}	>200	>200	8.7
SnO_3^{2-}	0.83	nt	10.8
SeO_4^{2-}	112	nt	85.5
TeO_4^{2-}	0.92	nt	16.7
$P_2O_7^{4-}$	48.50	nt	78.9
$V_2O_7^{4-}$	0.57	nt	18.5
$B_4O_7^{4-}$	0.95	nt	71.6
ReO_4^-	0.75	nt	0.93
RuO_4^-	0.69	nt	5.3
$S_2O_8^{2-}$	0.084	nt	8.7
$SeCN^-$	0.086	nt	0.91
CS_3^{2-}	0.0088	nt	0.097
$Et_2NCS_2^-$	3.1	nt	0.004
ClO_4^-	>200	nt	>200
BF_4^-	>200	nt	>200
FSO_3^-	0.46	nt	89.5
$NH(SO_3)_2^{2-}$	0.76	nt	7.7
$H_2NSO_2NH_2$	1.13	nt	0.0092
H_2NSO_3H	0.39	nt	0.093
$Ph–B(OH)_2$	23.1	nt	0.0098
$Ph–AsO_3H_2$	49.2	nt	0.090

[a]As sodium salt; nt = not tested.
[b] Errors were in the range of 3–5% of the reported values, from three different assays.

Several of the investigated anions and small molecules showed efficient or very efficient inhibition of the PgiCA activity, with inhibition constants in the range of 4.0–97 M (Table X). They include thiocyanate, cyanide, azide, hydrogensulfide, trithiocarbonate, diethyldithiocarbamate, sulfamide, sulfamate, phenylboronic acid and phenylarsonic acid. It can be observed that the pseudohalides (thiocyanate, cya-

nide, azide) were much more active compared to the halides and cyanate (K_Is in the range of 41–93 M for the first group versus 0.71–8.7 mM for the second one). Hydrogensulfide and trithiocarbonate also had a similar activity (K_Is of 92– 97 M) whereas diethyldithiocarbamate was a highly effective PgiCA inhibitor, with an inhibition of 4.0 M (this was the best inhibitor detected in this study, apart acetazolamide). It is also interesting to note that sulfamide was an effective PgiCA inhibitor (K_I of 9.2 M) whereas the structurally related sulfamic acid was around 10 times a weaker PgiCA inhibitor (K_I of 93M). The same situation was observed for the pair phenylboronic acid/phenylarsonic acid, with the first compound being an efficient (K_I of 9.8 M) and the second one a less efficient (K_I of 90 M) PgiCA inhibitor. The inhibition profile of PgiCA is very different from that of CAM (the only other γ-CA investigated in some detail regarding its inhibition with various classes of compounds) or hCA II (which belongs to the α-class). This is a very encouraging finding, if one considers the fact that PgiCA was cloned from an important human pathogen and it should be targeted specifically without interference with the host enzymes.

6.5.2 PgiCAb (β-CA)

Anion inhibition study

We investigated the anion inhibition profile of the new enzyme with simple and complex anions, as well as small molecules inhibiting other CAs, among which (Table XI). **Perchlorate**, **tetrafluoroborate**, **azide**, **nitrate, hydrogensulfite and sulfate** were not inhibitors of PgiCAb, a behavior observed with most other α-, β- and γCAs investigated so far, for the first two anions, but for sure not for the last ones, which are rather effective inhibitors for other enzymes. For example azide has an inhibition constant of 73 μM against PgiCA and of 1.5 mM against hCA II, but it is not at all inhibitory against PgiCAb. A rather large number of anions, among which the halides, cyanide, bicarbonate, nitrite, selenate, diphosphate, divanadate, tetraborate, peroxodisulfate, hexafluorophosphate and triflate, were weak PgiCAb inhibitors with inhibition constants in the range of 5.4–21.4 mM. Interestingly, for the halogenides the fluoride and chloride had a similar behavior (K_Is of 7.5–7.8 mM) whereas the heavier halogenides were weaker inhibitors (K_Is of 15.9–21.4 mM). Usually the opposite is true, with the heavier halogenides being inhibitorier than the light ones (e.g., for hCA II and other α- or β-class CAs). It is also interesting to note

the difference of inhibitory power between bicarbonate (K_I of 7.3 mM) and carbonate (KI of 3.7 mM), as these anions are in equilibrium with CO_2, the substrate

Table XI Inhibition constants of anionic inhibitors against the α-CA (human) isoform hCA II, the γ-CAs PgiCA (Porphyromonas gingivalis), and the β-class enzyme PgiCAb (Porphyromonas gingivalis), for the CO_2 hydration reaction.

Inhibitor[a]	K_I[b] (mM)		
	hCA II	PgiCA	PgiCAb
F^-	>200	0.95	7.8
Cl^-	200	0.94	7.5
Br^-	63	0.92	15.9
I^-	26	8.7	21.4
CNO^-	0.03	0.71	0.76
SCN^-	1.6	0.093	1.9
CN^-	0.02	0.041	5.4
N_3^-	1.5	0.073	>200
HCO_3^-	85	0.96	7.3
CO_3^{2-}	73	0.89	3.7
NO_3^-	35	8.5	>200
NO_2^-	63	3.1	7.8
HS^-	0.04	0.092	4.5
HSO_3^-	89	9.3	>200
SO_4^{2-}	>200	8.7	>200
SnO_3^{2-}	0.83	10.8	1.5
SeO_4^{2-}	112	85.5	9.2
TeO_4^{2-}	0.92	16.7	3.9
$P_2O_7^{4-}$	48.50	78.9	8.2
$V_2O_7^{4-}$	0.57	18.5	8.1
$B_4O_7^{2-}$	0.95	71.6	7.2
ReO_4^-	0.75	0.93	2.3
RuO_4^-	0.69	5.3	3.2
$S_2O_8^{2-}$	0.084	8.7	9.2
$SeCN^-$	0.086	0.91	2.4
CS_3^{2-}	0.0088	0.097	4.3
$Et_2NCS_2^-$	3.1	0.004	0.23
ClO_4^-	>200	>200	>200
BF_4^-	>200	> 200	>200
PF_6^-	nt	nt	8.2
$CF_3SO_3^-$	nt	nt	8.5
FSO_3^-	0.46	89.5	3.9
$NH(SO_3)_2^{2-}$	0.76	7.7	2.1
$H_2NSO_2NH_2$	1.13	0.0092	0.078
H_2NSO_3H	0.39	0.093	0.060
Ph-$B(OH)_2$	23.1	0.0098	0.077
Ph-AsO_3H_2	49.2	0.090	0.076

[a] As sodium salt; nt = not tested.
[b] Errors were in the range of 3–5% of the reported values, from three different assays.

of the enzyme. An even higher difference was observed between the very similar nitrate/nitrite, with the first one non-inhibitory and the second one with a K_I of 7.8 mM. Another group of anions, such as thiocyanate, carbonate, hydrogensulfide, stannate, tellurate, perrhenate, perruthenate, selenocyanide, trithiocarbonate,

fluorosulfonate and iminodisulfonate, were better PgiCAb inhibitors compared to anions discussed above, with inhibition constants in the range of 1.9–4.5 mM. Even more powerful inhibitors were on the other hand cyanate and diethylditiocarbamate, which had K_Is of 0.23–0.76 mM. The most efficient PgiCAb inhibitors detected so far were sulfamide, sulfamate, phenylboronic acid and phenylarsonic acid, with KIs ranging between 60 and 78l M. It is also interesting to note that all these compounds are also effective inhibitors of the γ-class enzyme from this bacterium, PgiCA, being by far less efficient hCA II inhibitors. Thus, even this preliminary study was able to detect leads with a good inhibitory power against the two pathogenic bacterium enzymes, and also with a good selectivity for the pathogenic over the host enzyme inhibition. The inhibition profile of PgiCAb is generally quite different from that of PgiCA as well as the human isoform hCA II

Chapter 7. *Plasmodium falciparum* CAs

In 2004, in genome of the protozoan *Plasmodium falciparum*, the causative agent of malaria Krungkrai and coworkers identified a gene encoding for a CA. This gene was identified in the GeneBank with the following accession number AAN35994.2. The open reading frame of the malarial CA enzyme (*P. falciparum* CA, accession number AAN35994.2, PlasmoDB: PF3D7_1140000) encodes a 600 amino acid polypeptide chain. In 2004, Krungkrai and coworkers cloned a truncated form of *Plasmodium falciparum* CA gene (GenBank: AAN35994.2) encoding for an active CA (named PfCA1) with a primary structure of 235 amino acid residues (Reungprapavut S., *et al.* 2004). The metalloenzyme showed a good esterase activity with 4-nitrophenylacetate as a substrate and was inhibited by known sulfonamide CA inhibitors (CAIs). The authors observed that the highly conserved α-CA active site residues, responsible for binding of the substrate and for catalysis, were present also in PfCA1 and considered thus the Plasmodium enzyme belonging to the α-CA class. Subsequent, it was showed that different Plasmodium spp. encoded CAs, all considered to belong to the α-class, and that primary sulfonamides inhibited in vitro and in vivo the growth of Plasmodium parasites. Recently, in the laboratory where I did my PhD, it was reanalyzed and realigned the amino acid sequence of the truncated PfCA1with the two human α-CA isoforms, hCAI and II, in order to identify other features of the protozoan enzyme (Figure 9). We observed that to have three histidines aligned with the three zinc-coordinating histidines of the human isoforms, it was necessary to ‘‘force’’ the alignment, introducing in the PfCA1 sequence a five-residues insertion and a six-residues deletion between residues 96–119. Nevertheless, the other residues crucial for the catalytic mechanism of the α-CAs, such as the proton shuttle His64 and one of the gatekeeper residues, Thr199, seemed to be not conserved in the Plasmodium enzyme (Del Prete S. *et al.* 2014; Vullo D. *et al.* 2015; Supuran C.T. & Capasso C. 2014) (Figure 9). The dyad Glu106-Thr199 is highly conserved in all α-CAs investigated so far, being involved in the orientation of the substrate for the nucleophilic attack by the zinc hydroxide species of the enzyme. Thus, the proposed alignment showed important amino acid substitutions that differentiated the sequence of Plasmodium enzyme from those of other α-CAs. Hence, a phylogenetic tree was constructed to better investigate the relationship of the Plasmodia amino acid sequences with CAs from prokaryotic and eukaryotic species belonging to different classes (α-, β-, γ-, δ-, and ζ-CAs). In Figure

30 has been represented only the branches with α-, δ-, η and ζ-CAs). It was observed that Plasmodia CAs clustered in a branch different from that of the α-CAs, although close to it, while they were well separated from the other CA classes (Figure 30). We hypothesized that the Plasmodia CAs were the result of modifications of an ancestral δ-CA gene, which originated a new class of CA that we denominated η-class.

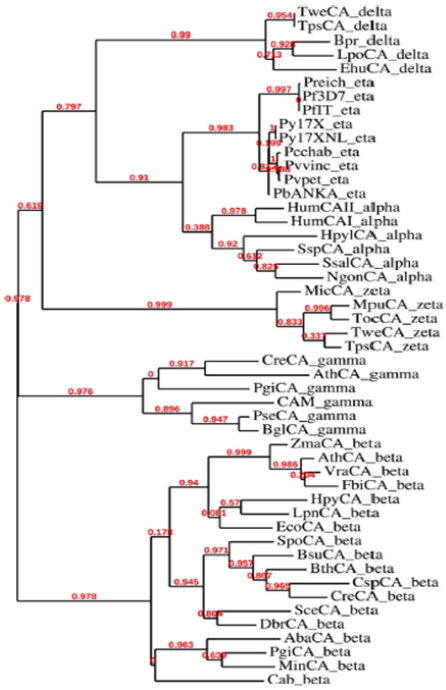

Figure 30. Phylogenetic tree that led to the discovery of η class in the genus Plasmodium, built using the amino acid sequences of the α-, β-, γ-, δ-, ζ- and η-CA of prokaryotic and eukaryotic organisms. To build the tree was used PhyML 3.0 program.

In collaboration with Dr. Giuseppina De Simone, we constructed, for homology modeling, the three-dimensional structure model of *P. falciparum* CA, aligning the entire shape of the CA of the protozoan (600 aa) with different amino acid sequences of α-CA with known crystallographic structure (De Simone G., *et al.* 2015) such as *Neisseria gonorrhoeae*, *Thermovibrio ammonificans*, *Homo sapiens, Chlamydomonas reinhardtii*, *Aspergillus oryzae* and *Dunaliella salina*. In figure 31 it is shown a detail of the structural model of *P. falciparum* CA catalytic site.

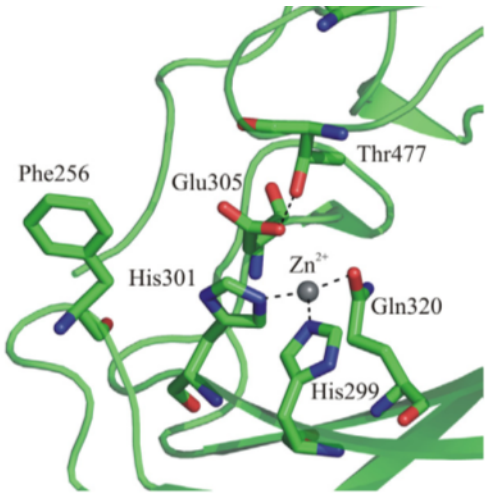

Figure 31. Parcticular of CA catalytic site of *Plasmodium falciparum* modeled on the three-dimensional structure of known CAs.

From that model, it shows that the metal is coordinated with two His residues (corresponding to residues 94 and 96 in the sequence of hCA I) and a residue of glutamine (which corresponds to residue His119 in sequence hCA I) (Figure 31). This coordination pattern was never observed in any of the CAs gene family. It is probable that the event, which triggered the separation of η- from α -class, has been the mutation of one of the histidine residues that coordinate the zinc ion with the residue of glutamine. Moreover, the separation of the class η- from the α-class, is also characterized by the replacement of the His residue in position 64 with a tyrosine residue (De Simone, G. *et al*, 2015).

In collaboration with Prof. Claudiu Supuran, were determined the kinetic constants of this new class of CA. PfCA1, showed the following kinetic properties for the CO_2 hydration reaction to bicarbonate and protons: k_{cat} of $1.4 \times 10^5 s^{-1}$ and a k_{cat} / K_M of $5.4 \times 10^6\ M^{-1} \times s^{-1}$. In Table XII were compared the kinetic constants of PfCA1 with those of other classes of CAs from different organisms. It can be noted as PfCA1 presents a significant catalytic action with a k_{cat} of value in the same order of magnitude of hCA I and of the CA from *Flaveria bidentis*, while it is about 28 times less efficient than the hCA II. Moreover, the activity of PfCA1 is effectively inhibited by acetazolamide (K_I = 170nM). Although the η- and α-CAs share many similar features, strongly suggesting the first ones to be evolutionary derived from the last, there are significant differences between the two families to allow some optimism for the drug design of selective inhibitors for the parasite over the host enzymes. However, these studies are still in their initial phase and further work by X-

ray crystallography should validate the model proposed in order to detect inhibitors with high affinity and selectivity for the η-CAs over the α-CAs

Table XII. Kinetic parameters for the hydration reaction of CO_2 catalyzed by different CA belonging to different families. α class : hCA I and II and the bacterial enzyme SazCA (*Sulfurihydrogenibium azorense*). β class : CH2 (*Criptococcus neoformans*) and FbiCA1 (*Flaveria bidentis*). γ class : is represented by PgiCA (*Porphyromonas gingivalis*) and that of η class from PfCA1 of *Plasmodim falciparum*.

	Class	**Organism**	**k_{cat} (s^{-1})**	**k_{cat}/K_M ($M^{-1} s^{-1}$)**	**K_I (nM) (acetazolamide)**
hCA I	α	Mammal	$2,0 \times 10^5$	$5,0 \times 10^7$	250
hCA II	α	Mammal	$1,4 \times 10^6$	$1,5 \times 10^8$	12
SazCA	α	Bacteria	$4,4 \times 10^6$	$3,5 \times 10^8$	0,9
Can2	β	Fungi	$3,9 \times 10^5$	$4,3 \times 10^7$	10,5
FbiCA1	β	Plant	$1,2 \times 10^5$	$7,5 \times 10^6$	27
PgiCA	γ	Bacteria	$4,1 \times 10^5$	$5,4 \times 10^7$	324
PfCA1	η	Protozoan	$1,4 \times 10^5$	$5,4 \times 10^6$	170

7.1 η-CA inhibition studies

The protozoa *Trypanosoma cruzi* encodes a α-class CA (TcCA) in its genome, while *Leishmania donovani chagasi*, another parasitic protozoa, encodes a β-class CA (LdcCA). TcCA is inhibited significantly by sulfonamides, thiols and anions, similarly LdcCA is inhibited by sulfonamides and thiols and some of these were effective in reduction of the growth of this parasite in vitro. We hypothesize that inhibition of protozoan CAs may lead to therapeutic agents that act with a novel mechanism of action. To help aid in testing this hypothesis, here we extend our knowledge of inhibition of pathogen CAs, specifically targeting the recently characterized *Plasmodium falciparum* enzyme PfCA. A selection of representative CA inhibitor scaffolds bearing sulfonamides and sulfamate functionality, compounds **1–24** as well as **15 clinically** used or clinically tested agents, were investigated (Figure 23 of the present thesis). The inhibition data against the human isoforms hCA I and hCA II, and protozoan CAs from *T. cruzi* (TcCA), *L. donovani chagasi* (LdcCA) and *P. falciparum* (PfCA) with the compounds **1–24** and the **15 clinically** used/ tested drugs are provided in Table XIII.

Table XIII. Inhibition of human isoforms hCA I and hCA II, of the protozoan ones from *T. cruzi* (TcCA), *L. donovani chagasi* (LdcCA) and *P. falciparum* η-class enzyme (PfCA) with sulfonamides **1–24** and the clinically used drugs AAZ–HCT

Inhibitor/enzyme class	K_I^* (nM)				
	hCA I α	hCA II α	TcCA α	LdcCA β	PfCA η
1	28,000	300	25,460	5960	581
2	25,000	240	57,300	9251	5800
3	79	8	63,800	8910	5885
4	78,500	320	44,200	>100,000	5580
5	25,000	170	7231	>100,000	3650
6	21,000	160	9238	>100,000	758
7	8300	60	8130	15,600	5545
8	9800	110	6925	9058	6175
9	6500	40	8520	8420	5440
10	7300	54	9433	9135	6310
11	5800	63	842	9083	12,450
12	8400	75	820	4819	4140
13	8600	60	534	584	618
14	9300	19	652	433	744
15	5500	80	73,880	927	4490
16	9500	94	71,850	389	704
17	21,000	125	66,750	227	726
18	164	46	84,000	59.6	6780
19	109	33	810	>100,000	5250
20	6	2	88.5	95.1	6705
21	69	11	134	50.2	12,800
22	164	46	365	136	15,000
23	109	33	243	87.1	14,600
24	95	30	192	73.4	8400
AAZ	250	12	61.6	91.7	170
MZA	50	14	74.9	87.1	198
EZA	25	8	88.2	51.5	131
DCP	1200	38	128	189	542
DZA	50,000	9	92.9	806	963
BRZ	45,000	3	87.3	764	260
BZA	15	9	93.6	236	1330
TPM	250	10	85.5	>100,000	295
ZNS	56	35	867	>100,000	246
SLP	1200	40	87.9	>100,000	1170
IND	31	15	84.5	316	308
VLX	54,000	43	82.7	338	226
CLX	50,000	21	91.1	705	217
SLT	374	9	71.9	834	132
HCT	328	290	134	50.2	153

* Errors in the range of 5–10% of the shown data, from three different assays.

All compounds showed CA inhibitory activity, with multiple inhibitors possessing K_{IS} <100 nM identified for the α-class TcCA. and β-class LdcCA, however no compound with a KI <100 nM was detected for the η-class PfCA. The best PfCA inhibitors were ethoxzolamide **EZA** and sulthuame **SLT**, with K_{Is} of 131–132 nM, followed by acetazolamide **AAZ**, methazolamide **MZA**, and hydrochlorothiazide

HCT (K_{Is} ranging from 153 to 198 nM, Table XIII). A striking observation is that these CAIs belong to a variety of scaffolds and chemical classes, ranging from aromatic primary sulfonamides (**SLT**), to monocyclic heterocyclic derivatives (**AAZ, MZA**) and bicyclic such derivatives (**EZA, HCT**). While additional studies are required, this observation may provide chemical starting points for development of CAIs that target the η-class CAs. Of the remaining clinically used compounds brinzolamide **BRZ,** topiramate **TPM**, zonisamide **ZN**S, indisulam **IND**, valdecoxib **VLX** and celecoxib **CL**X showed moderate inhibition of PfCA, with K_{Is} ranging from 217 to 308 nM. As for the stronger inhibitors, these moderate inhibitors similarly comprise heterogeneous structural motifs. The least effective PfCA inhibitors from the set of clinically tested compounds were dichlorophenamide **DC**P, dorzolamide **DZA**, benzola- mide **BZA** and sulpiride **SLP**, with K_{Is} ranging from 542 to 1170 nM (Table XIII).

Compounds **1–24** are simpler in structure than the clinically tested compounds and comprise either the benzene sulfonamide or thiadiazole sulfonamide scaffold decorated with small substituents on the aryl/heteroaryl ring or structures with two aromatic rings separated by variable spacer groups. Many of these simpler compounds showed effective, albeit moderate to weak inhibitory activity of PfCA. Compounds **1, 6, 12, 13, 16** and **17** had K_{Is} in the range of 581–758 nM and are medium potency PfCA inhibitors. The remaining sulfonamides are weaker inhibitors with K_{Is} in the range of 3.65–15.0 μM (Table XIII). In general compounds **1–24** are substantially weaker PfCA inhibitors than the clinically used compounds. The halogen substitution of the sulfanilamide scaffold **2** (PfCA K_I = 5.8 μM) either does not improve inhibition or is detrimental to inhibition (compare K_I values of **2** with halogenated derivatives **7–9**, **10** and **12**). Secondly, the length of the alkyl spacer group present in compounds **5, 6** and **15–17** impacts on the PfCA inhibitory activity, inhibition improves from a methylene linker in 5 (PfCA K_I = 3.6 μM) and 15 (PfCA K_I = 4.5 μM) to the ethyl and propyl linkers of **6**, **16** and **17** (PfCA K_{Is} 0.7 μM). Finally, the sulfanylated sulfanilamides **21– 24** showed very weak PfCA inhibition (PfCA K_{Is} 8.4–15.0 μM).

Considering the small number of inhibition studies reported at this moment for the η-CAs, these results demonstrate it is quite probable that effective, low nanomolar inhibitors may be developed. Moreover, some dendrimers investigated showed a better inhibitory power compared to acetazolamide. The main conclusion is that this class of molecules may lead to important developments in the field of anti-

infective CA inhibitors. Given that drug resistance has emerged against most antimalarial in clinical use, the discovery of η-CA -specific inhibitors may lead to a novel therapeutic approach for malaria once the biology of η-CA has been further investigated in different life cycle stages.

Chapter 8. *Malassezia Globosa*

Malassezia yeasts are almost exclusively the single eukaryotic members of the microbial flora of the skin. Malassezia have been recognized for more than 150 years, as members of the human cutaneous flora and etiologic agents of certain skin diseases. At the begining of 1800, it was noted that yeast cells and filaments were present in the skin scales of patients with pityriasis versicolor, whereas yeast cells, but no filaments, were observed in scales from healthy scalp, seborrheic dermatitis scalp, and dandruff. Dandruff is a frequent pathological skin condition confined to the scalp and is characterized by flaking with minimal to absent inflammation. Malassezia genus includes seven species, the three former taxa (*M. furfur, M. pachydermatis, and M. sympodialis*) and four newtaxa (*M. globosa, M. obtusa, M. restricta, and M. slooffiae*). With the exception of M. pachydermatis, all species afore-mentioned require lipids for their growth. Moreover, *M. globosa* and *M. restricta* are found on the skin of practically all humans. It has been demonstrated that oleic acid responsible of the sebum of the scalp is produced from the hydrolysis of triglycerides by *M. globosa* lipases. These data highly implicate M. globosa in the pathogenesis of dandruff. Several strategies and treatments are available for dandruff, the majority of which aim to target growth of the fungi. A common active ingredient in anti-dandruff shampoos is zinc pyrithione, also known as zinc pyridinethione **A**, its effect being most likely mediated through disruption of fungal membrane activities. **Ketoconazole B**, an azole antifungal agent interfering with the biosynthesis of fungal sterols is also used in many shampoos. Other azoles have been used in anti-dandruff treatments, as they interfere with the synthesis of ergosterol, a key component of fungal cell walls. However the effectiveness of **A** and **B** for preventing/treating dandruff is not very high, and additional therapeutic strategies are being explored, such as, for example, inhibition of the lipase present in Malassezia spp., or inhibition of the β-carbonic anhydrase (MgCA), which is the single CA-class encoded by its genome. Thus, MgCA has been proposed as a novel anti-dandruff target.

8.1 Construct preparation, protein expression and purification

The GeneArt Company, specialized in gene synthesis, designed the synthetic *M. globosa* gene encoding for the β-CA, and containing 4 base pair sequences (CACC) necessary for directional cloning at the 5’ end of the MgCA gene. The fragment was

subsequently cloned into the expression vector pET100D-Topo (Invitrogen, Carlsbad, CA), creating the plasmid pET100D-Topo/MgCA. In order to confirm the integrity of the M. globosa gene and the fact that no errors occurred at the ligation sites, the vector containing the fragment was sequenced. Competent Escherichia coli BL21 (DE3) Codon Plus cells were transformed with pET100/D-Topo/MgCA, grown at 37°C, induced with 1mM IPTG. $Zn(SO4^{2-})$ was added after 30 min and after additional growth for 3 h, cells were harvested and disrupted by sonication at 4°C in 20mM buffer phosphate, pH 8.0. Following sonication, the sample was centrifuged at 1200g at 4°C for 30 min. The supernatant was dialyzed against 0.02M phosphate buffer (pH 8.0) containing 0.01 M imidazole and 0.5M NaCl at 4°C and loaded onto a His-select HF Nickel affinity column. The column was equilibrated with 0.02M phosphate buffer (pH 8.0) containing 0.01 M imidazole and 0.5M NaCl at a flow rate of 1.0 ml/min. The MgCAb was eluted with 0.02M phosphate buffer (pH 8.0) containing 0.5 M NaCl and 0.25mM imidazole at a flow rate of 1.0 ml/min. Active fractions (1 ml) were collected and combined for a total volume of 5 ml. Subsequently, they were dialyzed, concentrated and analyzed by SDS-PAGE. At this stage of purification, the enzyme was at least 95% pure (Figure 32).

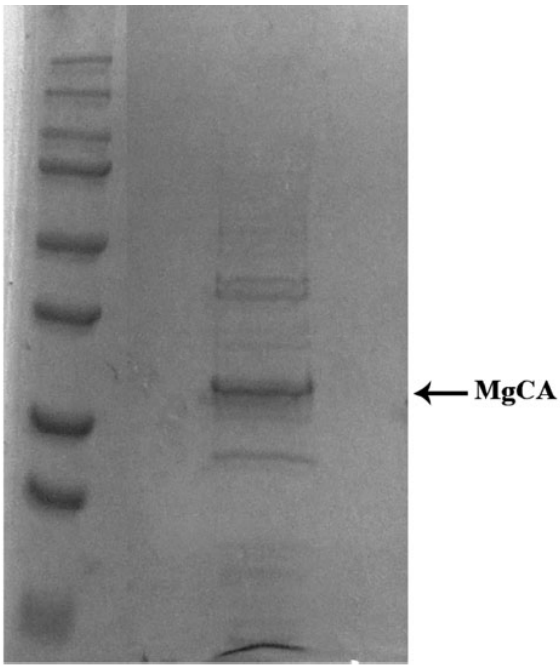

Figure 32. SDS-PAGE of the recombinant MgCA purified from E. coli codon plus cells. Lane A, molecular markers, M.W starting from the top: 250, 150, 100, 75, 50, 37, 25 and 20; Lane B, purified MgCA from Histag affinity column.

8.2 Protonography

Wells of 12% SDS-gel were loaded with bCA and MgCA mixed with loading buffer without 2-mercaptoethanol and without boiling the samples, in order to avoid protein denaturation. The gel was run at 180V until the dye front ran off the gel. Following the electrophoresis, the 12% SDS-gel was subject to protonographyto detect the bCA and MgCA hydratase activity on the gel. The analysis by protonography of MgCA showed a band of about 29 kDa (monomeric form) under reducing condition (Figure 33).

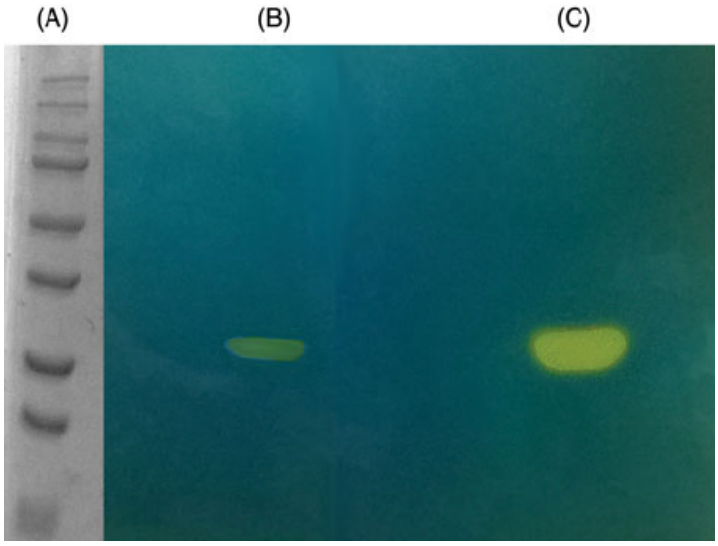

Figure 33. MgCA protonogram. The yellow bands correspond to the hydratase activity on the gel responsible for the drop of pH from 8.2 to the transition point of the dye. Incubation time was of 60 s. bCA is present in the monomeric (29 kDa) form. Lane A, molecular markers, M.W. starting from the top: 250, 150, 100, 75, 50, 37, 25 and 20 kDa; Lane B: MgCA; Lane C: commercial bovine CA (bCA).

8.3 Kinetic constants

Using the stopped-flow technique, the kinetic parameters were determined for the newly purified recombinant MgCA using CO_2 as a substrate. MgCA showed a significant catalytic activity, with a kcat of $9.2x10^5$ s^{-1} and a kcat/Km of $8.3x10^7$ $M^{-1}xs^{-1}$. Table XVIII shows a comparison of the kinetic parameters of MgCA with those of MG-CA (β-CA cloned as GST-fusion protein), hCA I and II (α-CA from Homo sapiens, isoform I and II, respectively) and Can2 (β-CA from C. neoformans).

It may be observed that MgCA and MG-CA showed kinetic parameters about 2 times higher than the other β-CA reported in Table XIV (Can2), and four times higher than the human α-CA isoform I. Moreover, MgCA cloned as Hisfusion protein has kinetic data similar to those of the GST-fusion protein reported earlier, but the activity of the His-tagged MgCA is better. It is interesting to note that both proteins obtained with two different cloning strategies are not affected by acetazolamide inhibition. Intriguingly, this lack of effectiveness of AAZ for inhibiting a β-class enzyme has been observed only for Cab, an enzyme isolated and characterized from the Archaeon Methanobacterium thermoautotrophicum.

Table XIV. Kinetic parameters for the CO2 hydration reaction catalyzed by MG-CA (GST-fusion protein), MgCA (His-fusion protein), hCA I and II (α-CA from H. sapiens, isoform I and II, respectively) and Can2 (β-CA from C. neoformans).

Cryptonym	Activity level	Class	K_{cat} (s^{-1})	k_{cat}/k_m $M^{-1} \times s^{-1}$	K_I (Acetazolamide) μM
hCA I	Moderate	α	2.0×10^5	5.0×10^7	0.25
hCA II	Very high	α	1.4×10^6	1.5×10^8	0.012
Can2	Moderate	β	3.9×10^5	4.3×10^7	0.010
MgCA	Moderate	β	9.2×10^5	8.3×10^7	74
MG-CA	Moderate	β	8.6×10^5	6.9×10^7	76

8.4 Inhibition studies

Inorganic (complexing) anions represent an interesting class of derivatives, which bind metal ions in many types of metalloenzymes. Their chemical simplicity represents both a disadvantage as well as an advantage when investigating them as CAIs. The disadvantage consists in the fact that due to their propensity to coordinate metal ions in solution or in metalloenzyme active sites, usually this class of inhibitors is non-selectively binding to many metals present in such enzymes, and furthermore, their activities are normally those of weak inhibitors (in the milli-molar, rarely tens of micromolar ranges). However, the advantage of this chemical simplicity (but also diversity, since a large number of inorganic/organic anions can be envisaged) is represented by the fact that many such compounds can be considered as lead molecules and further elaborated for leading to highly effective inhibitors. Data of Table XV show a very interesting inhibition profile of MgCA with anions and small molecules. The following salient features were observed:

Anions known to possess weak affinity for Zn(II) in other CAs,a such as perchlorate and tetrafluoroborate were also not inhibitory against MgCA (as for hCA I and II, the two major red blood cell isoforms, which may be considered as the main off targets when investigating parasite CAs, like the enzyme considered here). Surprisingly,

carbonate, bisulfite and peroxydisulfate showed the same activity, with no inhibition of MgCA up to 100 mM concentrations of inhibitor.

Some other anions with poor inhibitory properties against MgCA were bromide, azide, hydrogen sulfide, perrhenate, and sulfate, diphosphate, divanadate, tetraborate, selenocyanide, trithiocarbonate, triflate, hexafluorophosphate, and fluorosulfonate.

One may see that this is a highly heterogeneous group of anions, incorporating either highly simple ones (halides) as well as complex ones, which differ considerably in their affinity for metal ions in solutions. Obviously, the environment within the active site dramatically interfereswhich had K_Is in the range of 11.9–45.2 mM (Table XIV). The sulfate data is interesting, as this anion usually has a low affinity for Zn(II) in many CAs (e.g., hCA II and I), whereas azide, which is a very weak MgCA inhibitor acted as a highly potent one for many α-CAs (e.g., it has a K_{Is} in the micromolar rage against hCAI).

The largest majority of anions investigated here showed a medium potency inhibitory power against MgCA with K_{Is} in the low millimolar range (1.73–8.82 mM). Among themnare the halides (except bromide), cyanate, thiocyanate, cyanide, nitrate, nitrite, stannate, selenate, tellurate, perosmate, with the binding, favoring some and probably inducing a less favored binding for other of them, which explains the rather small variation in the inhibition constants for this large group of inhibitors.

A very interesting observation is that among the best anion inhibitors detected here were bicarbonate (K_I of 0.59 mM) and diethyldithiocarbamate (K_I of 0.30 mM).

It should also be noted the inhibition data between carbonate (not an inhibitor) and trithiocarbonate (K_I of 1.77 mM) which is one of the efficient inhibitors in the group of medium potency anions.

The best MgCA inhibitors were sulfamide, sulfamate, phenylboronic acid and phenylarsonic acid, which had inhibition constants in the range of 83‑90 μM (comparable with acetazolamide, K_I of 74l M, see discussion above). Thus, as for other pathogenic enzymes investigated ultimately, this study allowed us to reveal that small molecule inhibitors such as dithiocarbamates, sulfamide, sulfamate, phenylboronic acid and phenylarsonic acid show an interesting potential for designing CAIs with an improved potency.

Table XV. Inhibition constants of anion inhibitors against α-CAs from mammals (hCA I, and II, human isoforms, and the protozoan enzyme from T. cruzi, TcCA), and the η-CA PfCA from P. falciparum, for the CO_2 hydration reaction, at 20°C and pH 7.5

Inhibitor[§]	K_I (mM)		
	hCA I	hCA II	MgCA
F^-	>300	>300	7.13
Cl^-	6	200	7.98
Br^-	4	63	18.6
I^-	0.3	26	8.73
CNO^-	0.0007	0.03	6.81
SCN^-	0.2	1.60	8.39
CN^-	0.0005	0.02	7.19
N_3^-	0.0012	1.51	45.2
HCO_3^-	12	85	0.59
CO_3^{2-}	15	73	>100
NO_3^-	7	35	8.13
NO_2^-	8.4	63	7.56
HS^-	0.0006	0.04	11.9
HSO_3^-	18	89	>100
SnO_3^{2-}	0.57	0.83	5.07
SeO_4^{2-}	118	112	7.41
TeO_4^{2-}	0.66	0.92	5.75
OsO_5^{2-}	0.92	0.95	6.16
$P_2O_7^{4-}$	25.77	48.50	6.03
$V_2O_7^{4-}$	0.54	0.57	6.89
$B_4O_7^{2-}$	0.64	0.95	8.45
ReO_4^-	0.11	0.75	16.7
RuO_4^-	0.101	0.69	8.82
$S_2O_8^{2-}$	0.107	0.084	>100
$SeCN^-$	0.085	0.086	1.73
CS_3^{2-}	0.0087	0.0088	1.77
$Et_2NCS_2^-$	0.00079	0.0031	0.30
$CF_3SO_3^-$	nt	nt	2.28
PF_6^-	nt	nt	6.47
SO_4^{2-}	63	>200	19.5
ClO_4^-	>200	>200	>100
BF_4^-	>200	>200	>100
FSO_3^-	0.79	0.46	4.06
$NH(SO_3)_2^{2-}$	0.31	0.76	21.4
$H_2NSO_2NH_2$	0.31	1.13	0.094
H_2NSO_3H	0.021	0.39	0.083
Ph-$B(OH)_2$	58.6	23.1	0.089
Ph-AsO_3H_2	31.7	49.2	0.090

§ As sodium salt, except sulfamide, phenylboronic acid and phenylarsonic acid.

8.5 Activation studies

Recently we have extended the CA activation studies to the β-class enzymes from pathogenic fungi, such as MgCA. Infact, we report the first activation study of MgCA with a series of amines and amino acids (of types 1‑19,figure 34.), which were investigated earlier for their interactions with mammalian α-CAs as well as more recently with the β- and γ-class enzymes from the Archaea domain and from pathogenic fungi, respectively. This study may help a better understanding of the β-CA catalytic/activation mechanism, as the natural proton shuttling residue in this class of enzymes has not been yet identified, unlike the α-CAs for which it is known that a His residue placed in the middle of the active site cavity (His64, hCA I numbering) plays this function.

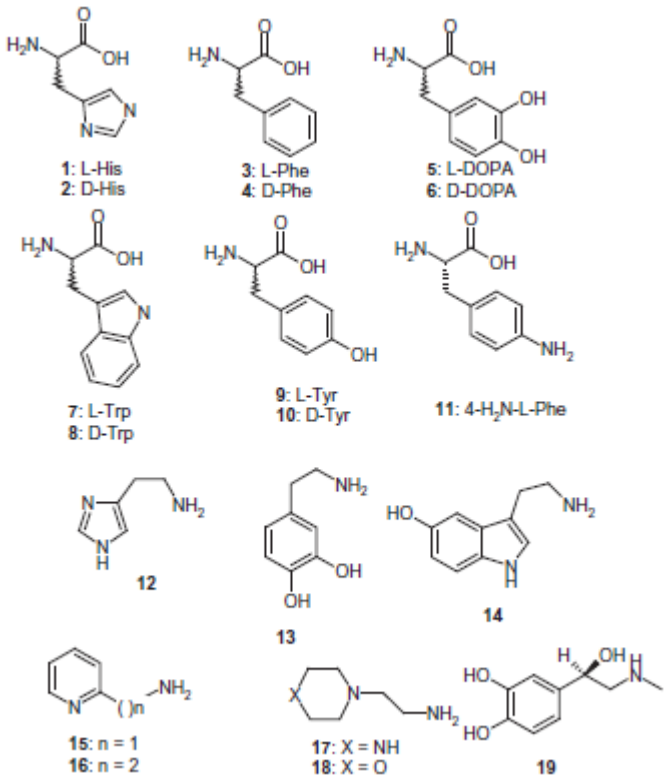

Figure 34. Structure of activators 1–19 investigated in the present study.

Data of Table XVI show that all amino acids and amines 1‑19, which have been investigated in this study, act as CAAs against the fungal enzyme MgCA. However, the activation profiles of these compounds against MgCA are different from other recently investigated α- and β-class enzymes, such as hCA II, ScCA and CgCA, which were included in Table XVI for comparison. The following structure activity

relationship (SAR) can be observed for the activation of MgCA with compounds 1‑19. Several amino acids, such as L-/D-His, L-Phe, D-DOPA, D-Trp, L-/D-Tyr, 4-amino-L-phenylalanine, as well as serotonin 14, showed activation constants in the range of 12.5‑29.3 μM, therefore they are considered as moderate MgCA activators. However, it may be observed that most of these derivatives (except L-Phe, L-/D-Tyr and D-Trp) are much weaker activators of the C. glabrata enzyme CgCA. ScCA on the other hand has completely different activation profiles with these derivatives, being poorly activated by all amino acids (but slightly more susceptible to activation by serotonin). hCA II is highly activated by most amino acids, sometimes with activation constants in the nanomolar range11‑14 (e.g., L-/D-Phe; L-/D-Tyr). A second group of derivatives, including D-Phe, L-DOPA, L-Trp, as well as amines 12, 13, 15, 16 and 18, acted as more effective MgCA activators when compared to the compounds discussed above, with activation constants ranging between 5.82 and 10.9 μM. Thus, it may be observed that the amines were generally better MgCA activators compared to the carboxylic acids with which they are structurally related (compare Histamine with L/D-His, or dopamine with L-/D-DOPA, e.g.). The heterocylic amines incorporating pyridyl, piperazine, and morpholine rings were more effective MgCA activators compared to histamine, dopamine or serotonin. The most potent MgCA activators were L-adrenaline 19 and 1-(2-aminoethyl) piperazine 17, with activation constants of 0.72‑0.81 μM. Thus, small structural modifications in the scaffold of the amine activator (e.g., compare dopamine 13 with L-adrenaline 19) lead to drastic changes of the activating effect, with 19 being 13-times a better activator compared to 13.

Table XVI. Activation constants of hCA II (cytosolic α-isozyme), yeast β-CAs from S. cerevisiae (ScCA), C. glabrata (CgCA) and MgCA (Malassezia globosa) with amino acids and amines

No.	Compound	K_A (μM)			
		hCA II	ScCA	CgCA	MgCA
1	L-His	10.9	82	37.0	29.3 ± 1.2
2	D-His	43	85	21.2	18.1 ± 0.9
3	L-Phe	0.013	86	24.1	34.1 ± 2.7
4	D-Phe	0.035	86	15.7	10.7 ± 0.8
5	L-DOPA	11.4	90	23.3	8.31 ± 0.6
6	D-DOPA	7.8	89	15.1	13.7 ± 1.1
7	L-Trp	27	91	22.8	10.1 ± 0.6
8	D-Trp	12	90	12.1	12.5 ± 1.2
9	L-Tyr	0.011	85	9.5	15.7 ± 1.0
10	D-Tyr	0.058	84	7.1	25.1 ± 1.9
11	4-H_2N-L-Phe	0.15	21.3	31.6	13.4 ± 0.8
12	Histamine	125	20.4	27.4	10.9 ± 0.9
13	Dopamine	9.2	13.1	27.6	9.43 ± 0.7
14	Serotonin	50	15.0	16.7	14.2 ± 1.3
15	2-Pyridyl-methylamine	34	16.2	15.0	6.12 ± 0.3
16	2-(2-Aminoethyl)pyridine	15	11.2	16.3	7.30 ± 0.3
17	1-(2-Aminoethyl)-piperazine	2.3	9.3	14.9	0.81 ± 0.07
18	4-(2-Aminoethyl)-morpholine	0.19	10.2	10.1	5.82 ± 0.4
19	L-Adrenaline	96	0.95	10.8	0.72 ± 0.05

Chapter 9. Evolutionary aspects

The analysis of the Gram-positive and Gram-negative genomes conducted by similarity sequence searching programs, such as Blasta and Fasta, revealed a very complex distribution of the different classes of CAs in the two groups of bacteria. In fact, the genome of some of them encodes for all three classes of CAs (α, β and γ), while for others the genome encodes for two or one classes of CAs. Interestingly, the α-CAs are only present in the genome of Gram-negative and not in that of Gram-positive bacteria. By analyzing these results, in this thesis we will try to answer the following questions: 1) Why the α-CA are present only in Gram-negative? 2) What is the physiological role of α-CA in bacteria? 3) Why the α-CAs are not present in all Gram-negative? 4) Why there are species of bacteria whose genome does not code for CA?

A characteristic common to the α-CA identified in Gram-negative bacteria, it is the presence of a signal peptide to the N-terminal of the amino acid sequence (Figure 35 marked in red). This sequence directs the newly synthesized α-CA towards the periplasmic space, i.e. the space between the inner and outer membrane, which is absent in Gram-positive bacteria. The presence, then, of the periplasmic space would explain why the α-CA are present only in Gram-negative bacteria.

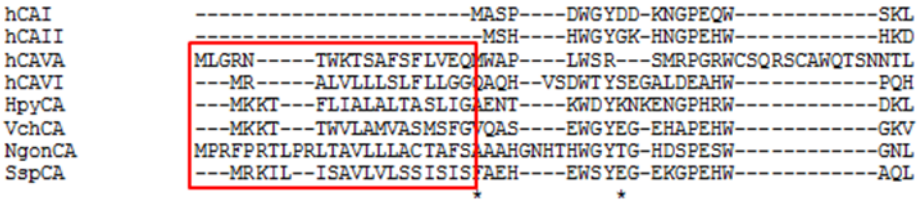

Figure 35. A detail of the multialignment of the α-CA amino acid sequences identified in the genome of mammalian and Gram-negative bacteria. The signal sequence included in the red rectangle is absent in the two human isoforms hCA I and II, while it is present in the mitochondrial form (hCA VA) for localization in the intermembrane space, in the hCA VI for secretion in saliva, and in the α- CA for bacterial localization in the periplasmic space.

To understand the role played by α-CA in Gram-negative, need to refer to some bacteria characterized by the presence of periplasmic α-CA. *Helicobacter pylori* is a pathogenic bacterium, Gram-negative, flagellated acidophilus, whose natural habitat is the gastric mucus of the human stomach. Its genome encodes for a α-, a β- and a γ-

CA (Nishimori I., *et al.* 2008; Morishita S., *et al.* 2008; Chirica L.C., *et al.* 2002). The α-CA has a periplasmic location, the β-CA has a cytoplasmic localization while still nothing is known about the expression and localization of γ-CA. *H. pylori* has developed unique adaptive mechanisms for growth in highly acidic environments such as the stomach. These mechanisms involve urease and CAs. In acidic conditions, urea penetrates into the cell through the channel and urea, in bacterial cytoplasm is hydrolyzed to CO_2 and $2NH_3$ (Supuran C.T. 2008) (Figure 36). In the bacterial cytoplasm, the CO_2 is hydrated by β-CA, while the CO_2 diffuses into the periplasm is converted to HCO_3^- by periplasmic α-CA. The ions H^+ products are used by NH_3 to form NH_4^+ in the periplasm and cytoplasm, respectively. Then, as shown in figure 32, the role of periplasmic α-CA and cytoplasmic β-CA it is to produce HCO_3^- and protons to neutralize the acid input. In *H. pylori*, then, the periplasmic α-CA is crucial for the acid acclimatization of the pathogen within the stomach. (Marcus E.A., *et al.* 2005; Sachs G., *et al.* 2005).

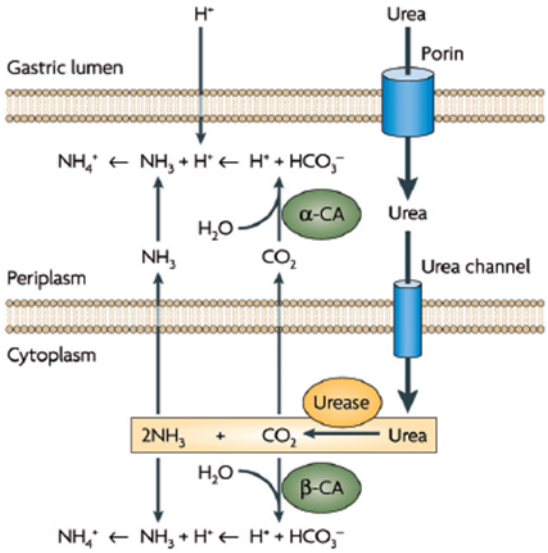

Figure 36. Schematization of the role of the α- and β-CA in maintaining periplasmic pH in *Helicobacter pylori*.

A similar mechanism has been reported for the Gram-negative bacterium *Ralstonia eutropha* (Gai C.S., *et al.* 2014). The genome of this bacterium encode for an α-, a β- and γ-CA. The α-CA has a periplasmic localization and assists the transport of bicarbonate across the cell membrane (Gai C.S., *et al.* 2014). Concerning the bacterium *Vibrio cholerae*, the α-CA, probably located in the periplasmic space, could be involved in the production of bicarbonate, an inducer of gene expression of

the virulence of the pathogen. In addition, the two bacteria belonging to the genus *Sulfurihydrogenibium*, *S. yellowstonense* and *S. azorense*, which live at temperatures up to 110°C, exhibit α-CA characterized by a signal peptide for periplasmic localization of this enzyme. These observations allow assuming that in the course of evolution, in Gram-negative bacteria, a signal peptide place at the 'N-terminal of a primordial CA, has generated a new class of CAs, namely the α class, with localization in the periplasmic compartment. Dr. Clemente Capasso and Prof. Claudiu Supuran, have speculated that the α-CA are able to convert the CO_2 to bicarbonate diffused in the periplasmic space, ensuring the survival and/or satisfying the metabolic needs of the microorganism. Instead, the β- and γ-CA localized in the cytoplasm are responsible for the supply of CO_2 to the carboxylase or for the homeostasis of intracellular pH and other functions (Capasso C. & Supuran C.T. 2014).

Not all Gram-negative bacteria, however, have α-CAs. Probably the α-CAs are not required when the Gram-negative bacteria colonize habitats defined as adverse to their survival or limiting for their metabolic needs (Capasso C. & Supran C.T. 2014).

There are also bacteria whose genome does not code for any class of CAs. A very interesting study has shown that knockout mutants for the CAs of *Ralstonia eutropha*, *Escherichia coli* and *Saccharomyces cerevisiae* are able to grow only in the presence of atmosphere with a CO_2 level of between 2 and 5% (Ueda K., *et al.* 2012). High levels of CO_2, in fact, generate high concentrations of bicarbonate spontaneously, through the reaction not catalyzed. These microorganisms lacking the CAs, at low concentrations of CO_2 (0.035%) are not able to grow, if not by providing a sufficient amount of bicarbonate. This shows that the CAs are not necessary for microbial growth in environments with high concentrations of CO_2 as the intestine, the sea water and in conditions of syntrophism and commensalism, but become necessary when this gas is present in low concentrations. The bacteria belonging to the genera Buchnera and Rickettsia, living in habitats with high concentration of CO_2, such as soil, seawater or the intestine, do not need CAs.

We also wondered if there was a relationship between the evolutionary history of bacterial CAs and evolution of Gram-positive and Gram-negative bacteria. The phylogenetic tree (Figure 37) obtained by aligning the amino acid sequences of the α-, β- and γ-CA identified in the genome of Gram-positive and negative bacteria, showing that the γ-CA by Gram-positive and negative are closely associated to each

other, as meaning that they form mixed groups of γ-CA from Gram-positive and Gram-negative bacteria.

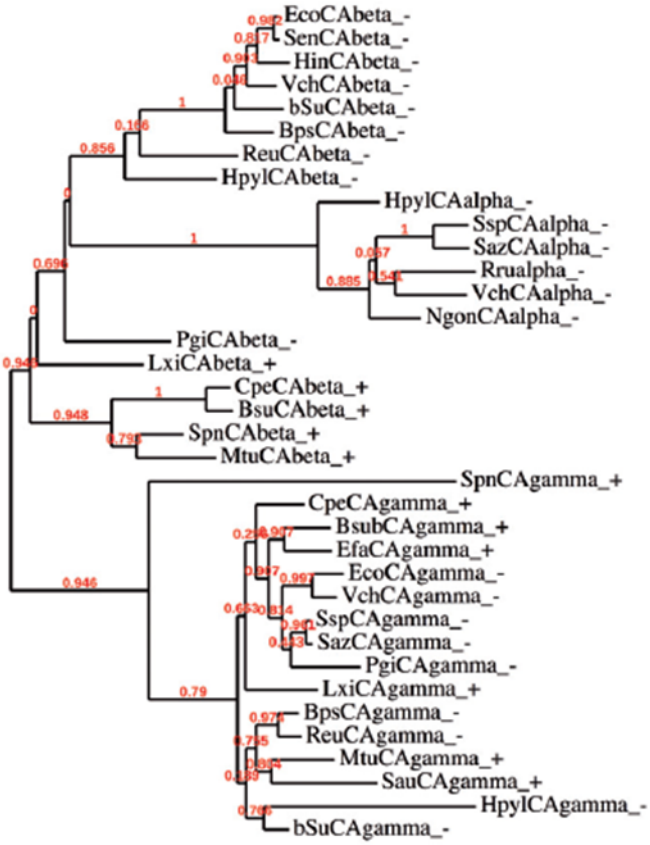

Figure 37. Phylogenetic analysis of α-, β and γ-CA of Gram-positive and negative. For the construction of the dendrogram it was used the program PhyML 3.0.

The β-CAs, unlike the γ-CAs, with the exception of LxiCAbeta_+ and PgiCAbeta_-, form two separate clusters, one containing the β-CAs only from Gram-negative bacteria and the other containing β-CAs only from Gram-negative bacteria positive. This could be the result of a gene duplication event. The α-CAs, found only in Gram-negative bacteria, form a separate cluster, located in the same cluster of β-CAs of Gram-negative bacteria (Capasso C. & Supuran C.T. 2014).

The results that come from the phylogenetic analysis is that the ancestral CAs are represented by the γ-class. In fact, even if the γ-class is widely distributed in all three domains, it is the only mainly identified in archaea, the oldest living organisms on our planet (Zimmerman S., *et al.* 2004; Tripp B.C., *et al*. 2001 -2004; Smith K.S., *et al.* 1999).

This is in agreement with the theory that supports a close relationship between the archaea and bacteria Gram-positive and considers phylogenetically distinct the Gram-negative bacteria.

From the γ-class would be originated the β-class of Gram-positive and then that of the Gram-negative bacteria. Subsequently, from an ancestral β-CA of a Gram-negative bacterium, they would originate the α-CAs, the latter exclusively present in Gram-negative bacteria. This hypothesis can also be corroborated by the theory of "enzyme promiscuity" (Baas B.J., *et al.* 2013; Chakraborty S., *et al.* 2013; Khersonsky O., *et al.* 2010), i.e. the ability of an enzyme to catalyze additional reactions to the primary role. Tawfick considers, in fact, promiscuity a key factor in the evolution of a new function of the same protein (Khersonsky O. & Tawfik D.S. 2010). In fact, it has been noted that the γ-CAs use only the CO_2 as substrate, while the β-CAs can hydrolyze in addition to CO_2, also hydrogen sulfide and carbonyl sulfide. Instead, the αCA not only catalyze the reaction of hydration of CO_2 and carbon disulphide, but also possess esterase and thioesterasic activity. Furthermore, by analyzing the size of the catalytic site bacterial of α-, β- and γ- CAs, it has been seen that the catalytic pocket is rather small for the γ-CAs, a bit bigger for β-CAs and wide for α-CAs (Figure 38).

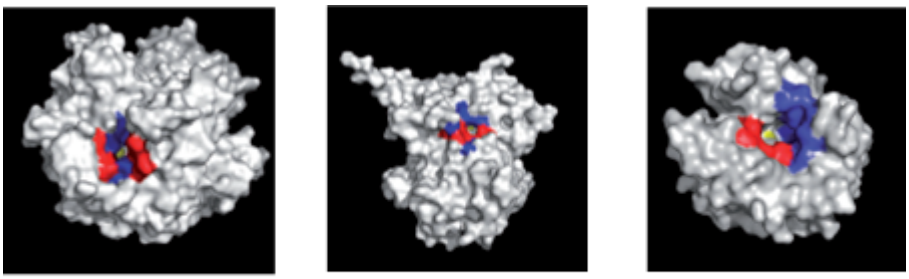

Figure 38. Three-dimensional structure of the catalytic site of the γ-(Cam), β-(Can2) and α-(hCA II)-CAs.

Overall, the catalytic efficiency of γ-CA is lower than the β-CA, which in turn represent the catalysts less efficient than α-CA (Capasso C. & Supuran C.T. 2014). We can conclude that phylogenetic analysis and theory of enzyme promiscuity support the hypothesis that the most recent CA is that of α-class (with additional catalytic activities), while the γ-CA is the class ancestral, that catalyzes only the reaction of hydration of CO_2 (with a catalytic efficiency rather low). These results are in agreement with the evolutionary theory according to which the Gram-positive

bacteria, characterized by a simple cellular structure, have appeared before the Gram-negative bacteria with a more complex cell structure (outer membrane and inner membrane).

Chapter 10. Discussion

Infectious diseases are still today the second leading cause of death worldwide, and the abuse and/or inappropriate use of antibiotics have led to a wide spread of the phenomenon of the antibiotic resistance of pathogenic microorganisms (Sacarlal J., *et al.* 2009; Nour N.M. 2012). As a general rule antibiotics inhibit the growth of the pathogen by acting on metabolic "pathways" such as cell wall biosynthesis, biosynthesis of proteins, biosynthesis of DNA and RNA, biosynthesis of folates (Gaynor M. & Mankin A.S. 2003). In recent years, many research groups have focused their interest of study on CAs of bacteria, fungi and protozoa, since they constitute a class of enzymes whose inhibition, as reported in literature, can slow or stop the growth of the pathogen through a different mechanism of action respect to those reported for antibiotics. CAs are target molecules of many antibacterial or antifungal drugs. It has been proved, in fact, that the CA are essential to the life cycle of the microorganisms (Capasso C. & Supuran C.T. 2013; Rusconi S., *et al*. 2004; Supuran C.T. 2012). In many pathogenic microorganisms have been identified and characterized CAs from at least four gene families α, β, γ and η. Usually bacteria encode for CA belonging to the classes α, β and γ. It has been reported in literature that the in vivo inhibition with sulfonamides and phenolic derivatives of the bacterial CAs identified in *Helicobacter pylori*, *Mycobacterium tuberculosis* and *Brucella suis*, hindered the growth of microorganisms. The acetazolamide and ethoxzolamide have been used in the clinic in the 80th and 90th as anti-ulcer agents and has been shown that the inhibition of CA from *Helicobacter pylori* represented a valid alternative for the control of the disease. The crystallographic structure of *Helicobacter pylori* α-CA complexed to acetazolamide or methazolamide represents a useful template for designing highly selective inhibitors for the bacterial CAs with few side effects. Fungi express α- and β-CA and it was found that the inhibition of these enzymes with sulfonamides, thiols and dithiocarbamates, block the in vivo growth of *Malassezia globosa*, *Candida albicans* and *Crytpococcus neoformans*. Protozoa, however, encode for α- β- or η-CA. It has been shown that sulphonamidic inhibitors, thiols and idroxamates actually cause the death of some microorganisms in vivo such as *Trypanosoma cruzi*, *Leishmania donovani chagasi* and *Plasmodium falciparum*.

***Vibrio cholerae* CAs**

In the present thesis it has been shown that the sulfonamides and their relative bioisosteres and, anions inhibited *in vitro* the three classes of CAs identified in the genome of ***Vibrio cholerae,*** indicated with the acronyms **VchCA (α), VchCAβ (β) and VchCAγ (γ)**. The three enzymes are efficient catalysts for CO_2 hydration, with k_{cat} values ranging between (3.4 − 8.23) × 10^5 s^{-1} and k_{cat}/K_M of (4.1 − 7.0) × 10^7 M^{-1} s^{-1}. We also compared the thermostability of three CAs from the bacterial pathogen *Vibrio cholera*. The results demonstrated that VchCA (α-CA) was more stable with respect to the β and γ-CAs identified in the genome of *V. cholerae*. The inhibition study with a panel of sulfonamides and one sulfamate led to the detection of a large number of nanomolar VchCA, VchCAβ and VchCAγ inhibitors, including simple aromatic/heterocyclic sulfonamides (compounds **2-9**, **11**, **13-15**, **24**) as well as **EZA**, **DZA**, **BRZ**, **BZA**, **TPM**, **ZNS**, **SLP**, **IND** (K_{IS} in the range of 66.2-95.3 nM). A set of inorganic anions and small molecules was investigated for inhibition of these enzymes. Perchlorate and tetrafluoroborate were not active inhibitors (K_Is > 200 mM), whereas sulfate was a moderate inhibitor of VchCA and VchCAγ (K_Is of 0.85–9.65 mM). The most potent VchCAγ inhibitors were N,N-diethyldithiocarbamate, sulfamate, sulfamide, phenylboronic acid and phenylarsonic acid, with K_I values in a range from 44 to 91 μM. The most active VchCA inhibitors were hydrogensulfite, bisulfite, trithiocarbonate, N,N-diethyldithiocarbamate, sulfamide, sulfamate, phenylboronic acid and phenylarsonic acid, with K_I values between 8 and 88 μM; while the most effective VchCAβ inhibitors were sulfamide, sulfamate, phenylboronic acid and phenylarsonic acid, with K_I values between 54 and 86 μM. As it was proven that bicarbonate is a virulence factor of this bacterium and since ethoxzolamide was shown to inhibit this virulence in vivo, we propose that VchCA, VchCAβ and VchCAγ may be a target for antibiotic development, exploiting a mechanism of action rarely considered up until now, i.e., interference with bicarbonate supply as a virulence factor. The inhibition profile of VchCA, VchCAβ or VchCAγ was different from that of the other bacterial or mammalian CAs investigated up until now, proving that probably it will be possible to design VchCA, VchCAβ or VchCAγ selective inhibitors using the scaffold of leads detected here.

Moreover, the X-ray crystal structure of the VchCAβ was solved at 1.9Å resolution from a crystal that was perfectly merohedrally twinned, revealing a tetrameric type II β-CA with a closed active site in which the zinc is tetrahedrally

coordinated to Cys42, Asp44, His98 and Cys101. The substrate bicarbonate was found bound in a noncatalytic binding pocket close to the zinc ion, as reported for a few other β-CAs, such as those from *Escherichia coli* and *Haemophilus influenzae*.

***Porhyromonas gingivalis* CAs**

The oral pathogenic bacterium *Porphyromonas gingivalis*, the main causative agent of periodontitis, encodes for two CAs one belonging to the β-class (PgiCAb) and another one to the γ-class (PgiCA). These bacterial CAs, produced as recombinant enzyme, showed a good catalytic activity for the CO_2 hydration reaction, comparable to that of the human isoform hCA I. PgiCA has been characterized for its inhibition profile with various classes of CA inhibitors, such as the sulfonamides and anions, whereas PgiCAb has been analyzed only for the anion inhibition profile. The PgiCA inhibition profile obtained using a wide range of pharmalogical and not-pharmacological sulfonamides was very different when compared with that obtained for the human isoenzymes, hCAI and II, CAM and the β-CA from a protozoan parasite. Dichlorophenamide, topiramate and many simple aromatic/heterocyclic sulfonamides were ineffective as PgiCA inhibitors whereas the best inhibition was observed with halogenosulfanilamides incorporating heavy halogens, 4-hydroxy- and 4-hydroxyalkyl-benzenesulfonamides, acetazolamide, methazolamide, zonisamide, indisulam, celecoxib, saccharin and hydrochlorothiazide (K_Is in the range of 131–380 nM). Inorganic anions such as thiocyanate, cyanide, azide, hydrogen sulfide, sulfamate and trithiocarbonate were effective PgiCA inhibitors with inhibition constants in the range of 41–97 μM. Other effective inhibitors were diethyldithiocarbamate, sulfamide, and phenylboronic acid, with K_Is of 4.0–9.8 μM. PgiCAb has a good catalytic activity for the CO_2 hydration reaction, with k_{cat} 2.8×10^5 s^{-1} and k_{cat}/K_m of 1.5×10^7 M^{-1} s^{-1}, being inhibited by cyanate and diethyldithiocarbamate in the submillimolar range (K_Is of 0.23-0.76 mM) and more efficiently by sulfamide, sulfamate, phenylboronic acid and phenylarsonic acid (K_Is of 60-78 μM).

The role of these enzymes as a possible virulence factor of *P. gingivalis* is poorly understood at the moment but its good catalytic activity and the possibility to be inhibited by a large number of compounds may led to interesting developments in the field. The anion inhibition profile of the two *P. gingivalis* enzymes is very different. Identification of selective inhibitors of PgiCAb/PgiCA may lead to pharmacological tools useful for understanding the physiological role(s) of these enzymes, since this

bacterium is the main causative agent of periodontitis and few treatment options are presently available.

***Plasmodium falciparum* CA**

For the treatment of diseases such as malaria, for example, several drugs are available, but over the years, their effectiveness is greatly diminished and, thus, remains the problem of antibiotic resistance. Protozoa, such as *Plasmodium falciparum*, utilize purines and pyrimidines for DNA/RNA synthesis during its exponential growth and replication. Plasmodia synthesize pyrimidines de novo from HCO_3^-, which is the substrate of the first enzyme involved in the Plasmodia pyrimidine pathway. HCO_3^- is generated from CO_2 through the action of a CA. Our studies have shown that PfCA, the CA identified in the genome of *Plasmodium falciparum*, belongs to a new class of CAs, called η. The metal ion coordination pattern of the η-CA from the malaria producing protozoa *P. falciparum* is unique among all seven genetic families encoding for such enzymes, comprising two His and one Gln residues, in addition to the water molecule/hydroxide ion acting as nucleophile in the catalytic cycle. The inhibition study of the η-CA against a panel of sulfonamides and one sulfamate compound, some of which are clinically used, showed that the strongest inhibitors identified were ethoxzolamide and sulthiame, with K_{Is} of 131-132 nM, followed by acetazolamide, methazolamide and hydrochlorothiazide (K_{Is} of 153-198 nM). Brinzolamide, topiramate, zonisamide, indisulam, valdecoxib and celecoxib also showed significant inhibitory action against PfCA, with K_{Is} ranging from 217 to 308 nM. An interesting observation was that the more efficient PfCA inhibitors are representative of several scaffolds and chemical classes, including benzene sulfonamides, monocyclic/bicyclic heterocyclic sulfonamides and compounds with a more complex scaffold (i.e., the sugar sulfamate derivative, topiramate, and the coxibs, celecoxib and valdecoxib). This study provides a platform for the development of next generation novel PfCA inhibitors. In fact, the inhibition of the CA of pathogenic microorganisms such as bacteria, protozoa and fungi, can represent an alternative approach for the design of antibacterial/pesticides/antifungal with a novel mechanism of action. α-CAs are potential drug targets, as shown by the use of sulfonamides in the clinic for the treatment of infection by *Helicobacter pylori* (Puscas I. 1984) and for the β-, γ- or η-class CAs there is a great interest in identifying selective inhibitors, since they are absent in humans and other mammals.

***Malassezia globosa* CA**

Malassezia globosa is highly implicated in the pathogenesis of dandruff and its genome encodes for only one carbonic anhydrases belonging to the β-class (MgCA). In the past, MgCA was cloned as GST-fusion protein, but the yield was rather low and the protein was often found in inclusion bodies. Here, we cloned the recombinant MgCA as His-Tag fusion protein. This procedure resulted in a good method to express and purify the active recombinant MgCA, and the protein recovery was better with respect to that used for preparing MG-CA (β-CA cloned as GST-fusion protein). Here, it has been reported an extensive anion inhibition study. It was demonstrated that metal complexing anions such as cyanate, thiocyanate, cyanide, azide are weak MgCA inhibitors (K_{Is} ranging between 6.81 and 45.2 mM), whereas bicarbonate (K_{Is} of 0.59 mM) and diethyldithiocarbamate (K_{Is} of 0.30 mM) together with sulfamide, sulfamate, phenylboronic acid and phenylarsonic acid were the most effective inhibitors detected (K_{Is} ranging between 83 and 94 μM). Carbonate, similar to perchlorate or tetrafluoroborate, did not inhibit MgCA up to 100 mM. This study allowed a deep understanding of inhibition mechanisms with these classes of compounds and led to interesting drug design campaigns and the discovery of CAIs with a good selectivity ratio for inhibiting enzyme classes or isoforms of medicinal interest.

Phylogenetic analysis

The complex distribution of the various CA classes in Gram-positive and negative bacteria allowed us to find a correlation between the evolutionary history of the bacteria and the three CA classes (α, β and γ) identified in their genome. Prokaryotes appeared on the Earth 3.5-3.8 billion years ago, while eukaryotes were dated 1.8 billion years ago. During the first 2.0-2.5 billion years the Earth's atmosphere not contained oxygen, thus the first organisms were anaerobic. Eukaryotic organisms almost aerobes developed on the Earth when the atmosphere was characterized by stable and relatively high oxygen content. All the oldest part of the evolutionary history of the planet and more than 90% of the phylogenetic diversity of life can be attributed to the microbial world. Moreover, the fact that the archaea are distinct from other prokaryotes is demonstrated by the existence of protein sequences that are present in archaea, but not in eubacteria (Gupta R.S. 1998). Many phylogenetic methods support a close correlation of archaea with Gram-positive bacteria, while

Gram-negative bacteria form a separate clade, indicating their phylogenetic distinction. Gupta et al. believe that the Gram-positive bacteria occupy an intermediate position between archaea and Gram-negative bacteria, and that they evolved precisely from archaea. Phylogenetic analysis of carbonic anhydrases identified in bacteria Gram-positive and negative, showed that the ancestral CA is represented by γ-class. In, fact, the γ-CA is the only CA class, which has been identified in archaea (Zimmerman S., *et al*. 2004; Tripp B.C., *et al.* 2001-2004; Smith K.S., *et al.* 1999). This is consistent with the theory that maintains a close relationship between the archaea and the Gram-positive bacteria, considering Gram-negative arising from the latter. Furthermore, phylogenetic analysis of bacterial CAs showed that the α-CAs, exclusively present in Gram-negative bacteria, were the most recent CAs. These results have been corroborated by the enzymatic promiscuity theory, which is the ability of an enzyme to catalyze a side reaction in addition to main reaction (Torrance J.W., *et al.* 2007). In fact, as described in the Results section, the α-CAs can catalyze secondary reaction, such as the hydrolysis of p-NpA or thioester, in addition to its primary reaction consisting in the CO_2 hydration.

Protonography

Protonography is a new technique, which allows the detection of carbonic anhydrases activity on a SDS polyacrylamide gel. The name ‘‘protonography’’ was chosen because CA activity produces hydrogen ions (protons) during the catalyzed reaction. These protons are responsible of the change of color that appears on the gel, in correspondence of the CO_2 hydrase activity. The advantage of this technique is that on the basis of molecular weight markers, recombinant or native CAs with different molecular weights can be detected and quantified rapidly on a single gel. Another improvement of this technique is the possibility to reveal CAs in biological systems, such as tissues or bacterial extracts from which only the genome information is so far available. In this case, protonography might be the method of choice for CAs screening, identification and characterization. Furthermore, protonography coupled with mass spectrometry for protein identification will make possible the broader mapping of active CAs present in protein extract from various sources, allowing the detection of distinct CA isoforms.

Chapter 11. Conclusions

My PhD project brought new insights in the field of carbonic anhydrases. It has been demonstrated: *a*) the studies carried out on the CAs from pathogens have identified selective inhibitors to be used as anti-infective; *b*) the discovery of the η-CA, a new genetic families of CAs; *c*) the introduction of a new technique, named protonography, useful for the identification of CA activity on a polyacrylamide gel; and *d*) it was speculated on the evolution of the CA classes (α, β and γ) identified in the Gram-negative and -positive bacteria. Our main hypothesis is that from the ancestral sequence of CA, the γ-class arose first, followed by the β-class; the α-class CAs came last and it is found only in the Gram-negative bacteria.

Bibliography

Aguilera, J., Van Dijken, J. P., De Winde, J. H. & Pronk, J. T. (2005b). Carbonic anhydrase (Nce103p): an essential biosynthetic enzyme for growth of Saccharomyces cerevisiae at atmospheric carbon dioxide pressure. Biochem J 391, 311–316.

Alber B.E., Ferry J.G. A carbonic anhydrase from the archaen Methanosarcina thermophila. Proc Natl Acad Sci U S A. 1994; 91(15):6909-13.

Alp S. Putative virulence factors of Aspergillus species. Mikrobiyoloji Bulteni 2006; 40:109-119.

Andrews K.T., Fisher G.M., Sumanadasa S.D., Skinner-Adams T., Moeker J., Lopez M., Poulsen S.A.. Antimalarial activity of compounds comprising a primary benzene sulfonamide fragment. Bioorg Med Chem Lett. 2013; 23(22):6114-7.

Armstrong J.M., Myers D.V., Verpoorte J.A., Edsall J.T. Purification and properties of human erythrocyte carbonic anhydrases. J Biol Chem. 1966; 241(21):5137-49.

Baas B.J., Zandvoort E., Geertsema E.M., Poelarends G.J. Recent advances in the study of enzyme promiscuity in the tautomerase superfamily. Chembiochem. 2013; 14(8):917-26.

Bahn, Y. S., Xue, C., Idnurm, A., Rutherford, J. C., Heitman, J. & Cardenas, M. E.(2007). Sensing the environment: lessons from fungi. Nat Rev Microbiol 5, 57–69.

Bahn, Y. S., Cox, G. M., Perfect, J. R. & Heitman, J. (2005). Carbonic anhydrase and CO2 sensing during Cryptococcus neoformans growth, differentiation, and virulence. Curr Biol 15, 2013–2020.

Boron W.F. Evaluating the role of carbonic anhydrases in the transport of HCO3--related species. Biochim Biophys Acta. 2010; 1804(2):410-21. Review.

Bostanci N., Belibasakis G.N. *Porphyromonas gingivalis*: an invasive and evasive opportunistic oral pathogen. Molecular Microbiology 2012; 333:1-9.

Capasso C., Supuran C.T. An overview of the alpha-, beta- and gamma-carbonic anhydrases from Bacteria: can bacterial carbonic anhydrases shed new light on evolution of bacteria? J Enzyme Inhib Med Chem. 2014; 30(2):325-32.

Capasso C., Supuran C.T. Anti-infective carbonic anhydrase inhibitors: a patent and literature review. Expert Opin Ther Pat. 2013; 23(6):693-704.

Capasso C., Supuran C.T. Bacterial Carbonic Anhydrases as Drug Targets. The Carbonic Anhydrases as Biocatalyst 2015; 271-281.

Cardoso T., Ribeiro O., Aragao I.C., et al. Additional risk factors for infection by multidrug-resistant pathogens in healthcare-associated infection: a large cohort study. BioMed Central Infectious Disease 2012; 12:375.

Cash R.A., Music S.I., Libonati J.P., Snyder M.J., Wenzel R.P., Hornick R.B. Response of man to infection with *Vibrio cholerae*. I. Clinical, serologic, and bacteriologic responses to a known inoculum. J Infect Dis. 1974;129(1):45-52.

Cash R.A., Music S.I., Libonati J.P., Snyder M.J., Wenzel R.P., Hornick R.B. Response of man to infection with *Vibrio cholerae*. I. Clinical, serologic, and bacteriologic responses to a known inoculum. J. Infect. Dis. 1974; 129, 45−52.

Chakraborty S., Minda R., Salaye L., Dandekar A.M., Bhattacharjee S.K., Rao B.J. Promiscuity-based enzyme selection for rational directed evolution experiments. Methods Mol Biol. 2013; 978:205-16.

Chegwidden W.R., Carter N.D., Edwards Y.H. The Carbonic Anhydrases: New Horizons, 2000; 12-28.

Chirica L.C., Elleby B., Jonsson B.H., Lindskog S. The complete sequence, expression in Escherichia coli, purification and some properties of carbonic anhydrase from *Neisseria gonorrhoeae*. Eur J Biochem. 1997; 244(3):755-60.

Chirica L.C., Petersson C., Hurtig M., Jonsson B.H., Borén T., Lindskog S. Expression and localization of alpha- and beta-carbonic anhydrase in *Helicobacter pylori*. Biochim Biophys Acta. 2002; 1601(2):192-9.

Clare B.W. and Supuran C.T. Carbonic anhydrase activators. 3: structure-activity correlations for a series of isozyme II activators. J Pharm Sci. 1994; 83(6):768-73.

Cleves, A. E., Cooper, D. N., Barondes, S. H. & Kelly, R. B. (1996). A new pathway for protein export in Saccharomyces cerevisiae. J Cell Biol 133, 1017–1026.

Cox G.M., McDade H.C., Chen S.C., Tucker SC, Gottfredsson M, Wright LC, Sorrell TC, Leidich SD, Casadevall A, Ghannoum MA et al. Extracellular phospholipase activity is a virulence factor for *Cryptococcus neoformans*. Molecular Microbiology 2001; 39:166-75.

Cox G.M., Mukherjee .J, Cole G.T., et al. Urease as a virulence factor in experimental cryptococcosis. Infection and Immunity 2000; 68:443-487.

Cronk J.D., Endrizzi J.A., Cronk M.R., O'Neill J.W., Zhang K.Y.J. Crystal structure of *E. coli* beta-carbonic anhydrase, an enzyme with an unusual pH-dependent activity. Protein Sci 2001; 10: 911-922.

De Luca V., Del Prete S., Supuran C.T., Capasso C. Protonography, a new technique for the analysis of carbonic anhydrase activity. J Enzyme Inhib Med Chem. 2015; 30(2):277-82.

De Simone G., Di Fiore A., Capasso C., Supuran C.T. The zinc coordination pattern in the η-carbonic anhydrase from Plasmodium falciparum is different from all other carbonic anhydrase genetic families. Bioorg Med Chem Lett. 2015; 25(7):1385-9.

De Simone G., Supuran C.T. (In)organic anions as carbonic anhydrase inhibitors. J Inorg Biochem. 2012; 111:117-29.

De Simone, G., Di Fiore, A., Supuran C.T., Are carbonic anydrase inhibitors suitable for obtaining antiobesity drugs. Current Pharmaceutical Design 2008; 14, 655–660.

Del Prete S., De Luca V., Scozzafava A., Carginale V., Supuran C.T., Capasso C. Biochemical properties of a new alpha-carbonic anhydrase from the human pathogenic bacterium, *Vibrio cholerae* . J Enzyme Inhib Med Chem 2014; 29 : 23 – 7.

Del Prete S., De Luca V., Vullo D., Scozzafava A., Carginale V., Supuran C.T., Capasso C. Biochemical characterization of the γ-carbonic anhydrase from the oral pathogen *Porphyromonas gingivalis*, PgiCA. J Enzyme Inhib Med Chem. 2014; 29(4):532-7.

Del Prete S., Isik S., Vullo D., De Luca V., Carginale V., Scozzafava A., Supuran C.T., Capasso C. DNA cloning, characterization, and inhibition studies of an α-carbonic anhydrase from the pathogenic bacterium *Vibrio cholerae*. J Med Chem. 2012; 55(23):10742-8.

Del Prete S., Vullo D., De Luca V., AlOthman Z., Osman S.M., Supuran C.T., Capasso C. Biochemical characterization of recombinant β-carbonic anhydrase (PgiCAb) identified in the genome of the oral pathogenic bacterium *Porphyromonas gingivalis*. J Enzyme Inhib Med Chem. 2014; 1-5.

Del Prete S., Vullo D., De Luca V., Supuran C.T., Capasso C. Biochemical characterization of the δ-carbonic anhydrase from the marine diatom *Thalassiosira weissflogii*, TweCA. J Enzyme Inhib Med Chem. 2014; 29(6):906-11.

Del Prete S., Vullo D., Fisher G.M., Andrews K.T., Poulsen S.A., Capasso C., Supuran CT. Discovery of a new family of carbonic anhydrases in the malaria pathogen *Plasmodium falciparum*--the η-carbonic anhydrases. Bioorg Med Chem Lett. 2014 ; 24(18):4389-96.

Di Fiore A., Alterio V., Monti S.M., De Simone G., D'Ambrosio K. Thermostable Carbonic Anhydrases in Biotechnological Applications. Int J Mol Sci. 2015; 8;16(7):15456-80. doi: 10.3390/ijms160715456.

Di Fiore A., Capasso C., De Luca V., Monti S.M., Carginale V., Supuran C.T., Scozzafava A., Pedone C., Rossi M., De Simone G. X-Ray structure of the first "extremo-'-carbonic anhydrase", a dimeric enzyme from the thermophilic bacterium, *Sulfurihydrogenibium yellostonense* YO3AOP1. Acta Crystallographica Section D: Biological Crystallography, 2013; 69.6: 1150-1159.

Dogne, J. M., Hanson, J., Supuran, C.T., Pratico, D. Coxibs and cardiovascular side-effects: from light to shadow. Curr Pharm Des 2006; 12, 8, 971-975.

Edsall J.T. Multiple molecular forms of carbonic anhydrase in erythrocytes. Ann N Y Acad Sci. 1968; 151(1):41-63.

Elleuche, S. & Po¨ ggeler, S. (2009a). Evolution of carbonic anhydrases in fungi. Curr Genet 55, 211–222.

Falkowski P., Scholes R.J., Boyle E., Canadell J., Canfield D., Elser J., Gruber N., Hibbard K., Högberg P., Linder S., MacKenzie F.T., *et al* The Global Carbon Cycle: A Test of Our Knowledge of Earth as a System. Science 2000; 290 (5490): 291–296

Forsman C., Behravan G., Osterman A., Jonsson B.H. Production of active human carbonic anhydrase II in E. coli. Acta Chem Scand 1988; 42:314–318.

Gaynor M., Mankin A.S. Macrolide antibiotics: binding site, mechanism of action, resistance. Curr Top Med Chem 2003; 3:949-61.

Go¨ tz, R., Gnann, A. & Zimmermann, F. K. (1999). Deletion of the carbonic anhydrase-like gene NCE103 of the yeast Saccharomyces

cerevisiae causes an oxygen-sensitive growth defect. Yeast 15, 855–864.

Gupta R.S. What are archaebacteria: life's third domain or monoderm prokaryotes related to gram-positive bacteria? A new proposal for the classification of prokaryotic organisms. Mol Microbiol. 1998; 29(3):695-707. Review.

Harris J.B., LaRocque R.C., Qadri F., Ryan E..T, Calderwood S.B. Cholera. Lancet. 2012; 379(9835):2466-76.

Innocenti A., Zimmerman S., Casini A., Ferry J.G., Scozzafava A., Supuran C.T. Carbonic anhydrase inhibitors. Inhibition of the zinc and cobalt gamma-class enzyme from the archaeon Methanosarcina thermophila with anions Bioorg Med Chem Lett 2004; 14: 3327- 31.

Innocenti, A., Leewattanapasuk, W., Muhlschlegel, F. A., Mastrolorenzo, A. & Supuran, C. T. (2009). Carbonic anhydrase inhibitors. Inhibition of the beta-class enzyme from the pathogenic yeast Candida glabrata with anions. Bioorg Med Chem Lett 19, 4802– 4805.

Joseph P, Ouahrani-Bettache S, Montero JL, Nishimori I, Minakuchi T, Vullo D, Scozzafava A, Winum JY, Kohler S, Supuran CT. 2011. A new beta-carbonic anhydrase from Brucella suis, its cloning, characterization, and inhibition with sulfonamides and sulfamates, leading to impaired pathogen growth. Bioorg Med Chem 19: 1172-1178.

Joyce S.A., Watson R.J., Clarke D.J. The regulation of pathogenicity and mutualism in Photorhabdus. Current Opinion in Microbiology 2006;9:127-132.

Khersonsky O., Tawfik D.S. Enzyme promiscuity: a mechanistic and evolutionary perspective. Annu Rev Biochem. 2010; 79:471-505.

Klengel, T., Liang, W. J., Chaloupka, J., Ruoff, C., Schro¨ ppel, K., Naglik, J. R., Eckert, S. E., Mogensen, E. G., Haynes, K. & other authors (2005). Fungal adenylyl cyclase integrates CO2 sensing with cAMP signaling and virulence. Curr Biol 15, 2021–2026.

Kimber M.S., Pai E.F. The active site architecture of *Pisum sativum* β-carbonic anhydrase is a mirror image of that of α-carbonic anhydrases. EMBO J 2000; 19: 2323-2330.

Knudsen J.F., Carlsson U., Hammarstrom P., Sokol G.H., Cantilena L.R. The cyclooxygenase-2 inhibitor celecoxib is a potent inhibitor of human carbonic anhydrasem II. Inflammation 2004; *28,* 5, 285-290.

Köhler K. *et al.* Saccharin inhibits carbonic anhydrases: possible explanation for its unpleasant metallic aftertaste. Angewandte Chemie International Edition 46; 2007; 7697–7699.

Krebs H. A. Inhibition of carbonic anhydrase by sulphonamides. Biochem J 1948; 43, 4, 525-528.

Krissinel E. and Henrick K. Inference of macromolecular assemblies from crystalline state. J. Mol. Biol. 2007; 372, 774–797.

Krungkrai J., Supuran C.T. The alpha-carbonic anhydrase from the malaria parasite and its inhibition. Curr Pharm Des. 2008; 14(7):631-40.

Krungkrai SR, Suraveratum N, Rochanakij S, Krungkrai J. 2001. Characterisation of carbonic anhydrase in *Plasmodium falciparum*. Int J Parasitol 31: 661-668.

Lee R. B.Y., Smith J A.C., Rickaby R.E.M.J. Phycol. 2013; 49, 170.

Marcus E.A., Moshfegh A.P., Sachs G., Scott D.R. The periplasmic alpha-carbonic anhydrase activity of *Helicobacter pylori* is essential for acid acclimation. J Bacteriol. 2005; 187(2):729-38.

Meldrum N.U., Roughton F.J. Carbonic anhydrase. Its preparation and properties. J Physiol. 1933; 80(2):113-42.

Menlove K.J., Clement M., Crandall K.A. Similarity searching using BLAST. Methods Mol Biol 2009; 537:1–22.

Mincione F., Scozzafava A. and Supuran C.T. (2009). Antiglaucoma carbonic anhydrase inhibitors as ophthalomologic drugs (pp. 139-154). Wiley: Hoboken (NJ).

Morishita S., Nishimori I., Minakuchi T., *et al*. Cloning, polymorphism, and inhibition of beta-carbonic anhydrase of *Helicobacter pylori*. J Gastroenterol 2008; 43:849–57.

Nishimori I., Minakuchi T., Kohsaki T., Onishi S., Takeuchi H., Vullo D., *et al*. Carbonic anhydrase inhibitors: the beta-carbonic anhydrase from Helicobacter pylori is a new target for sulfonamide and sulfamate inhibitors. Bioorg Med Chem Lett 2007; 17: 3585-94.

Nishimori I., Minakuchi T., Morimoto K., Sano S., Onishi S., Takeuchi H., *et al*. Carbonic anhydrase inhibitors: DNA cloning and inhibition studies of the alpha-carbonic anhydrase from *Helicobacter pylori*, a new target for developing sulfonamide and sulfamate gastric drugs . J Med Chem 2006; 49 : 2117 – 26.

Nishimori I., Onishi S., Takeuchi H., Supuran C.T. The alpha and beta classes carbonic anhydrases from *Helicobacter pylori* as novel drug targets. Curr Pharm Des 2008; 14:622–30.

Nishimori I., Onishi S., Vullo D., Innocenti A., Scozzafava A., Supuran C.T. Carbonic anhydrase activators: the first activation study of the human secretory isoform VI with amino acids and amines. Bioorg. Med. Chem. Lett. 2007; 17, 5351–5357.

Nour N.M. Premature delivery and the millennium development goal. Rev Obstet Gynecol 2012; 5:100-5.

Li, W., Zhou, P. P., Jia, L. P., Yu, L. J., Li, X. L. & Zhu, M. (2009). Limestone dissolution induced by fungal mycelia, acidic materials, and carbonic anhydrase from fungi. Mycopathologia 167, 37–46.

Pearson W.R. Using the FASTA program to search protein and DNA sequence databases. Methods Mol Biol. 1994; 24:307-31.

Puscas I. Treatment of gastroduodenal ulcers with carbonic anhydrase inhibitors. Ann NY Acad Sci 1984; 429:587–91.

Reungprapavut S., Krungkrai S.R., Krungkrai J. Plasmodium falciparum carbonic anhydrase is a possible target for malaria chemotherapy. J Enzyme Inhib Med Chem. 2004; 19(3):249-56.

Roux O., Cereghino R., Solano P.J., *et al.* Caterpillars and fungal pathogens: two co-occurring parasites of an ant-plant mutualism. PLoS One 2011; 6:e20538.

Rowlett RS, Hoffmann KM, Failing H, Mysliwiec MM, Samardzic D. Evidence for a bicarbonate "escort" site in Haemophilus influenzae beta-carbonic anhydrase.Biochemistry. 2010 May 4;49(17):3640-7. doi: 10.1021/bi100328j.

Scozzafava A., Mastrolorenzo A., *et al.* New advances in HIV entry inhibitors development. Curr Drug Targets Infect Disord 2004; 4:339-55.

Sacarlal J., Nhacolo A.Q., Sigauque B., *et al*. A 10 year study of the cause of death in children under 15 years in Manhica, Mozambique. BMC Public Health 2009; 9:67.

Sachs G., Weeks D.L., Wen Y., Marcus E.A., Scott D.R., Melchers K. Acid acclimation by Helicobacter pylori. Physiology (Bethesda). 2005; 20:429-38. Review.

Sainsbury P.D., Mineyeva Y., Mycroft Z., Bugg T.D.H. Chemical intervention in bacterial lignin degradation pathways: Development of selective inhibitors for intradiol and extradiol catechol dioxygenases. Bioorg Chem. 2015; 60:102-9.

Schaller M., Borelli C., Korting H.C., *et al*. Hydrolytic enzymes as virulence factors of *Candida albicans*. Mycoses 2005; 48:365-377.

Scozzafava A., Briganti F., Ilies M.A. & Supuran C.T. Carbonic anhydrase inhibitors. Synthesis of membrane-impermeant low molecular weight sulfonamides possessing *in vivo* selectivity for the membrane-bound versus the cytosolic isozymes. Journal of Medicinal Chemistry. 2000; 43, 292–300.

Sein K.K., Aikawa M. 1998. The pivotal role of carbonic anhydrase in malaria infection. Med Hypotheses 50: 19-23.

Smith K.S., Ferry J.G. A plant-type (β-class) carbonic anhydrase in the thermophilic methanoarchaeon *Methanobacterium thermoautotrophicum*. J Bacteriol 1999; 181: 6247-53.

Smith K.S., Ferry J.G. Prokaryotic carbonic anhydrases. FEMS Microbiol Rev 2000; 24: 335-66.

Smith K.S., Jakubzick C., Whittam T.S., Ferry J.G. Carbonic anhydrase is an ancient enzyme widespread in prokaryotes. Proc Natl Acad Sci U S A. 1999; 96(26):15184-9.

Soto W., Punke E.B., Nishiguchi M.K. Evolutionary perspectives in a mutualism of sepiolid squid and bioluminescent bacteria: combined usage of microbial experimental evolution and temporal population genetics. Evolution 2012; 66:1308-1321.

Strop P., Smith K.S., Iverson T.M., Ferry J.G., Rees D.C. Crystal structure of the "cab"-type beta class carbonic anhydrase from the archaeon *Methanobacterium thermoautotrophicum*. J Biol Chem 2001; 276: 10299-305.

Sun M.K. and Alkon D.L. Carbonic anhydrase gating of attention: memory therapy and enhancement. Trends Pharmacol. Sci. 2002; 23, 83–89.

Sun M.K. and Alkon D.L. Pharmacological enhancement of synaptic efficacy, spatial learning, and memory through carbonic anhydrase activation in rats. J. Pharmacol. Exp. Ther. 2001; 297, 961–967.

Supuran C.T. and Winum J.Y. In Drug Design of Zinc-Enzyme Inhibitors: Functional, Structural, and Disease Applications. Ophthalomologic Drugs. 2009; 139–154.

Supuran C.T. Bacterial carbonic anhydrases as drug targets: toward novel antibiotics? Front Pharmacol. 2011; 2:34

Supuran C.T. Carbonic anhydrase inhibition/activation: trip of a scientist around the world in the search of novel chemotypes and drug targets. Curr Pharm Des 2010; 16 : 3233 – 45.

Supuran C.T. Carbonic anhydrase inhibitors and activators for novel therapeutic applications. Future Med Chem. 2011; 3(9):1165-80. Review.

Supuran C.T. Carbonic Anhydrases – An Overview Current Pharmaceutical Design. Bentham Science Publishers Ltd, 2008; 14,603-614.

Supuran C.T. Carbonic anhydrases: novel therapeutic applications for inhibitors and activators. Nat Rev Drug Discovery 2008; 7:168 – 81.

Supuran C.T. Inhibition of bacterial carbonic anhydrases and zinc proteases: from orphan targets to innovative new antibiotic drugs. Curr Med Chem 2012; 19:831-44.

Supuran C.T., Capasso C. The eta-class carbonic anhydrases as drug targets for antimalarial agents. Expert Opin Ther Targets 2014; 1-13.

Supuran C.T., De Simone G. Carbonic Anhydrase: An Overview. The Carbonic Anhydrases as Biocatalyst 2015; 3-11.

Supuran C.T., Di Fiore A., Alterio V., Monti S.M., De Simone G. Recent advances in structural studies of the carbonic anhydrase family: the crystal structure of human CA IX and CA XIII. Curr Pharm Des. 2010; 16(29):3246-54.

Supuran C.T., Diuretics: from classical carbonic anhydrase inhibitors to novel applications of the sulfonamides. Current Pharmaceutical Design 2008; 14, 641-648.

Supuran C.T., Scozzafava A., Conway J. (Eds.): Carbonic anhydrase- Its inhibitors and activators, CRC Press, Boca Raton (FL), USA, 2004; 1-363.

Supuran C.T., Scozzafava A., Ilies M.A. and Briganti F. Carbonic anhydrase inhibitors. Synthesis of sulfonamides incorporating 2,4,6-trisubstituted-pyridinium-ethylcarboxamido moieties possessing membrane-impermeability and *in vivo* selectivity for the membrane-bound (CA IV) versus the cytosolic (CA I and CA II) isozymes. Journal of Enzyme Inhibition and Medicinal Chemistry.2000; 15, 381–401.

Supuran CT. 2008. Carbonic anhydrases: novel therapeutic applications for inhibitors and activators. Nat Rev Drug Discov 7: 168-181.

Supuran, C.T, Ilies M.A. and Scozzafava A. Carbonic anhydrase inhibitors. Part 29. Interaction of isozymes I, II and IV with benzolamide-like derivatives. European Journal of Medicinal Chemistry. 1998; 33, 739–752.

Supuran, C.T., Di Fiore A., De Simone G. Carbonic anhydrase inhibitors as emerging drugs for the treatment of obesity. Expert Opinion on Emerging Drugs 2008; 13, 383-392.

Supuran, C.T., Scozzafava A., Conway J., Eds.; Carbonic Anhydrase. Its Inhibitors and Activators; CRC Press: Boca Raton (FL), USA, 2004; 1–363.

Tanc M., Carta F., Scozzafava A., Supuran C.T. α-Carbonic Anhydrases Possess Thioesterase Activity. ACS Med Chem Lett. 2015; 6(3):292-5.

Temperini C., Innocenti A., Scozzafava A., Mastrolorenzo A., Supuran C.T. Carbonic anhydrase activators: LAdrenaline plugs the active site entrance of isozyme II, activating better isoforms I, IV, VA, VII, and XIV. Bioorg. Med. Chem. Lett., 2007; 17, 628-635.

Temperini C., Innocenti A., Scozzafava A., Supuran C.T., Carbonic anhydrase activators: kinetic and X-.ray crystallographic study for the interaction of D- and L-tryptophan with the mammalian isoforms I-XIV. Bioorg. Med. Chem., 2008; 16, 8373-8378.

Temperini C., Scozzafava A., Puccetti L., Supuran C.T., Carbonic anhydrase activators: X-ray crystal structure of the adduct of human isozyme II with L-histidine as a platform for the design of stronger activators. Bioorg. Med. Chem. Lett., 2005; 15, 5136-5141.

Temperini C., Scozzafava A., Supuran C.T. Carbonic anhydrase activators: the first X-ray crystallographic study of an adduct of isoform I. Bioorg. Med. Chem. Lett. 2006; 16, 5152–5156.

Temperini C., Scozzafava A., Vullo D., Supuran C.T. Carbonic anhydrase activators. Activation of isozymes I, II, IV, VA, VII, and XIV with l- and d-histidine and crystallographic analysis of their adducts with isoform II: engineering proton-transfer processes within the active site of an enzyme. Chemistry, 2006; 12, 7057-7066.

Tibayrenc M., Ayala F.J. Reproductive clonality of pathogens: A perspective on pathogenic viruses, bacteria, fungi, and parasitic protozoa. Proc Natl Acad Sci USA 2012. 109: E3305-3313.

Torrance JW, Holliday GL, Mitchell JB, Thornton JM. The geometry of interactions between catalytic residues and their substrates.J Mol Biol. 2007 Jun 15;369(4):1140-52. Epub 2007 Mar 24.

Trevan M. Techniques of Immobilization. In: Immobilized Enzymes. An Introduction and Applications in Biotechnology (Trevan, M., ed.), 1980 Wiley, Chichester-New York, pp. 1–9.

Tripp B.C., Bell C.B. 3rd, Cruz F., Krebs C., Ferry J.G. A role for iron in an ancient carbonic anhydrase. J Biol Chem. 2004; 279(8):6683-7.

Tripp B.C., Smith K., Ferry J.G. Carbonic anhydrase: new insights for an ancient enzyme. J Biol Chem. 2001; 276(52):48615-8.

Ueda K., Nishida H., Beppu T. Dispensabilities of carbonic anhydrase in proteobacteria. Int J Evol Biol 2012; 2012:324549 (1–5).

Viparelli F., Monti S.M., De Simone G., Innocenti A., Scozzafava A., Xu Y., Morel F.M., Supuran C.T. Inhibition of the R1 fragment of the cadmium-containing zeta-class carbonic anhydrase from the diatom *Thalassiosira weissflogii* with anions. Bioorg Med Chem Lett. 2010; 20(16):4745-8.

Vullo D., Del Prete S., Fisher G.M., Andrews K.T., Poulsen S.A., Capasso C., Supuran C.T. Sulfonamide inhibition studies of the η-class carbonic anhydrase from the malaria pathogen *Plasmodium falciparum*. Bioorg Med Chem. 2015; 23(3):526-31.

Vullo D., Del Prete S., Osman S.M., Scozzafava A., Alothman Z., Supuran C.T., Capasso C. Anion inhibition study of the β-class carbonic anhydrase (PgiCAb) from the oral pathogen *Porphyromonas gingivalis*. Bioorg Med Chem Lett. 2014; 24(18):4402-6.

Vullo D., Isik S., Del Prete S., De Luca V., Carginale V., Scozzafava A., Supuran C.T., Capasso C. Anion inhibition studies of the α-carbonic anhydrase from the pathogenic bacterium *Vibrio cholera*. Bioorg Med Chem Lett. 2013; 23(6):1636-8..

Winum J.Y., Ram, M., Scozzafava A., Montero J.L., Supuran C.T. Carbonic anhydrase IX: a new druggable target for the design of antitumor agents. Med. Res. Rev., 2008; 28, 445-463.

Winum J.Y., Temperini C., El Cheikh K., Innocenti A., Vullo D., Ciattini S., Montero J.L., Scozzafava A., Supuran C.T. Carbonic anhydrase inhibitors: clash with Ala65 as a means for designing inhibitors with low affinity for the ubiquitous isozyme II, exemplified by the crystal structure of the topiramate sulfamide analogue. J. Med. Chem. 2006; 49, 7024–7031.

Xu Y., Feng L., Jeffrey P.D., Shi Y., Morel F.M. Structure and metal exchange in the cadmium carbonic anhydrase of marine diatoms. Nature. 2008; 452(7183):56-61.

Zimmerman S., Innocenti A., Casini A., Ferry J.G., Scozzafava A., Supuran C.T.Carbonic anhydrase inhibitors. Inhibition of the prokariotic beta and gamma-class enzymes from Archaea with sulfonamides. Bioorg Med Chem Lett. 2004; 14(24):6001-6.

Zimmerman A. , Jean-Francois Tomb, and James G. Ferry. Characterization of CamH from Methanosarcina thermophila, Founding Member of a Subclass of the γ- Class of Carbonic Anhydrases. journal of bacteriology, mar. 2010, p. 1353–1360 vol. 192, no. 5 0021-9193/10/12.00 doi:10.1128/jb.01164-09